CHARACTERIZATION OF THE BONE LOSS AND RECOVERY RESPONSE AT THE DISTAL FEMUR METAPHYSIS OF THE ADULT MALE HINDLIMB UNLOADED RAT

A Thesis

by

JOSHUA MORGAN DAVIS

Submitted to the Office of Graduate Studies of
Texas A&M University
in partial fulfillment of the requirements for the degree of

MASTER OF SCIENCE

December 2011

Major Subject: Mechanical Engineering

CHARACTERIZATION OF THE BONE LOSS AND RECOVERY RESPONSE AT THE DISTAL FEMUR METAPHYSIS OF THE ADULT MALE HINDLIMB UNLOADED RAT

A Thesis

by

JOSHUA MORGAN DAVIS

Submitted to the Office of Graduate Studies of
Texas A&M University
in partial fulfillment of the requirements for the degree of

MASTER OF SCIENCE

Approved by:

Co-Chairs of Committee,	Harry Hogan
	Susan Bloomfield
Committee Member,	Chii-Der Suh
Head of Department,	Jerald Caton

December 2011

Major Subject: Mechanical Engineering

ABSTRACT

Characterization of the Bone Loss and Recovery Response at the Distal Femur Metaphysis of the Adult Male Hindlimb Unloaded Rat. (December 2011)

Joshua Morgan Davis, B.S., Texas A&M University

Co-Chairs of Advisory Committee: Dr. Harry Hogan
Dr. Susan Bloomfield

Extended periods of mechanical unloading are known to be detrimental to bone health. Astronauts who spend months in microgravity aboard the International Space Station (ISS) are at particular risk. It is anticipated that NASA will not drastically increase the size of the astronaut corps, and this will mean increased likelihood of repeat missions for more astronauts. Thus, it is important to better understand the effects that prolonged, multiple bouts of unloading have on bone. This study utilized the hindlimb unloaded (HU) rat model to examine bone loss and recovery for single and double unloading bouts. Adult male Sprague-Dawley rats (6 months old) were randomized into the following groups: baseline (sacrificed at 6 months), 1HU7 (unloaded for 1 month, weight-bearing recovery for 3 months), 2HU10 (unloaded for 1 month, recovered for 2 months, unloaded for another month, and then recovered 2 months), 1HU10 (normal cage activity until 1 month HU ending at month 10, 2 month recovery followed), and aging controls (remained ambulatory throughout experiment). Every month (28 days),

animals were terminated and the left femurs were excised, resulting in n=15 per group for each time point. Mineral and geometric properties were measured using peripheral quantitative computed tomography (pQCT) at the distal femur metaphysis, and quasi-static reduced platen compression (RPC) was used to estimate the mechanical properties of cancellous bone. Strength indices based on pQCT parameters were calculated as predictors of mechanical properties.

Bone mass properties decreased due to HU and recovered within 2-3 months post-HU. A combination of increased periosteal apposition and endocortical resorption also occurred during HU. The initial HU bout suppressed normal age-related increases in mechanical properties and recovered within 1-2 months. Cancellous compressive strength index (CSI) most closely matched changes in mechanical properties. A second HU bout after two months recovery had a less detrimental effect on pQCT parameters but a greater negative impact on mechanical properties, when compared to pre-HU values. The opposite is true for mechanical properties if loss is characterized relative to aging controls. Recovery after the second HU period did not appear to be significantly affected by a previous bout of HU.

TABLE OF CONTENTS

Page

Page

LIST OF FIGURES

Page

Page

Page

LIST OF TABLES

Page

1. INTRODUCTION

1.1 Motivation and Rationale

One of the most serious health problems that astronauts face is the substantial loss of bone experienced during long-duration space flight. Studies have shown that bone mineral density (BMD) in the femoral neck of International Space Station (ISS) crew members drops 1-2% per month of space flight.[1] This is significantly greater than the rate of bone loss in elderly Caucasian and African-American women, which is less than 1% per year.[2] Drastically reduced BMD poses a risk for crew members performing physically demanding tasks while they are in space, as well as when they return to Earth. Research has also shown that those losses are not quick to recover. Lang et al. studied 16 ISS crew members who spent 4-6 months in space and found that losses in BMD had not fully recovered to preflight values even 12 months after returning to Earth.[3] A "discordant recovery dynamic" was also observed during this study: bone mineral content (BMC) recovered faster than BMD, and both recovered more quickly than did estimated strength. More recently, Carpenter et al. tracked a subset of 8 of the ISS crew members studied previously[3] with longer term follow-up scans that ranged from 2.5-4 years post-flight.[4] These results continue to raise concerns about astronaut skeletal health, especially those who make repeat missions or missions to other planets. These concerns are particularly critical given that current indications

---

This thesis follows the style of Journal of Bone and Mineral Research.

suggest that NASA may be forced to eliminate or reduce the addition of new members to the astronaut corps to save costs; this would require sending fewer astronauts into space more frequently. Such a scenario would also mean that the average age of crew members will be steadily increasing, yet systematic studies of the effects of age on physiological changes in astronauts are not available.

Animal models have several intrinsic advantages over human experiments. For one, greater control can be exercised over animals' activities and treatments. Because of this, it is often easier to conduct large-scale studies using animals instead of humans. This is especially true when investigating the effects of microgravity, as it is very expensive to send people into space and only a small portion of the population have spent extended periods in microgravity. Human bed rest studies, another ground-based analog, are also very expensive to perform. The hindlimb unloaded (HU) rat model is a commonly used ground-based analog to study the effects of microgravity and disuse.[5,6] Another advantage to using animal subjects is entire bones can be collected after undergoing a specific treatment, something that is impossible with humans. *Ex vivo* analysis allows researchers to examine myriad tissues and organs and perform tests that would be impossible with live human subjects. This is particularly true when it comes to measuring the mechanical strength of various skeletal sites. Directly measuring the mechanical properties of bone could be considered one of the most relevant outcome variables in bone research because of the strong relation to fracture risk, but this information cannot be gathered from living humans. Using an animal

model, however, permits direct testing of the effects of changes in loadbearing (e.g. hindlimb unloading) and interventions or countermeasures on bone strength and related properties.

One of the more important aspects of understanding how bone adapts is the desire to accurately predict strength from non-invasive assessments. To do this, we need experimental results to validate theories and assumptions. Strength indices for bending and compression[1,7] have been developed for the proximal femur region in an effort to estimate strength based on data acquired clinically using quantitative computed tomography (QCT) scanners. These types of estimated strength parameters can also be applied to other anatomic sites as well. As of now, BMD is commonly used as an indicator of overall bone condition, or at least in screening for risk of osteoporosis. BMD in most clinical cases is measured using dual-energy X-ray absorptiometry (DXA) scanners, with the most common sites being the proximal femur (hip) and the spine (lumbar vertebrae). It is well known, however, that BMD alone is not an accurate predictor of true bone quality or fracture risk.[8,9,10,11,12,13] Thus, yet another benefit of using an animal model is the ability to perform experiments to evaluate hypotheses and predictions about the relationships between non-invasive measures (primarily computed tomography based) and potential fractures.

A significant area of ongoing research in human clinical medicine regarding osteoporosis and fracture risk is the relative importance of cortical bone and cancellous bone in overall mechanical strength.[14,15,16,17,18,19] Osteoporotic fractures commonly

occur in the hip (which includes the proximal femur and femoral neck) and spine and both of these sites contain significant amounts of cancellous as well as cortical bone. It is therefore crucial to understand how cortical and cancellous bone contribute to the overall strength of these sites in order to predict the likelihood of fracture.

1.2 Objectives

The main purpose of this study is to quantify the loss and recovery characteristics of bone in the distal femur metaphysis of the adult male HU rat and assess its relevance as an appropriate model for loss and recovery behavior of astronauts' proximal femur. Male rats are commonly considered "skeletally mature" at 6 months of age and thus considered adult. Further, previous studies have shown that 28 days of HU leads to relative losses in bone mass and density similar to those of astronauts undergoing long term spaceflight[6,20] (4-6 months). As a mixed bone site, the distal femur metaphysis provides an opportunity to study the response to unloading (and reloading) for cortical and cancellous bone separately, and also as an integral "composite" system. The specific objectives of this study are as follows:

1. To quantify the loss and recovery characteristics of geometric, densitometric, and strength parameters of the cortical, cancellous and total (integral) compartments in the distal femur metaphysis of an adult hindlimb unloaded male rat using pQCT scanning and reduced platen compression (RPC) mechanical testing. I hypothesize that the animals will exhibit substantial losses

in bone mineral content (BMC), BMD, and strength in all compartments as a result of HU beginning at 6 months of age. Those animals that are allowed to recover for three recovery periods (3 times the duration of unloading) will show enough gains that they should not be significantly different than baseline or aging control values, with BMC recovering faster than BMD. I anticipate that bone strength will recover more slowly than BMD because, although the tissue may become mineralized, trabecular microstructure has been shown to recover more slowly.[21]

2. To determine the effects of a previous HU period on loss and recovery characteristics for a second HU period. Once again, geometric, densitometric, and strength parameters in the distal femur metaphysis of adult hindlimb unloaded male rats will be quantified using pQCT scanning and reduced platen compression (RPC) mechanical testing. The first 28-day HU period will start when the animals are 6 months old. This will be followed by 56 days of recovery and then a second 28-day HU exposure starting when the animals are 9 months old. In order to account for possible confounding effects of age, another group of animals will undergo a single bout of HU starting at 9 months of age. This will also permit addressing a related objective: to assess the effects of age on a single exposure to 28 days of HU, initiated at 6 or 9 months of age. I predict that the first HU bout will have a negative effect on the second HU exposure, making losses (relative to immediate pre-HU groups) greater for the second HU bout.

Recovery from the second HU (also relative to immediate pre-HU groups) will be less substantial than recovery from the first.

3. To compare the measured strengths obtained via RPC testing to currently used estimated strength calculations. Lang et al. used indices calculated from pQCT data to estimate the strength of the astronaut femoral neck in both bending and compression.[1,3] However, it remains to be determined how accurately they track with actual strength values. I hypothesize that measured strengths will closely match the strengths predicted by the cancellous compressive strength index (cancellous CSI) because the cancellous bone being tested will primarily be in compression. The bending strength index (BSI) will track less well but may still provide some insight into the behavior of the bone because it takes the material's estimated elastic modulus and spatial distribution into account. Stress-strain index (SSI), a density-weighted strength index, is less likely to accurately predict the strength of cancellous bone in compression but could still provide valuable insight into the geometric and density changes occurring during HU and recovery.
4. To compare the mineral and geometric characteristics obtained via pQCT to currently published astronaut femoral neck data. Research has shown that mineral losses due to unloading are site and compartment specific[22] so there is reason to believe that some sites may behave differently than others. One of the goals of the overall project is to find out which skeletal sites on the rat, if

any, compare well with loss and recovery trends for astronaut data. I hypothesize that the distal femur metaphysis results will follow the same general trends as the astronaut femoral neck, but there could possibly be substantial differences between the two due to differences in cortical/cancellous composition between the two sites and the prevalent loading conditions that each site experiences during normal activity (distal femur primarily in compression vs. femoral neck in bending and compression).

2. BACKGROUND

2.1 General Anatomy of Bone

Bone is the primary load bearing organ in the human body. It provides several mechanical functions, such as protecting other organs, creating a frame to support the body and keep its shape, and providing a means for mobility via connective tissue. It also provides other physiological functions like blood production and calcium storage. Bone tissue comprises the load-bearing portion of the organ and is what we traditionally think of when we refer to “bone”. It is a highly mineralized connective tissue which is composed of both organic (collagen) and inorganic (hydroxyapatite mineral) components. Bone tissue is usually divided into two types based on structure and location: cortical and cancellous (Fig. 1). Both types of bone can be seen in. Cortical bone is the dense, stiff outer layer that bears most of the skeletal loads. It is usually composed of lamellar regions that are aligned along the axis of long bones. Cancellous bone, also called trabecular or spongy bone, is less stiff and more porous than cortical bone and is characterized by a large number of tiny rod-like structures, called trabeculae. Cancellous bone is usually found in vertebrae, at the ends of long bones, and in areas where tendons and other connective tissue attach. The structure and orientation of the trabeculae give the cancellous region its distinct spongy appearance.

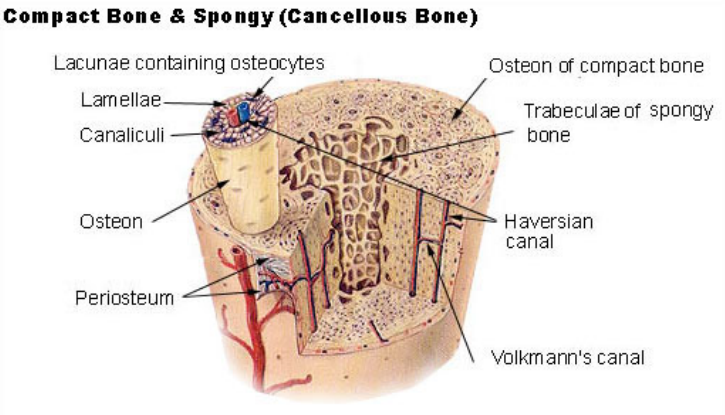

Fig. 1. Illustration showing the location of cortical and cancellous regions. Cortical bone is the dense, hard bone tissue which makes up the outer shell. Its structure is composed mostly of circular lamellar regions called osteons. Cancellous bone (or trabecular or spongy bone) is less dense and less hard than cortical bone. Its structure is easily identified by its spongy appearance, which is due to the presence and connectivity of tiny rod-like trabeculae.[23]

2.2 Adaptation of Bone to Loading and Disuse

Julius Wolff proposed in the 1870 that bone will adapt to the stresses it undergoes. Specifically, if a particular bone experiences significant loading it will gain mass and become stronger. Conversely, if it undergoes long periods of disuse the opposite will happen. Not only does the mass of bone change with loading scenarios, its geometry does as well. This is especially evident in cancellous bone, where trabeculae clearly align in the direction of principle stresses.[24]

Bone adapts via the activity of three cell types: osteoblasts, osteoclasts, and osteocytes (Fig. 2). Osteoblasts are the cells that add new bone by depositing osteoid, which will mature into mineralized bone tissue. Osteoclasts are cells that resorb bone. It seems counterproductive to have cells performing opposing jobs, but in healthy people their dual functions actually create stronger bones. Osteocytes are osteoblasts

that have become trapped inside the inner layers of bone. Because of their ubiquitous presence, it is thought that osteocytes play an important mechanosensing role, signaling when and where osteoblasts and osteoclasts should act.[25]

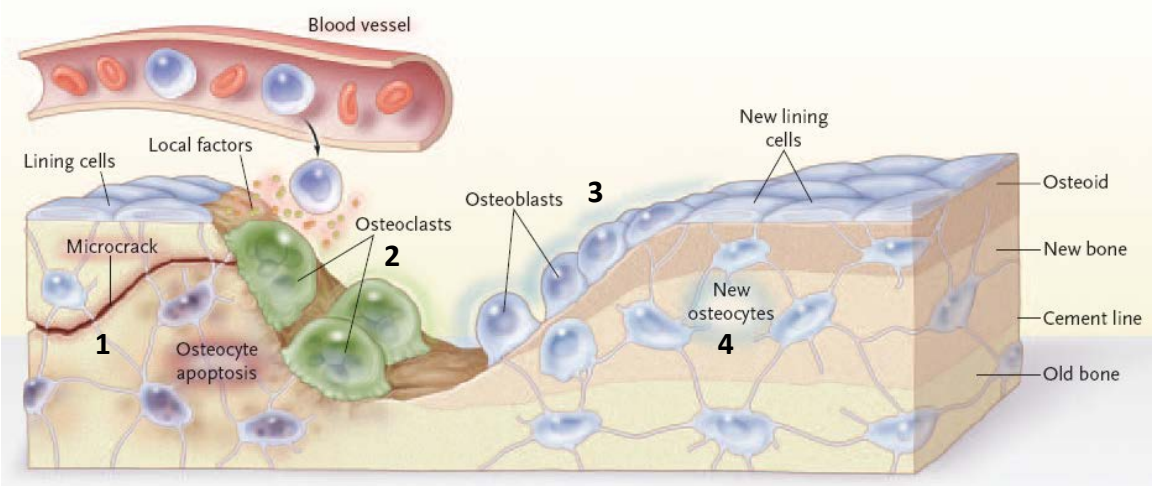

Fig. 2. The basic steps involved in the remodeling cycle of bone. 1) A microcrack occurs, causing osteocyte apoptosis, which sends out signaling proteins. 2) Osteoclasts attach to the damaged surface and resorb the damaged tissue and microcrack. 3) Osteoblasts deposit osteoid to fill in the void created by osteoclasts. 4) Eventually, bone tissue will surround some of the osteoblasts and new osteocytes will be formed.[10]

2.3 Distal Femur Metaphysis of the Rat

The femur is the longest bone in the body and is composed of a cortical region in the middle, called the diaphysis, and two ends consisting of an epiphysis and a metaphysis. The distal femur metaphysis of a rat (Fig. 3) is a good candidate for trying to model the astronaut femoral neck because it has a mix of cortical and cancellous bone (Fig. 4).

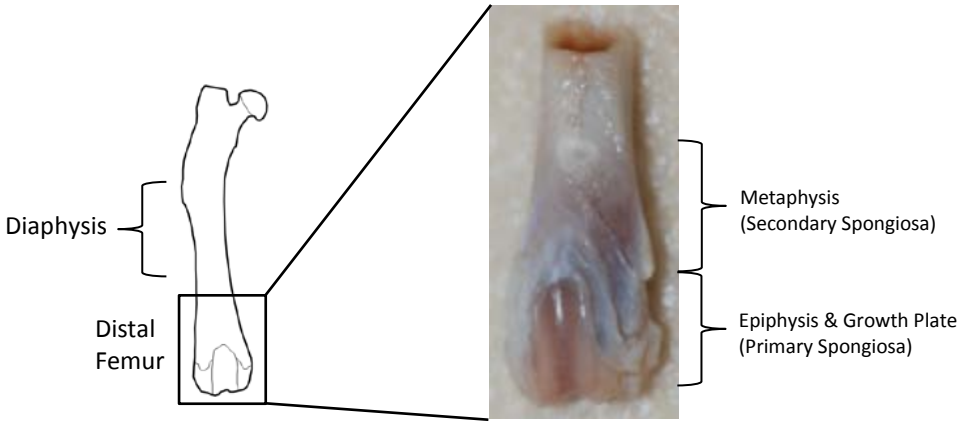

Fig. 3. Illustration of a whole rat femur with a window showing a picture of the distal portion of the femur.

The inclusion of cancellous bone is important because research has shown that it loses BMD more substantially than cortical bone when unloaded.[3,22] The primary spongiosa region is very close to the growth plate (Fig. 5) and, therefore, is less responsive to unloading than the secondary spongiosa region. It is for this reason that the secondary spongiosa region was examined in this study.

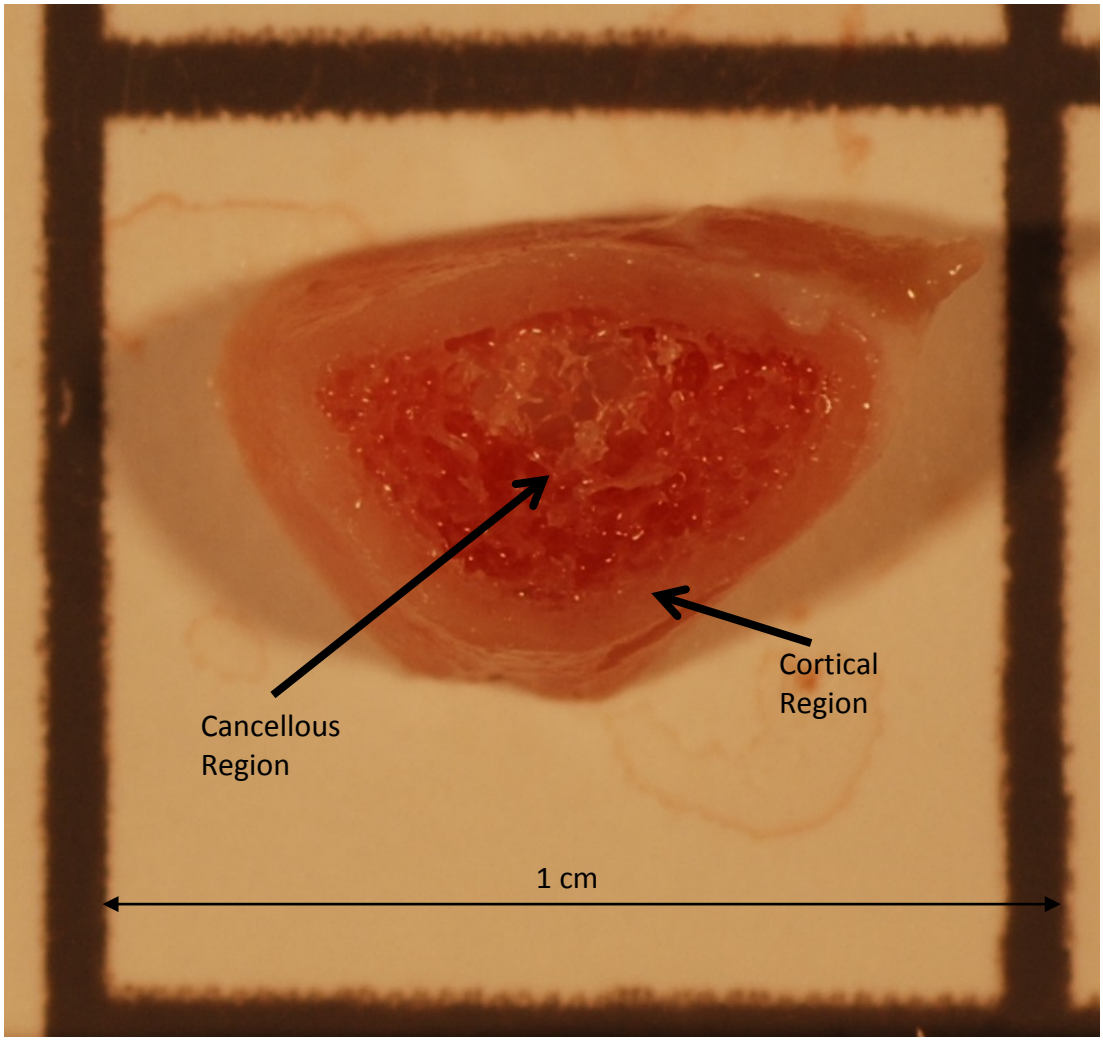

Fig. 4. Photograph of a transverse cross-section of a rat distal femur metaphysis immediately after being cut.

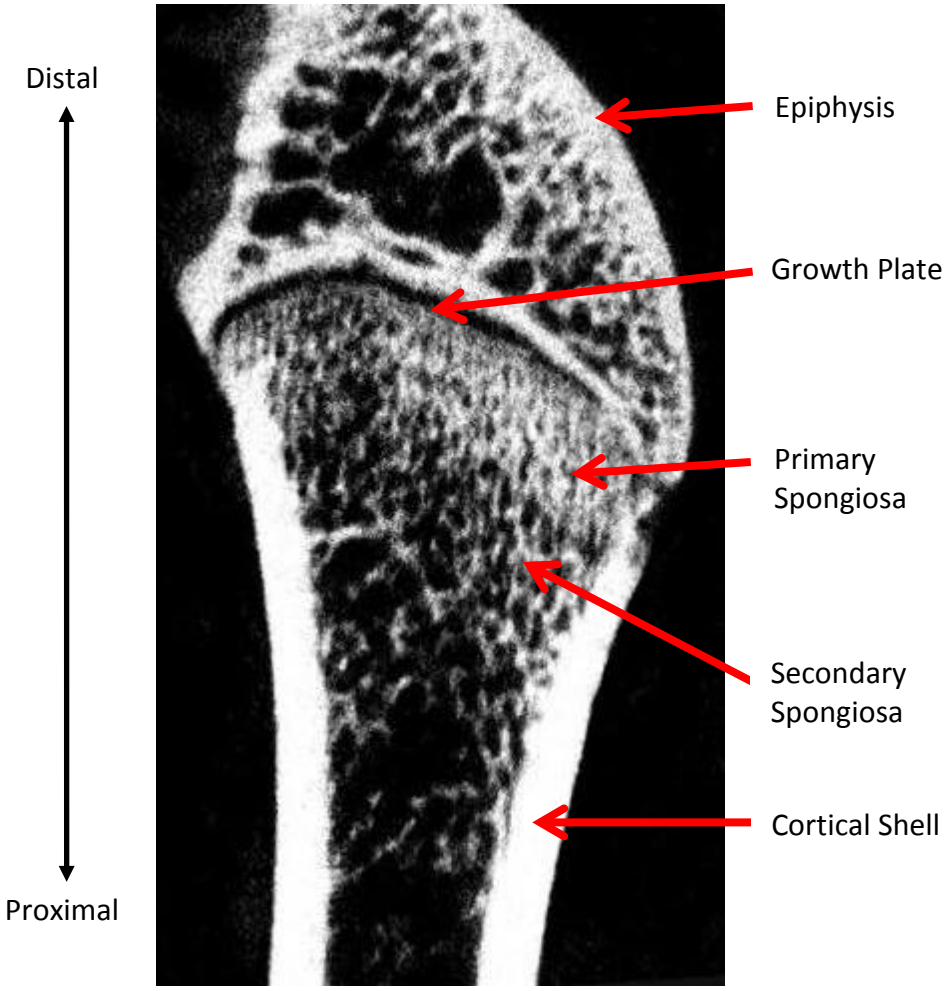

Fig. 5. Micro-CT image of the sagittal view of a rat distal femur. As proximal distance from the growth plate increases, the trabecular region becomes less dense and the cortical shell becomes thicker.[26]

2.4 Mechanical Testing Methods for Rat Distal Femur Metaphysis

Several approaches have been taken to mechanically test cancellous bone in the rat distal femur metaphysis. One method uses a 1.6-mm indenter to penetrate 2-mm into the cancellous region of a 4-mm section which was cut proximal to the femoral condyle.[27,28,29] While this method is useful for determining extrinsic properties, it does not give any information about intrinsic properties. Another method uses the same

type of specimen but uses a platen to load the entire cross-section in compression.[30] Results from this procedure do not give any direct information about the cancellous region, only the composite behavior. Another method, called reduced platen compression (RPC), was developed in Texas A&M University's Bone Biomechanics Lab. This method involves using a platen to compress only the cancellous compartment.[31] A direct comparison of RPC and whole cross-section compression was performed by Hogan et al.[31] on the proximal tibia of OVX and sham rats. Percent differences between intrinsic and extrinsic parameters of OVX and sham rats were much more dramatic using the RPC method. Even though OVX has a greater impact on cancellous bone, the dramatic declines would not be captured using whole bone compression because the cortical shell bears most of the load.

2.5 Reduced Platen Compression Mechanical Testing

The initial RPC method developed by Hogan et al.[31] calculated an average endocortical circle for a group of specimens and then used a single platen size to test all of them. This introduces some error because the size of specimens varies. A subsequent modification was put forth by Oxlund et al.[32] where a range of platen sizes were used to ensure that the platen was the same size as the specimen's endocortical circle. A more recent modification out of the Bone Biomechanics Lab sized the platens so that they were 70% of the diameter of the endocortical circle, reducing the influence

of cortical bone.[26] This version of the RPC method is the one that will be utilized in this study (Fig. 6).

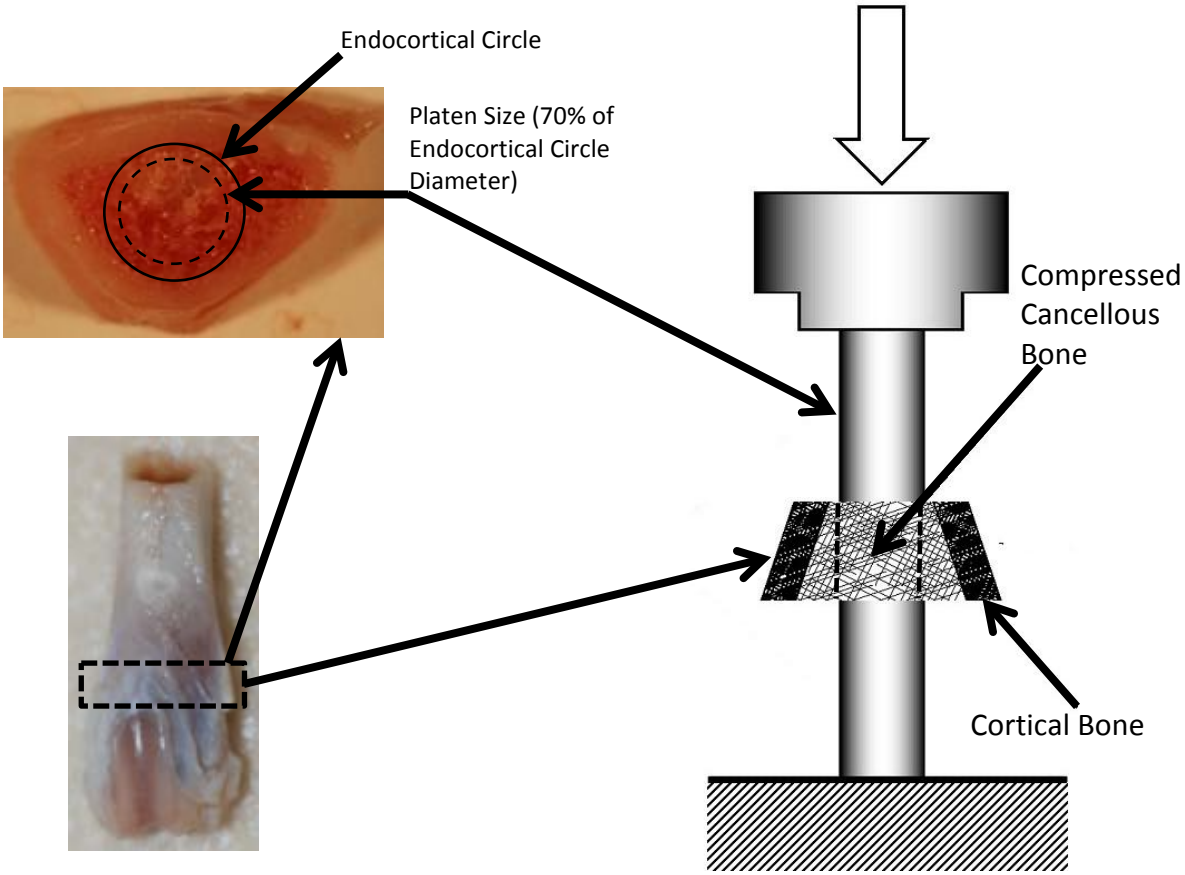

Fig. 6. Excised RPC specimen location and RPC test setup. The metaphysis section is removed from the distal femur and platens are sized to approximately 70% of the maximum endocortical diameter. (Portion taken from Lemmon H.[26])

2.6 Strength Indices

Because of the complex composition and geometry of bone, it is hard to make an accurate indicator of how strong it is. For clinical purposes, BMD is an easily obtainable predictor of bone strength, but it does not take the total mass and geometry

of the bone into consideration. Lang et al. used a compressive strength index (CSI) (Eq. 1) and a bending strength index (BSI) (Eq. 2) to approximate the bending and compressive strength of astronauts' femoral neck before a mission, immediately after returning, and after one year of recovery.[1]

$$CSI = vBMD^2 \times CSA_{min} \quad (1)$$

$$BSI = \frac{I_X + I_Y}{W} \quad (2)$$

where *vBMD* is total volumetric BMD, CSA_{min} is the minimum cross-sectional area of the total cross-section. BSI is similar to a structure's section modulus (*Z*) (Eq. 3), which is defined in beam theory as the ratio of a cross-section's moment of inertia (*I*) to the distance between the neutral axis and the most extreme fiber (*c*). *W* is the diameter of the equivalent circular cross-section, and I_X (Eq. 4) and I_Y (Eq. 5) are the elastic modulus-weighted moments of inertia.

$$Z = \frac{I}{c} \quad (3)$$

The calculations used to determine I_X and I_Y are given in Equations 4 and 5.

$$I_X = \frac{1}{e_b} \Sigma e_i \times \left(x_i - \bar{x}\right)^2 dA \quad (4)$$

$$I_Y = \frac{1}{e_b} \Sigma e_i \times \left(y_i - \bar{y}\right)^2 dA \quad (5)$$

where e_b is the elastic modulus of cortical bone (18,600 MPa)[33], e_i is the estimated elastic modulus of a voxel, $\bar{x}$ and $\bar{y}$ are the coordinates of the elastic modulus

weighted centroid, x_i and y_i are the voxel coordinates, and dA is the voxel area. It should be noted that the *vBMD-e_i* relation used by Lang et al. was developed Keyak et al.[34] while the relation that was used in this study (Eq. 6) was developed by Cory et al.[35] through the mechanical testing of bones from normal, ovariectomized, and partially nephrectomized rats .

$$e_i = 3711.4 \times \left(BMD_{app}\right)^{1.87} \quad (6)$$

Another strength index, called the stress-strain index (SSI) (Eq. 7), has been developed for use with pQCT scanners.[36]

$$SSI = \sum \frac{r_i^2 a_i \frac{CD_i}{ND}}{r_{max}} \quad (7)$$

where r_i is a voxel's distance from the center of mass, a_i is a voxel's area, CD_i is the apparent density of a voxel, ND is the normal density of cortical bone (1200 mg/cm^3), and r_{max} is the distance from the density-weighted center of mass to the most extreme voxel in the bone cross-section.

2.7 Adult Rat Hindlimb Unloading Model

The HU rat model is a commonly used ground-based analogue for simulating the effects of microgravity on the skeletal system.[5,6] This model involves suspending the hindlimbs of a rat by fastening a harness along the base of their tail (Fig. 7). By elevating the lower portion of their body, several important characteristics of microgravity are reproduced, including cephalic fluid shift and significantly reduced external loading of

the hindlimbs. Also, unlike some other animal hindlimb disuse studies, this method does not restrict the movement of their limbs.

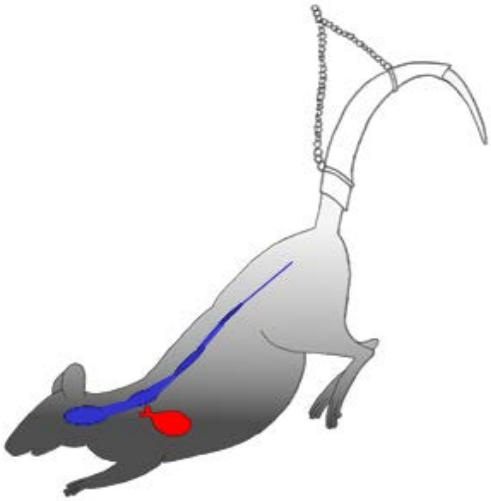

Fig. 7. Illustration of a hindlimb unloaded (HU) rat. The HU rat is a commonly used ground-based analog for studying the effects of microgravity.A harness is fastened to the sides of the tail and raised so that no external loading will be exerted on the hindlimbs. This model also reproduces several other effects of microgravity, such as cephalic fluid shift. (Courtesy of K. Wilkerson)

3. MATERIALS AND METHODS

3.1 Study Design and Animals

This experiment took place at Texas A&M University and was performed jointly by the Bone Biomechanics Lab in the Department of Mechanical Engineering and the Bone Biology Lab in the Department of Health and Kinesiology. The overall goal of the broader project, which was funded with a grant from NASA, was to examine the effects of hindlimb unloading on several bone quality measures with the aim of elucidating information that could be used to better predict the impact of multiple missions on bone health of NASA's Astronaut corps.

Adult male Sprague-Dawley rats were obtained from Harlan (Houston, TX) at 5.5 months of age and allowed to acclimate for 14 days prior to initiation of the study. All animals were singly housed after arriving at our animal facility in a temperature-controlled (23 ± 2°C) room with a 12-hour light-dark cycle in an American Association for Accreditation of laboratory Animal Care-accredited animal care facility and were provided standard rodent chow (Harlan Teklad 8604) and water ad-libitum throughout the study. Animal care and all experimental procedures described in this study were approved by the Texas A&M University IACUC (AUP 2008-93). Rats undergoing hindlimb unloading (HU) were suspended for bouts of 28 days (1 month) at a time. This time span is commonly used with the HU model and has been shown to mimic many of the negative effects of spaceflight on human bone health and quality.[22,37,38,39] In an effort

to achieve the objectives stated above, animals were divided into 3 broad groups: 1) those sacrificed at the start of the experimental period, which are designated baseline (BL6); 2) aging control (AC) animals that did not experience any HU treatment at all; 3) animals that experienced one or more bouts of HU. A total of 210 rats were used to populate 14 specific groups (n=15 each) in order to have end points (for excised bone samples and other tissue) at times of interest (in 28d intervals). Animals were block assigned to groups based on body weight and total vBMD (from *in vivo* pQCT) values at the start of the experiment (day 0) so that there were no differences between groups for body weight and Total vBMD. The details of each group and the nomenclature used to distinguish them can be summarized as follows (see Fig. 8):

- BL6 – baseline animals that were sacrificed when they were 6 months old
- AC7, AC8, AC9, AC10, AC12 – aging control animals that remained ambulatory until they were sacrificed at 7, 8, 9, 10, and 12 months of age
- 1HU7 – animals that underwent a single 1-month bout of unloading that started at 6 months of age and ended at 7 months
- 1HU7+R1 – animals that underwent a 1-month bout of unloading that started at 6 months of age, ended at 7 months, and were allowed to recover for 1 month
- 1HU7+R2 – animals that underwent a 1-month bout of unloading that started at 6 months of age, ended at 7 months, and were allowed to recover for 2 months
- 1HU7+R3 – animals that underwent a 1-month bout of unloading that started at 6 months of age, ended at 7 months, and were allowed to recover for 3 months

- 1HU10 – animals that underwent a single 1-month bout of unloading that started at 9 months of age and ended at 10 months
- 1HU10+R2 – animals that underwent a 1-month bout of unloading that started at 9 months of age, ended at 10 months, and were allowed to recover for 2 months
- 2HU10 – animals that underwent two 1-month bouts of unloading, with the first starting at 6 months of age and ending at 7 months and the second starting at 9 months of age and ending at 10 months
- 2HU10+R2 – animals that underwent two 1-month bouts of unloading, with the first starting at 6 months of age and ending at 7 months, the second starting at 9 months of age and ending at 10 months, and then a period of recovery for 2 months

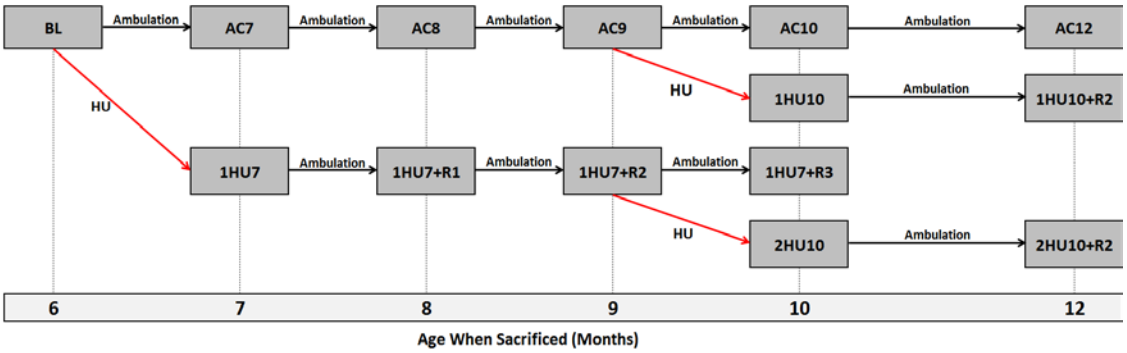

Fig. 8. Grouping of all rats, including the age at which they were sacrificed. Baseline (BL6) animals were sacrificed at 6 months of age. Aging controls (AC) were allowed normal cage activity until sacrificed. Group 1HU7 was hindlimb unloaded (HU) for 1 month, starting at 6-months-old. Recovery groups 1HU7+R1, 1HU7+R2, and 1HU7+R3 remained ambulatory for 1, 2, and 3 months after HU, respectively. The 1HU10 group experienced their first HU period and 2HU10 experienced their second HU period and were both sacrificed at 10 months. 1/2HU+R2 groups were allowed to recover for two months before being sacrificed.

The 1HU7 and recovery groups were used to examine the effects of a single HU bout and subsequent recovery. The 2HU10 and recovery groups were used to examine the effects of multiple bouts of HU and recovery. The 1HU10 and recovery groups were needed to detect whether changes occurring after the second HU bout were due to age or to multiple unloadings.

Details are provided in subsequent sections, with a brief overview of procedures outlined here. Once each of the animals was terminated, left femurs were excised and the distal metaphyseal region was scanned using a peripheral quantitative computed tomography (pQCT) scanner. After scanning, the whole bone was tested to failure by 3-point-bending, following which a 2 mm specimen was cut from the distal metaphysis. The sample from the distal metaphysis was tested in compression to estimate intrinsic material properties of the cancellous region following RPC testing procedures.

3.2 Harnessing and Hindlimb Unloading

Regardless of whether the animals were hindlimb unloaded at 6 or 9 months of age, the same harnessing procedure was followed. First, the rats were injected with 0.3 mL of a diluted atropine:saline (1:9) mixture to prepare them for anesthesia by minimizing fluid collection in airways. Then they were given a 0.3 mL dose of a Ketamine and DexaDomitor (3:2) cocktail to anesthetize them (25 mg/kg body weight). Once they were unconscious, their tails were scrubbed with a toothbrush and soapy water to remove dead tissue. Their tails were then dried using acetone and, once dry,

an adhesive spray was applied to the left and right sides of their tails. Harnesses fashioned from medical tape, bobby pins, and paper clips were then glued to their tails. To ensure that they did not dehydrate during harnessing, 1.5 mL of saline was administered subcutaneously. Once the glue dried and the harnesses were securely attached, they were awoken with a 0.1 mL shot of antisedan and then were placed in custom-built cages with harnesses attached to rods atop cages but with all limbs in contact with the floor. Twenty-four hours after they were harnessed, they were raised so that their hindlimbs could not touch the bottom of the cage to assure no weight-bearing by the hindlimbs. Daily health checks and cage cleaning were performed to ensure that the animals were in good condition and were not experiencing any undue stress. After 28 days (1 month), the animals were taken down and either terminated or allowed to recover in regular shoebox cages.

3.3 Ex Vivo *pQCT Scanning and Analysis*

Computed tomography is commonly used by physicians and researchers to examine what is happening inside the body. Using a series of X-ray images taken about an axis of rotation, it creates a two-dimensional slice (called a tomograph) of a volumetric region. Peripheral quantitative computed tomography (pQCT) scanners are commonly used to measure bone properties in peripheral sites of the body, such as the human forearm and rodent limbs.[40,41,42] A printout of how the densitometric data is organized and presented to the user can be found in the Appendix.

After the animals were sacrificed, femurs were excised, wrapped in gauze, and frozen in a vial filled with phosphate buffered saline (PBS) at -35˚F for storage. A peripheral quantitative computed tomography (pQCT) scanner (Norland Stratec XCT-Research M) belonging to Texas A&M University's Bone Biology Laboratory was used to obtain mineral and geometric data from the excised bones. Before scanning, the bones were taken out of their freezer and allowed to thaw. Left femurs were placed posterior-side up in a container filled with PBS to keep them hydrated during scanning. A scout scan was performed and the reference line was placed midway between the medial/lateral condyles and the intercondular fossa (Fig. 9). Four serial scan slices of 0.5 mm thickness were taken using a voxel resolution of 0.07 mm; the center of the slices were placed at distances of 3.5, 4.0, 4.5, and 5.0 mm proximal to the reference line, resulting in a total, continuous scanned length of 2 mm.

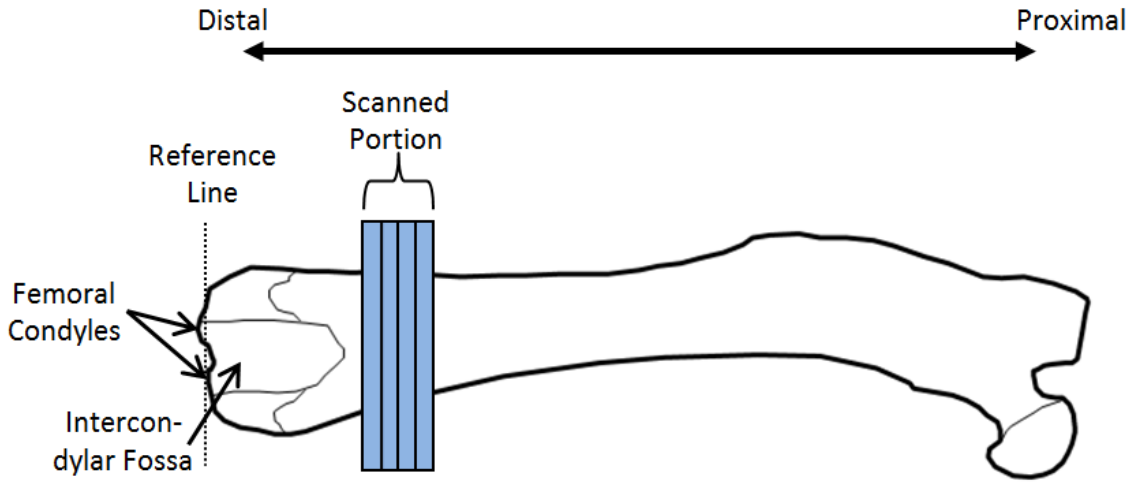

Fig. 9. Scan slice placement in the distal femur metaphysis. The reference line was placed mid-way between the intercondylar fossa and the medial/lateral condyles. The four scan slices have thicknesses of 0.5 mm and examine a section which is 3.25-5.25mm from the reference line.

After scanning, contour and peel algorithms provided by the Stratec XCT software (v6.00, Norland Corp., Fort Atkinson, WI) were selected to define the bone's outer edge and also determine the boundary between cortical and cancellous compartments (Fig. 10). Contour mode 3 was used, allowing the user to decide the BMD threshold which defines the periosteum. In this case, a BMD threshold of 450 mg/mm^3 was used; this value differentiates between the density of cortical bone and the surrounding water and was used to ensure that the precise definition of the periosteal edge was not compromised by partial volume effects (voxels along the periosteal edge which contain both bone and PBS). The peel algorithm determines the border separating cortical and cancellous regions and then "peels" the cancellous core away from the cortical shell, resulting in well-defined cancellous and cortical regions. This allows for separate analysis of the mineral and geometric properties of the cortical and cancellous regions, as well as the total (integral) bone, which includes both regions. Peel mode 4 was used with a user-defined threshold (800 mg/mm^3) and a 10% "scale-back factor" which ensures that highly dense cancellous bone is considered as such. Another algorithm was used to calculate the SSI, a predictor of bone strength[36], as well as other properties. For this algorithm, the same outer threshold of 450 mg/mm^3 was used.

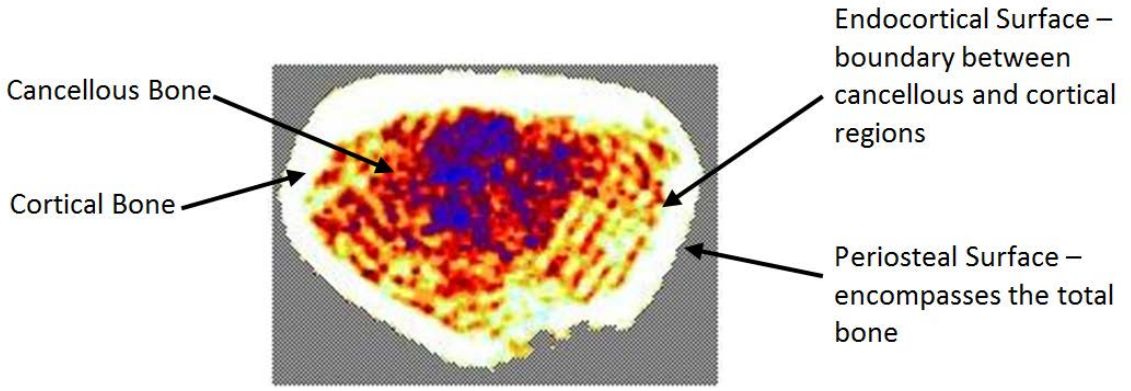

Fig. 10. pQCT cross-section of a distal femur metaphysis (annotations show important features). The periosteal surface defines the outer perimeter of the total (integral) bone, which includes the cancellous and cortical compartments. The endocortical surface separates the cortical from cancellous regions.

The outcome measures that were directly obtained from the pQCT software analysis are: total BMC, total vBMD, total area, cortical BMC, cortical vBMD, cortical area, cancellous BMC, cancellous vBMD, endocortical area (which is the area inside the cortical shell, where cancellous bone is located), SSI, and polar moment of inertia (I_P). Calculated measures that were derived from pQCT results are: cortical thickness, minimum and maximum moment of inertia (I_{MIN} and I_{MAX}), BSI, and total and cancellous CSI. Cancellous CSI uses the same formula as total CSI (Eq. 1), the only difference being that cancellous vBMD and minimum endocortical cross-sectional area are substituted for the total (integral) values. An average cortical thickness can be estimated by assuming that the cross-section is circular and subtracting the average radius of the cancellous region from the average radius of the total area (Eq. 8):

$$t_{cort} = r_{tot} - r_{canc} = \sqrt{\frac{A_{tot}}{\pi}} - \sqrt{\frac{A_{canc}}{\pi}} \quad (8)$$

Using relations derived from Mohr's circle, the maximum and minimum moments of inertia (Eqs. 9 and 10) were calculated.

$$I_{MAX} = \frac{I_X + I_Y}{2} + \sqrt{\left(\frac{I_X - I_Y}{2}\right)^2 + (I_{XY})^2} \quad (9)$$

$$I_{MIN} = \frac{I_X + I_Y}{2} - \sqrt{\left(\frac{I_X - I_Y}{2}\right)^2 + (I_{XY})^2} \quad (10)$$

These density-weighted moments of inertia will provide insight into changes in spatial distribution of the cross-section. I_{MAX} and I_{MIN} will be valuable because their changes will reflect how the geometry and bone mass are changing with respect to orthogonal axes that generally align with the medial-lateral (ML) axis and the anterior-posterior (AP) axis.

3.4 RPC Specimen Preparation & Platen Sizing

Before RPC testing took place, 3-point-bending was performed on the diaphysis of each left femur specimen; only the distal half of the femur was needed for RPC specimen collection. The diaphysis portion was clamped and fixed to a model 3242 Well Diamond Wire Saw with the metaphysis/epiphysis sticking out (Fig. 11). Diamond wire of 0.3 mm diameter was used to cut the RPC specimens. The first cut was made so that

the proximal side of the kerf was located exactly on the proximal apex of the anterior intercondylar fossa. A specimen cut from this location should ideally only contain secondary spongiosa. In fact, cuts at this location have been made in several other biomechanical studies examining the distal femur metaphysis.[26,35] Because a significant number of our HU specimens were predicted to have low BMD (relative to baseline and control animals), cutting at a more proximal location could potentially result in a large number of specimens being untestable due to the absence of cancellous bone. Once the first cut was made, the specimen was moved 2.3 mm in the proximal direction and a second cut (Fig. 12) was then made.

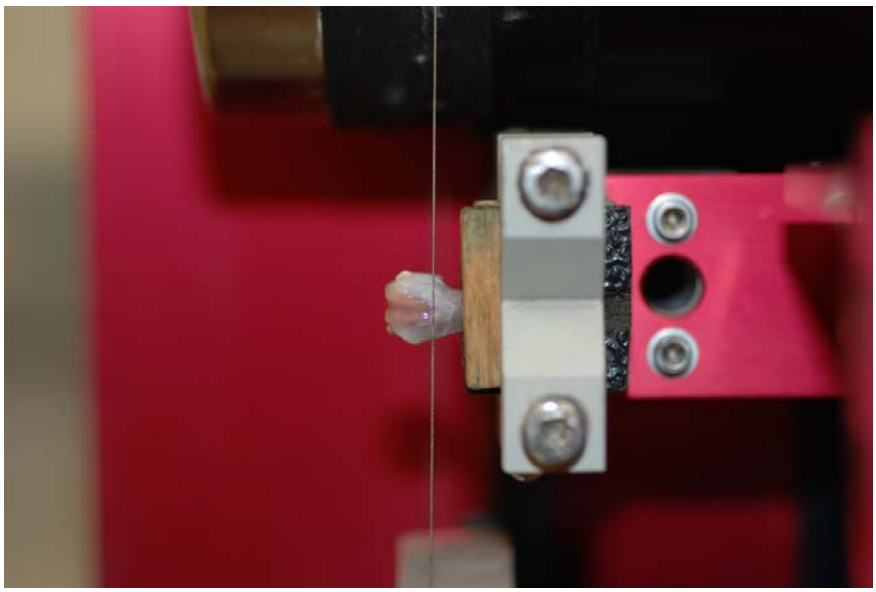

Fig. 11. Rat femur placement before RPC specimen cutting. The proximal portion of the bone is securely clamped in the fixture to prevent movement during cutting. Diamond wire is placed so that the first cut is made at the most distal peak of the intercondylar fossa.

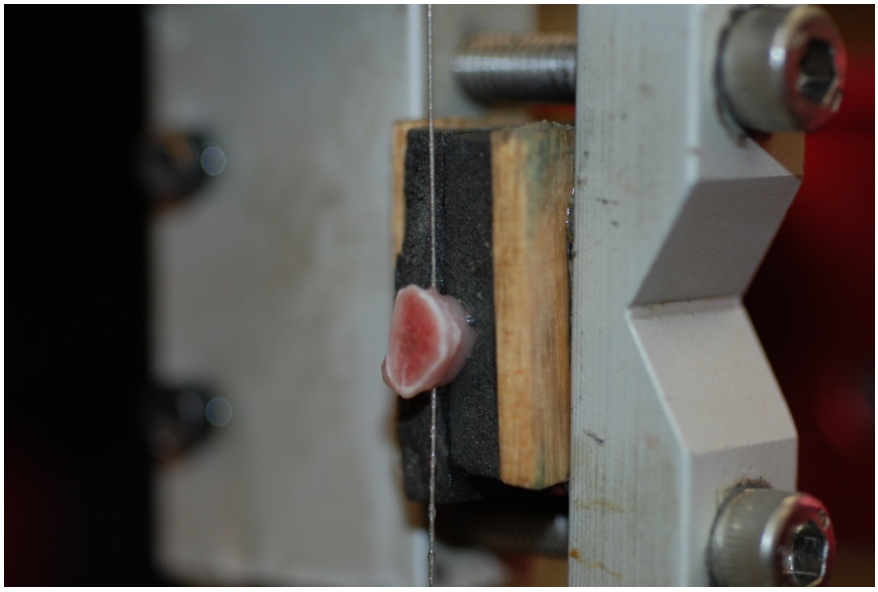

Fig. 12. Second cut being made to create the RPC specimen. The second cut was made proximal to the first cut. The nominal thickness of the specimen was 2 mm.

The proximal surface, which is the smaller of the two transverse surfaces, was then photographed next to a ruler and imported to Adobe Photoshop. Actual distances were converted from pixels using the ruler for scale. Using the Analysis Tool, the maximum endocortical diameter, or the largest circle that can be drawn inside the cancellous region, was measured and recorded. The endocortical diameter was multiplied by 0.7 (see Fig. 6); this was the optimal target, or desired, platen size. Platens were available in increments of 0.05 mm and the platen size closest to the target size was selected; this was the actual platen size. Actual platen sizes for the specimens in this study ranged from 1.45 mm to 2.25 mm. After photographing each specimen, they were wrapped in PBS-soaked gauze, cellophane, and aluminum foil. During this process, care was taken to ensure that no pressure was exerted on the cancellous surfaces.

3.5 RPC Mechanical Testing and Analysis

An Instron 3345 was used to perform the RPC tests. The 2-mm specimen was placed between two platens of previously determined size. The bottom platen was fixed to the base of the machine, making it stationary. The top platen was secured to the cross-head. Prior to testing each specimen, the platen positions were adjusted so that their transverse surfaces were aligned (Fig. 13).

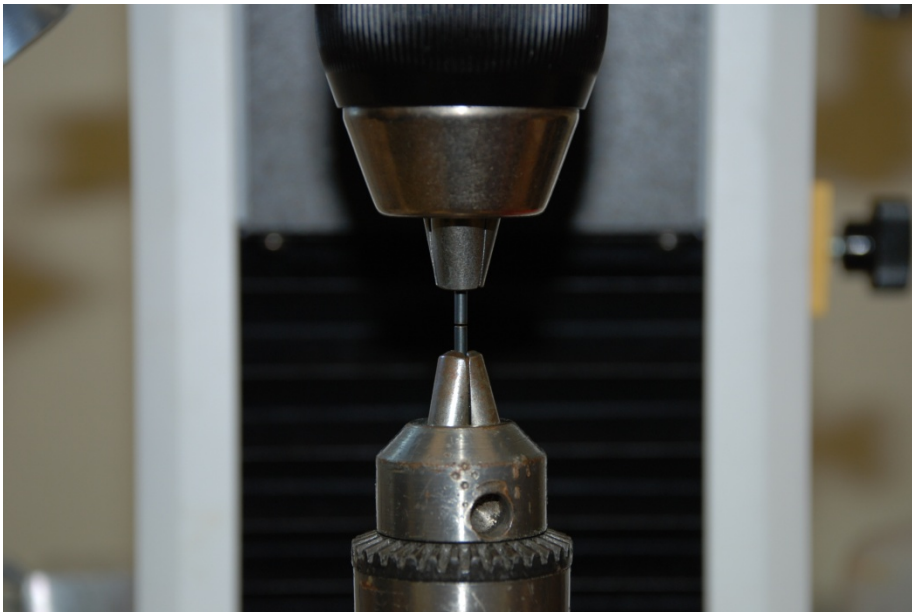

Fig. 13. Alignment of platens before RPC testing. To ensure that the cancellous region was purely in compression, platens of equal diameter were positioned coaxially with their transverse faces parallel to each other.

A 100 N Instron load cell was connected to the Instron 3345, which was connected to a PC via serial cable. The PC was running Instron's proprietary software, Bluehill (v2.14, Instron Bluehill). The specimen was placed with the larger, distal surface resting on the bottom platen. The top platen was then lowered until it was almost in

contact with the specimen. Having the platen so close to the surface made it possible to position the specimen so that the platens would be contacting the middle of the cancellous region. Once the specimen was properly positioned and the test was ready to begin (Fig. 14), the cross-head, with platen attached, was moved downward at a rate of 1.2 mm/min until a pre-load of 0.05 N was detected; this is when the Instron machine began recording force-displacement data. The cancellous region was compressed at a displacement rate of 0.25 mm/min. This value is well within the range of speeds usually used to test cancellous bone[27,31,32] and is commonly considered to be quasi-static loading. The displacement and corresponding compressive load were recorded by the PC at a rate of 20 Hz.

Fig. 14. An RPC test being performed. The bottom platen remains stationary while the top platen compresses the cancellous region at a rate of 0.25 mm/min.

The force, displacement, and stiffness data collected during the experiment are extrinsic (or structural) properties because they represent the response of the whole specimen. To estimate intrinsic, or "material" level, properties the extrinsic properties must be normalized to account for specimen size. Using the equations defined below, the following intrinsic properties were estimated stress (σ; Eq. 11), strain (ε_c, Eq. 12), and elastic modulus (E, Eq. 13). Engineering strain was calculated for the thickness deformation of the specimen.

$$\sigma = \frac{F_m}{A_{pl}} \tag{11}$$

$$\varepsilon_c = \frac{\Delta t}{t_0} = \frac{t_f - t_0}{t_0} \tag{12}$$

$$E = \frac{\sigma}{\varepsilon} = \frac{F_m t_0}{\Delta t A_{pl}} = \frac{k t_0}{A_{pl}} \tag{13}$$

where F_m is the measured force, A_{pl} is the cross-sectional area of the platen used, t_f is the final thickness of the compressed region, t_0 is the original thickness, Δt is the total compressive displacement, and k is the stiffness. Relevant intrinsic measures that were calculated from RPC mechanical testing are: ultimate stress, elastic modulus, energy to ultimate, ultimate strain, yield stress, energy to yield, and yield strain.

3.6 Data Analysis

The CT scans for all animals were printed out and examined and those scan slices that were determined to include the growth plate and primary spongiosa were

excluded. The analyzed CT data were then exported from the scanner and organized using Microsoft Excel. In most cases, 3 serial slices for each specimen were selected and their outcome measures were averaged together to give a single value.

An in-house MATLAB program was used to analyze raw data that was exported directly from the Instron machine. Once the user selected the specimen data to be analyzed, he/she is prompted to define the linear region. The slope of the linear region is the stiffness mentioned above and is used to calculate Elastic Modulus. The program then creates a linear function with the same y-intercept as the specified linear region but with 97% of its slope. The location where this function intersects the force-displacement data is determined to be the yield point. The ultimate point was simply the point of maximum force. Because of the complex structure of cancellous bone and the wide range of cancellous vBMD of test specimens, the point of failure was not always obvious. To maintain consistency, only one person examined the RPC force-displacment plots and identified the point at which failure occurred, being as consistent as possible across all specimens. The groups to which each specimen belonged were intentionally hidden during analysis in order to eliminate bias.

SigmaStat 3.5 software was used for all statistical analysis. Unpaired *t*-tests were performed on absolute raw values for each variable to determine differences between groups. Statistically significant differences were for p-values < 0.05. All values are expressed as mean ± SE (standard error of the mean).

4. RESULTS

Throughout the experiment, the body weights of the animals were recorded weekly (Fig. 15). These data are relevant to the effects of hindlimb unloading, especially as a possible indicator of animal stress levels. Despite being considered adult and skeletally mature, animals generally gained weight over the 6 month (24 week) duration of the study. Note in particular the mean values for the aging control (AC) group, which increase from 440g to 540g. The effects of HU are also evident as animal weights decrease slightly during the first week of HU (less than 10%) and then recover gradually. No drastic weight losses occurred of the magnitude that would be considered to be excessively stressful on the animals.[5]

Mineral, geometric, and strength data were obtained from the metaphyseal region of the left distal femur. The right distal femur was used for gene expression analysis and was, therefore, not available for pQCT scanning or mechanical testing. It should be noted that there are multiple ways to categorize recovery: relative to baseline (BL6), relative to age-matched AC groups, and relative to post-HU value for those groups that are allowed to resume normal loading. A group is deemed to be "fully recovered" if the outcome variable of interest for it and for a reference group are determined to be not significantly different ($p<0.05$) by an unpaired *t*-test. Information in the graphs will be presented as the percent difference relative to baseline.

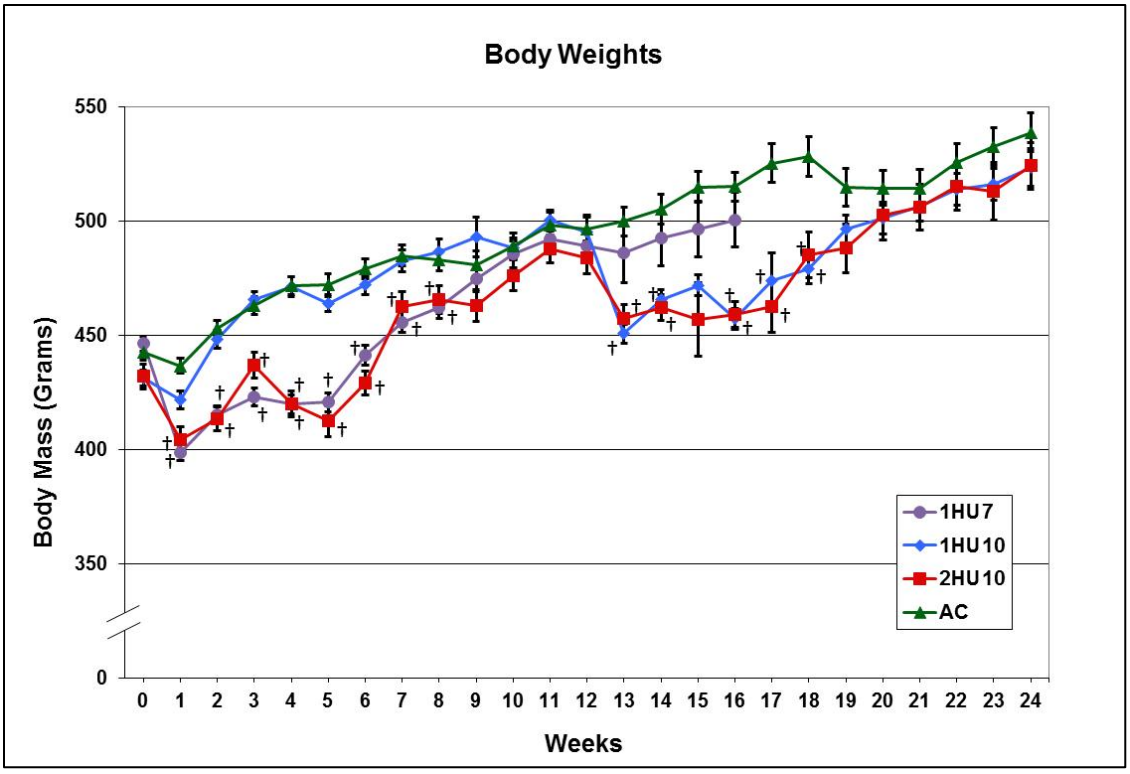

Fig. 15. Body weights for all groups beginning at 6 months of age (Week 0). All rats were weighed once a week until they were sacrificed.
Values are presented as mean ± SE.
† Indicates significant difference from age-matched control value at same time point; p<0.05, ANOVA.

In the following sections (4.1-4.4), data organized in tables are given in absolute numbers with native units while plots are shown as percent change from the baseline value. This should present a clear view of the actual and relative changes occurring during HU and recovery.

4.1 Densitometric Properties

Bone mass parameters (summarized in Table 1) were obtained through the use of pQCT scanning at the distal femur metaphysis. The specific densitometric variables

that were examined are: total vBMD (Fig. 16), cancellous vBMD (Fig. 17), cortical vBMD (Fig. 18), total BMC (Fig. 19), cancellous BMC (Fig. 20), and cortical BMC (Fig. 21). A common feature is that the initial HU (at 6 months) had detrimental effects on the mineral properties of both cortical and cancellous bone tissue, and the negative effects persisted at least for the first recovery period (1HU7+R1). That is, for all variables except cancellous BMC, the values for 1HU7 and 1HU7+R1 are both significantly different from baseline (BL6) and also from age-matched controls (AC7 and AC8, respectively). Cancellous BMC values are significantly lower than aging controls (both AC7 and AC8) but not different from BL6. Reductions from baseline due to the first HU (1HU7) were most dramatic for cancellous vBMD (-16.4%, p=.001), followed by total vBMD (-12.6%, p<.001). The variables least affected by the first HU were cortical vBMD (-2.9%, p<.001) and cancellous BMC (-4.1%, p=.538).

Recovery can be defined or considered in at least three ways in these studies. For each end point following an HU bout, recovery can be evaluated by comparing: a) to the pre-HU value, b) to the corresponding age-matched control value, or c) to the immediate, previous post-HU value (for those that are allowed to resume normal loading). In the first two cases, a lack of statistically significant differences would indicate “full” or “complete” recovery, whereas for the third case “significant” recovery could be considered to occur when a significant difference is reached. As mentioned previously, losses persisted for the first month following the 1HU7 bout, with no recovery for any variables. After a second recovery period (1HU7+R2), however, all

vBMD variables recovered fully, at least relative to age matched controls (AC9). Although the relative losses were mildest for cortical vBMD, this variable recovered completely by all three definitions. Both Total BMC and Cortical BMC were equivalent to BL6 (no significant differences) after two months of weight-bearing recovery; after another month of ambulation, these variables had recovered in terms of all three definitions.

Decreases resulting from the second HU period (2HU10) were not as dramatic as those seen during the first (1HU7), and cancellous BMC even increased slightly, although not significantly. In general, the age-matched, single-HU group (1HU10) showed losses similar to 2HU10, at least relative to pre-HU values. However, their absolute values were higher than those of 2HU10 in most cases. The recovery characteristics were generally similar for both 1HU10 and 2HU10 groups and they were also less complete than the 1HU7 recovery. However, the 2HU10 group tended to have slightly more complete recoveries relative to its pre-HU values, particularly for cortical bone. There were also no significant differences between the 1HU10+R2 and 2HU10+R2 groups.

Table 1. Mineral properties for cortical, cancellous, and total (integral) bone

	Total BMC (mg/mm)	Total vBMD (mg/cm^3)	Cancellous BMC (mg/mm)	Cancellous vBMD (mg/cm^3)	Cortical BMC (mg/mm)	Cortical vBMD (mg/cm^3)
6 Months Old						
BL6	12.15 (0.28)	656.4 (7.9)	3.64 (0.17)	338.0 (10.6)	8.51 (0.17)	1076.7 (5.7)
7 Month Old						
AC7	12.95 (0.28)	653.6 (11.4)	4.04 (0.19)	349.9 (15.8)	8.91 (0.14)	1067.1 (4.4)
1HU7	11.29 (0.20) *†	573.9 (9.9) *†	3.49 (0.17) †	282.4 (11.8) *†	7.80 (0.13) *†	1045.6 (6.0) *†
8 Months Old						
AC8	12.68 (0.30)	629.8 (10.4) *	4.09 (0.23)	333.6 (14.4)	8.59 (0.15)	1069.3 (6.5)
1HU7+R1	11.10 (0.17) *†	561.3 (8.1) *†	3.49 (0.15) †	277.7 (12.0) *†	7.60 (0.17) *†	1043.8 (6.2) *†
9 Months Old						
AC9	12.51 (0.21)	622.8 (11.6) *	3.73 (0.12)	311.2 (11.5)	8.78 (0.14)	1077.1 (4.9)
1HU7+R2	11.69 (0.22) †	596.3 (11.2) *	3.57 (0.18)	294.9 (12.4) *	8.12 (0.15) †	1065.8 (6.8) ◊
10 Months Old						
AC10	12.31 (0.21)	609.6 (11.8) *	3.64 (0.14)	297.3 (9.0) *	8.67 (0.15)	1075.5 (7.8)
1HU7+R3	12.52 (0.28) ◊	617.5 (11.9) *◊	3.85 (0.14)	314.5 (12.0)	8.67 (0.19) ◊	1073.8 (4.1) ◊
1HU10	11.98 (0.15) #	572.8 (9.0) *†#	3.53 (0.12)	269.2 (7.0) *†#	8.45 (0.14) ¤	1063.8 (7.6) ¤
2HU10	11.47 (0.22) †‡	555.2 (8.1) *†#‡	3.72 (0.14)	279.2 (5.4) *‡	7.75 (0.17) *†‡¤	1037.5 (8.2) *†#‡¤
12 Months Old						
AC12	12.75 (0.24)	610.0 (7.6) *	3.72 (0.20)	290.5 (12.4) *	9.03 (0.14) *	1091.7 (7.0)
1HU10+R2	12.45 (0.23)	574.4 (6.0) *†#	3.82 (0.17)	278.6 (7.9) *#	8.63 (0.16)	1062.6 (5.9) †
2HU10+R2	12.02 (0.25) †	576.3 (5.7) *†◊	3.63 (0.18)	276.6 (8.1) *	8.39 (0.15) †◊	1066.2 (6.2) †◊

Values are presented as mean ± SE.

*** Indicates significant difference from baseline value; p<0.05, unpaired t-test.**

† Indicates significant difference from age-matched control value at same time point; p<0.05, unpaired t-test.

 # Indicates significant difference from month 9 pre-HU value within same group (i.e. 1HU10(+R2) or 2HU10+(R2)); p<0.05, unpaired t-test.

◊ Indicates significant difference from immediate preceding post-HU value within same group; p<0.05, unpaired t-t est.

‡ Indicates significant difference between 1HU7+R3 and 2HU10; p<0.05, unpaired t-test.

¤ Indicates significant difference between 1HU10 and 2HU10 at the same time point; p<0.05, unpaired t-test.

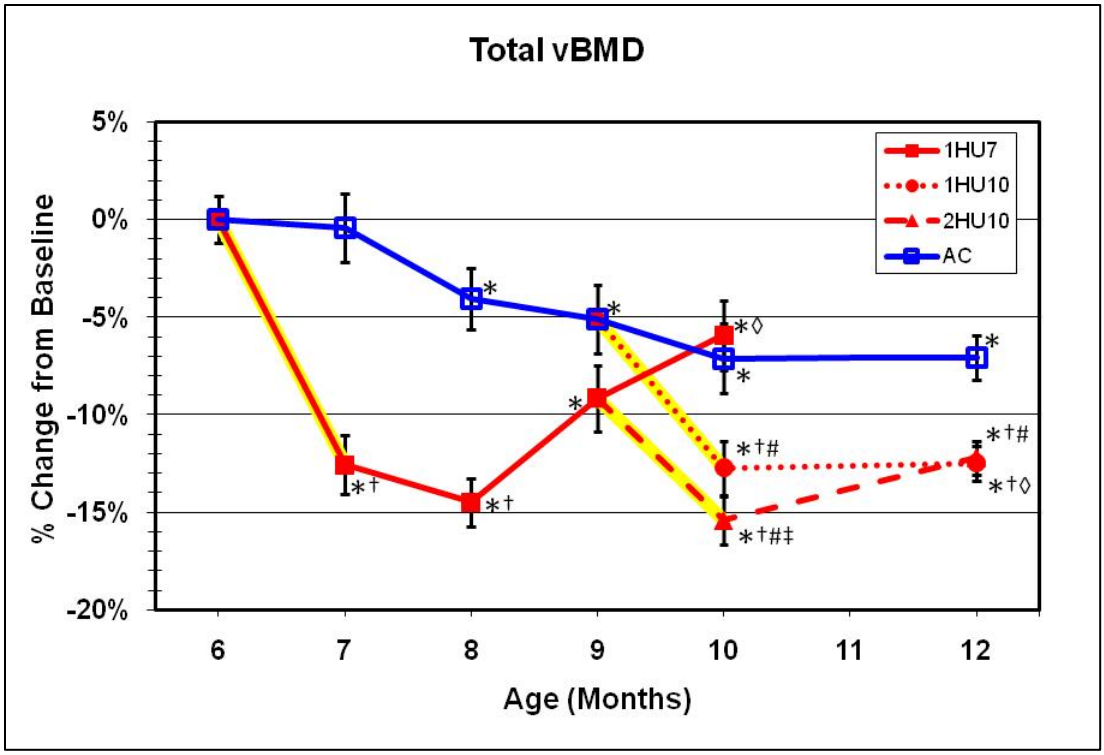

Fig. 16. Changes in total vBMD of the distal femur metaphysis as a result of hindlimb unloading and ambulatory recovery. Yellow highlighting indicates periods of HU. Numerical values for total vBMD are contained in Table 1. 1HU7 lost 12.6% from its pre-HU value (p<.001) and 1HU7+R1 continued to lose BMD, resulting in a value 10.9% lower than AC8 (p=.006). The gradual decline of the AC groups indicates bone loss due to aging. The recovery for 1HU7, however, does not follow the same downward trend as the control animals, showing that unloading-induced losses are reversible. Losses for both HU bouts starting at 9 months were significant (post-HU vs. pre-HU) but milder than the losses for the 6 to 7 month HU. The decline was 6.9% for 2HU10 (p=.005) and 8.0% for 1HU10 (p=.002). 2HU10+R2 was 3.8% higher than 2HU10 (p=.041) but was still 5.5% lower than AC12 (p=.001). There was no significant recovery for 1HU10.

Values are presented as mean ± SE.

*** Indicates significant difference from baseline value; p<0.05, unpaired t-test.**

† Indicates significant difference from age-matched control value at same time point; p<0.05, unpaired t-test.

 # Indicates significant difference from month 9 pre-HU value within same group (i.e. 1HU10(+R2) or 2HU10+(R2)); p<0.05, unpaired t-test.

◊ Indicates significant difference from immediate preceding post-HU value within same group; p<0.05, unpaired t-t est.

‡ Indicates significant difference between 1HU7+R3 and 2HU10; p<0.05, unpaired t-test.

¤ Indicates significant difference between 1HU10 and 2HU10 at the same time point; p<0.05, unpaired t-test.

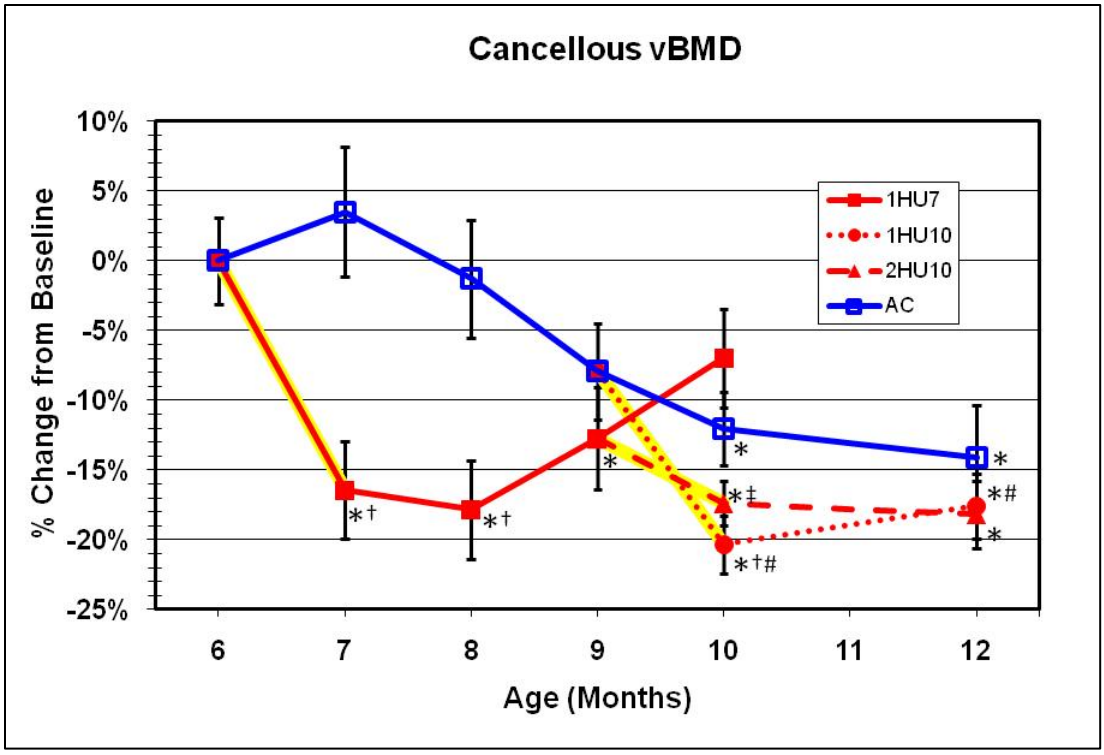

Fig. 17. Changes in cancellous vBMD of the distal femur metaphysis as a result of hindlimb unloading and ambulatory recovery. Yellow highlighting indicates periods of HU. Numerical values for cancellous vBMD are contained in Table 1. 1HU7 was 16.4% less than BL6 (p=.001) and 19.3% less than AC7 (p=.002). Age-related declines for controls (AC) are rather substantial after 7 months of age. Recovery relative to controls occurred at month 9 (p=.344) and recovery relative to BL6 occurred at month 10 (p=.262). The second HU period was detrimental to recovery following the first HU, as 2HU10 was 11.2% lower than the 1HU7+R3 group (p=.009). Losses for 2HU10 were -5.3% compared to the pre-HU group (p=.247), but losses relative to the pre-HU group for the 1HU10 bout were much greater (-13.5%) and significantly different (p=.003). Recovery for both HU10 groups was incomplete to non-existent relative to immediate post-HU values, but at 12 months both recovery groups were very similar to the aging control (AC12).

Values are presented as mean ± SE.

*** Indicates significant difference from baseline value; p<0.05, unpaired t-test.**

† Indicates significant difference from age-matched control value at same time point; p<0.05, unpaired t-test.

 # Indicates significant difference from month 9 pre-HU value within same group (i.e. 1HU10(+R2) or 2HU10+(R2)); p<0.05, unpaired t-test.

◊ Indicates significant difference from immediate preceding post-HU value within same group; p<0.05, unpaired t-t est.

‡ Indicates significant difference between 1HU7+R3 and 2HU10; p<0.05, unpaired t-test.

¤ Indicates significant difference between 1HU10 and 2HU10 at the same time point; p<0.05, unpaired t-test.

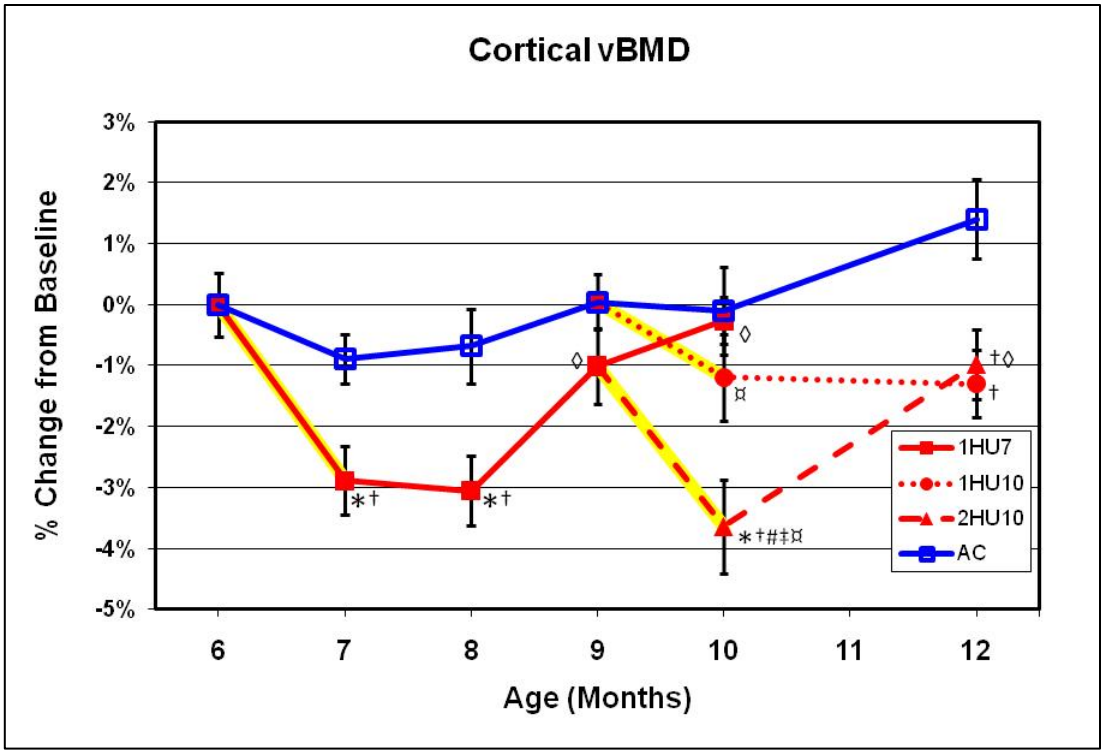

Fig. 18. Changes in cortical vBMD of the distal femur metaphysis as a result of hindlimb unloading (HU) and ambulatory recovery. Yellow highlighting indicates periods of HU. Numerical values for cortical vBMD are contained in Table 1. 1HU7 was 2.9% below BL and recovery was suppressed for 1 month thereafter, ultimately reaching BL6 and aging control values at months 9 and 10. The 2HU10 group experienced an absolute loss just slightly less than that of the first HU (2.6% vs. 2.9%, respectively), but the reduction due to 1HU10 was insignificant (p=.172). There was substantial recovery following 2HU10 resulting in nearly identical values at 12 months (1HU10+R2 and 2HU10+R2). Neither were significantly different from BL6 at this point, but both were significantly lower than corresponding age-matched controls (AC12).

Values are presented as mean ± SE.

*** Indicates significant difference from baseline value; p<0.05, unpaired t-test.**

† Indicates significant difference from age-matched control value at same time point; p<0.05, unpaired t-test.

 # Indicates significant difference from month 9 pre-HU value within same group (i.e. 1HU10(+R2) or 2HU10+(R2)); p<0.05, unpaired t-test.

◊ Indicates significant difference from immediate preceding post-HU value within same group; p<0.05, unpaired t-t est.

‡ Indicates significant difference between 1HU7+R3 and 2HU10; p<0.05, unpaired t-test.

¤ Indicates significant difference between 1HU10 and 2HU10 at the same time point; p<0.05, unpaired t-test.

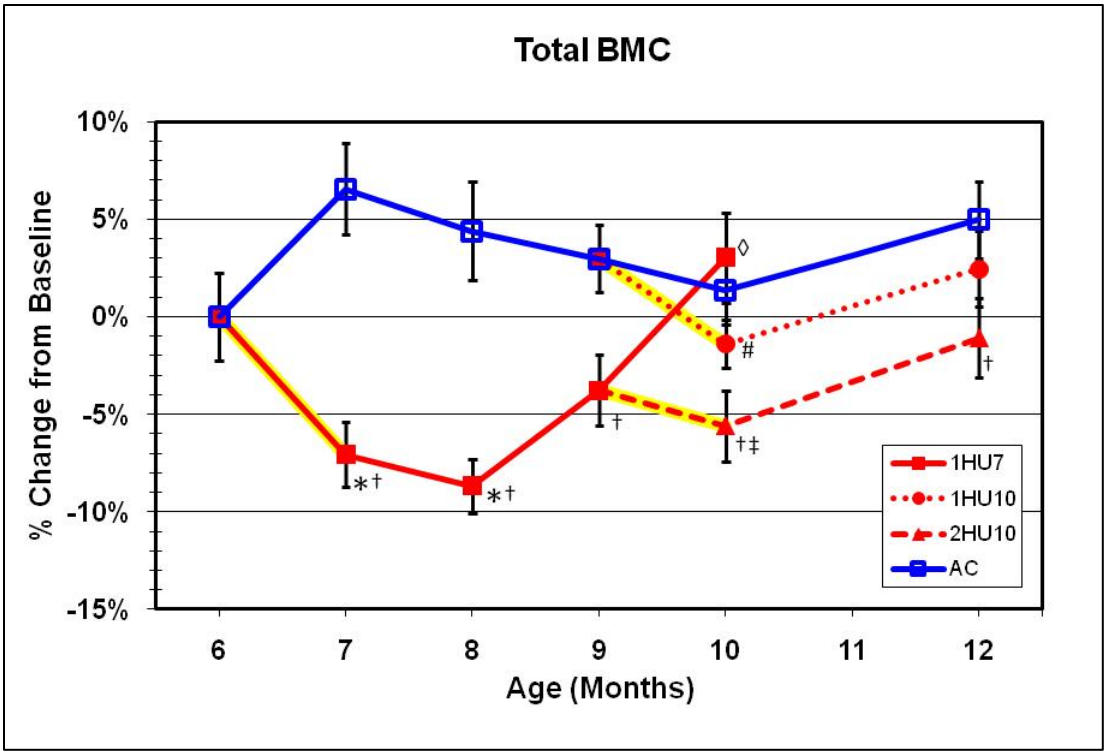

Fig. 19. Changes in total BMC of the distal femur metaphysis as a result of hindlimb unloading (HU) and ambulatory recovery. Yellow highlighting indicates periods of HU. Numerical values for total BMC are contained in Table 1. Total BMC was reduced by 7.1% relative to BL6 during the HU bout between months 6 and 7 (p=.017) and dropped another 1.6% during the first recovery period (p=.006). The difference relative to age-matched controls for 1HU7 was more substantial, however, with a mean value 12.8% lower than AC7 (p<.001). The 1HU7+R2 group recovered to be not different from BL6 (p=.228), although the mean was still 3.8% lower. Following another month of loading, the 1HU7+R3 group became similar to the AC10 group (p=.560). The 2HU10 and 1HU10 groups experienced decreases of 1.9% (p=.482) and 4.2% (p=.043) relative to their pre-HU values. Recovery following both HU10 bouts was similar.

Values are presented as mean ± SE.

*** Indicates significant difference from baseline value; p<0.05, unpaired t-test.**

† Indicates significant difference from age-matched control value at same time point; p<0.05, unpaired t-test.

 # Indicates significant difference from month 9 pre-HU value within same group (i.e. 1HU10(+R2) or 2HU10+(R2)); p<0.05, unpaired t-test.

◊ Indicates significant difference from immediate preceding post-HU value within same group; p<0.05, unpaired t-t est.

‡ Indicates significant difference between 1HU7+R3 and 2HU10; p<0.05, unpaired t-test.

¤ Indicates significant difference between 1HU10 and 2HU10 at the same time point; p<0.05, unpaired t-test.

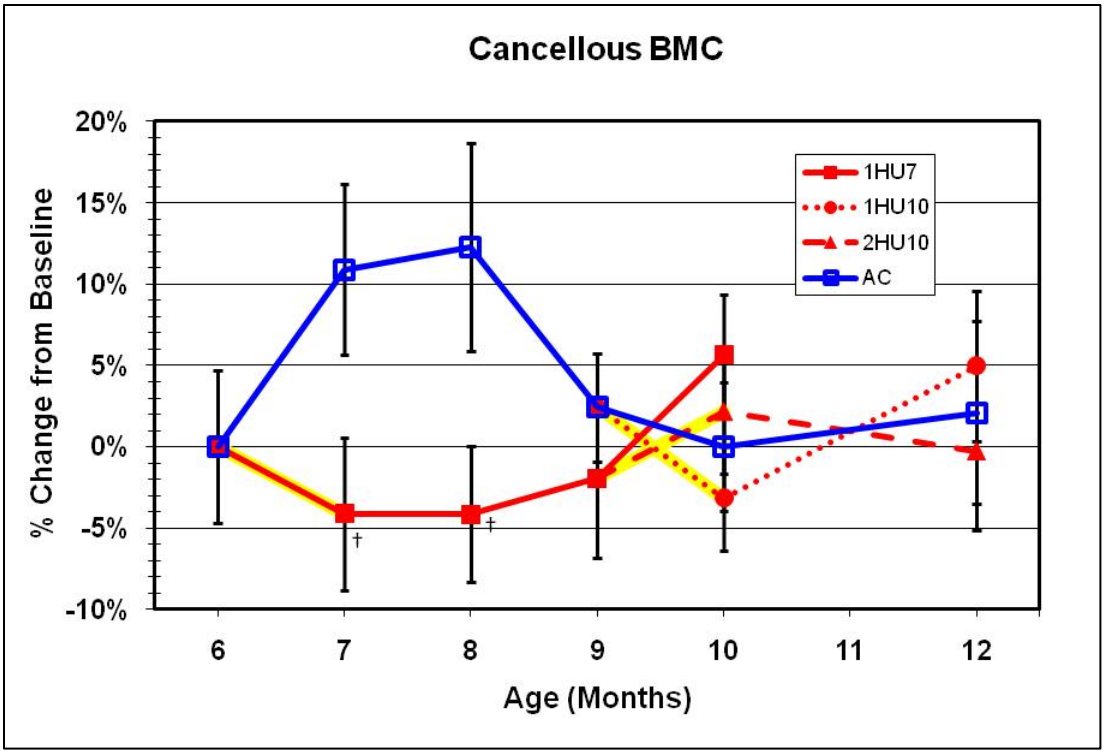

Fig. 20. Changes in cancellous BMC of the distal femur metaphysis as a result of hindlimb unloading (HU) and ambulatory recovery. Yellow highlighting indicates periods of HU. Numerical values for cancellous BMC are contained in Table 1. Cancellous BMC experienced a slight decline during the first HU but was not significantly different from BL6. Variability was highest for this outcome variable, so there are only two cases of statistically significant differences. Specifically, the 1HU7 and 1HU7+R1 groups were significantly different from their age-matched control groups by -13.5% (p=.040) and -14.6% (p=.044), respectively.

Values are presented as mean ± SE.

*** Indicates significant difference from baseline value; p<0.05, unpaired t-test.**

† Indicates significant difference from age-matched control value at same time point; p<0.05, unpaired t-test.

 # Indicates significant difference from month 9 pre-HU value within same group (i.e. 1HU10(+R2) or 2HU10+(R2)); p<0.05, unpaired t-test.

◊ Indicates significant difference from immediate preceding post-HU value within same group; p<0.05, unpaired t-t est.

‡ Indicates significant difference between 1HU7+R3 and 2HU10; p<0.05, unpaired t-test.

¤ Indicates significant difference between 1HU10 and 2HU10 at the same time point; p<0.05, unpaired t-test.

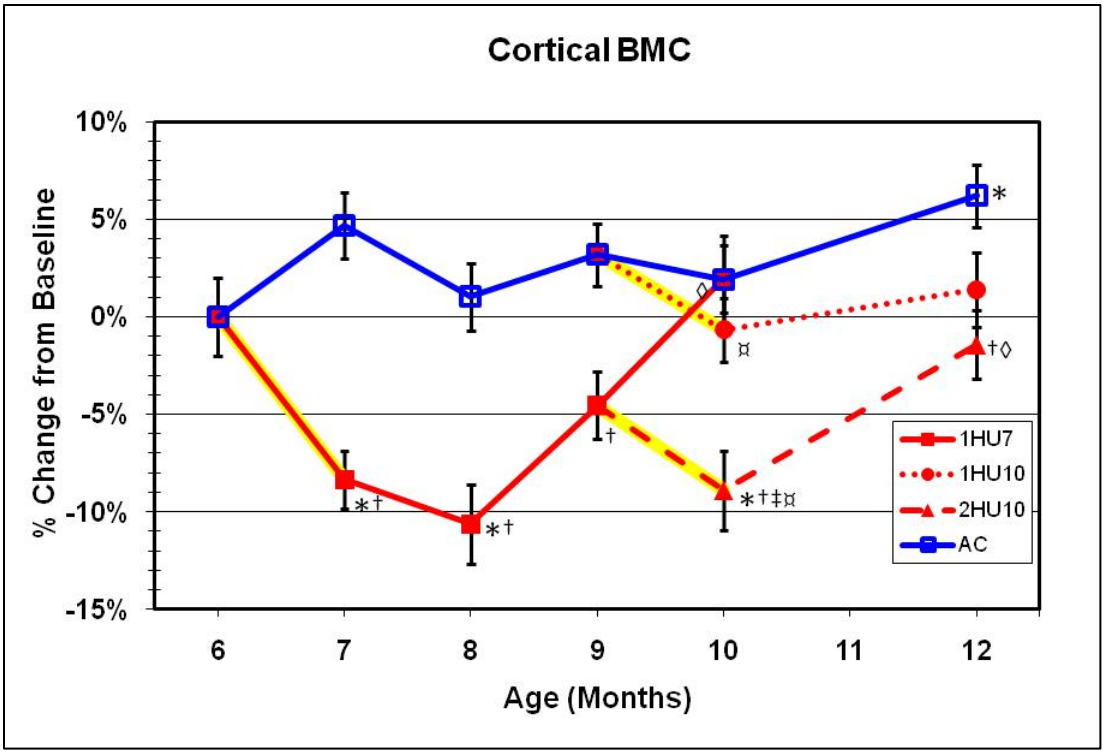

Fig. 21. Changes in cortical BMC of the distal femur metaphysis as a result of hindlimb unloading (HU) and ambulatory recovery. Yellow highlighting indicates periods of HU. Numerical values for cortical BMC are contained in Table 1. Cortical BMC dropped 8.3% relative to BL6 (p=.002) during the initial HU and dropped a further 2.3% during the first month of ambulation (p=.001). Full recovery relative to both HU and BL6 did not occur until after 3 months of ambulation. No significant losses were observed for either HU bout at 9 months (1HU10 or 2HU10). Values are presented as mean ± SE.

*** Indicates significant difference from baseline value; p<0.05, unpaired t-test.**

† Indicates significant difference from age-matched control value at same time point; p<0.05, unpaired t-test.

 # Indicates significant difference from month 9 pre-HU value within same group (i.e. 1HU10(+R2) or 2HU10+(R2)); p<0.05, unpaired t-test.

◊ Indicates significant difference from immediate preceding post-HU value within same group; p<0.05, unpaired t-t est.

‡ Indicates significant difference between 1HU7+R3 and 2HU10; p<0.05, unpaired t-test.

¤ Indicates significant difference between 1HU10 and 2HU10 at the same time point; p<0.05, unpaired t-test.

4.2 Geometric Properties

Cross-sectional geometry and related properties (Table 2) were also obtained from pQCT scans of the distal femur metaphysis.. Total area (Fig. 22) trended upward throughout the experiment for all groups, indicating periosteal apposition. Recall that total area is simply the area enclosed by the outer perimeter of the bone. Increased

total area was most evident during the first month for both aging controls and HU animals (1HU7). There was also a trend toward increased periosteal apposition for both of the HU bouts that started at 9 months. However, unloading per se did not have a statistically significant effect on total area, as none of the HU or reloaded groups differed significantly from the controls. Considering endocortical area (Fig. 23), cortical area (Fig. 24), and cortical thickness (Fig. 25), it is apparent that endocortical resorption was accelerated by HU, as evidenced by increases in endocortical area. However, the differences between groups within time points disappeared 1-2 months after the HU bouts ended. Cortical area decreased 5.8% between baseline and 1HU7 ($p=.020$), which gave rise to a decrease in cortical thickness of 10.2% ($p<.001$). Animals that were unloaded starting at 9 months (1HU10 and 2HU10) also lost cortical area over the period of HU (2.7% and 2.1%, respectively), but the differences were not statistically significant. The corresponding reductions in cortical thickness, however, were indeed statistically significant and roughly twice as high at 5.4% ($p=.008$) for 1HU10 and 5.5% ($p=.02$) for 2HU10. Taken together, these results clearly indicate that bone was lost more extensively at the endocortical surface than it was being deposited on the expanding periosteal surface during HU exposure.

Considering the recovery periods following HU bouts, there was very little change or response during recovery for total area and endocortical area. For cortical area and cortical thickness, however, reductions due to the first HU (1HU7) persisted

and even worsened slightly during the first month of recovery. For the second and third recovery periods (ending at 9 and 10 months), both cortical area and cortical thickness increased significantly to return to aging control levels (AC10). This indicates that recovery of the cortical bone compartment was explained by gain of bone at the periosteal surface.

Post hoc analysis showed that the principle axes for I_{MAX} (Fig. 26) and I_{MIN} (Fig. 27) are oriented predominantly in the anterior-posterior and medial-lateral directions, respectively. None of the moment of inertia measures exhibited any significant differences comparing post-HU values to pre-HU values, although there were differences between aging controls and post-HU animals at 7 and 8 months for I_{MAX} and I_P (Fig. 28). Exposure to HU had no appreciable effects on these moment of inertia measures when it was performed at the older stage (9 months).

Table 2. Geometric properties for cortical, cancellous, and total (integral) bone

	Total Area (mm^2)	Endocortical Area (mm^2)	Cortical Area (mm^2)	Cortical Thickness (μm)	I_{MAX} (mm^4)	I_{MIN} (mm^4)	I_P (mm^4)
6 Months Old							
BL6	18.54 (0.42)	10.64 (0.31)	7.90 (0.16)	589.8 (8.6)	31.37 (1.23)	15.80 (0.74)	47.17 (1.92)
7 Month Old							
AC7	19.85 (0.34) *	11.5 (0.27) *	8.35 (0.14) *	600.9 (8.7)	35.53 (1.16) *	17.57 (0.56)	53.10 (1.63) *
1HU7	19.73 (0.28) *	12.28 (0.27) *†	7.45 (0.10) *†	529.8 (7.9) *†	29.99 (0.85) †	16.96 (0.45)	46.94 (1.24) †
8 Months Old							
AC8	20.18 (0.41) *	12.14 (0.33) *	8.04 (0.14)	569.3 (7.7)	35.45 (1.27) *	17.75 (0.69)	53.21 (1.86) *
1HU7+R1	19.82 (0.38) *	12.54 (0.28) *	7.28 (0.15) *†	513.8 (7.9) *†	29.80 (0.89) †	16.84 (0.63)	46.64 (1.48) †
9 Months Old							
AC9	20.16 (0.36) *	12.01 (0.30) *	8.15 (0.12)	578.5 (7.2)	35.37 (0.92) *	17.72 (0.55)	53.09 (1.43) *
1HU7+R2	19.68 (0.40)	12.07 (0.34) *	7.62 (0.12) †	544.2 (8.4) *†	32.22 (1.09) †	16.66 (0.56)	48.89 (1.60)
10 Months Old							
AC10	20.29 (0.47) *	12.24 (0.42) *	8.06 (0.12)	569.7 (8.9)	34.30 (1.16)	18.29 (0.73) *	52.59 (1.82)
1HU7+R3	20.32 (0.35) *	12.13 (0.28) *	8.08 (0.17) ◊	569.5 (10.7) ◊	34.89 (1.13) ◊	18.08 (0.62) *	52.97 (1.68) *◊
1HU10	21.00 (0.30) *	12.07 (0.29) *#	7.93 (0.10) ¤	547.3 (8.0) *#¤	35.20 (0.76) *¤	18.40 (0.44) *	53.60 (1.08) *
2HU10	20.73 (0.41) *	12.21 (0.36) *#‡	7.46 (0.13) *†‡¤	514.4 (8.6) *†#‡¤	32.50 (1.00) ¤	17.66 (0.67)	50.17 (1.63)
12 Months Old							
AC12	20.94 (0.36) *	12.67 (0.31) *	8.27 (0.11)	574.5 (6.7)	38.36 (1.01) *	18.80 (0.61) *	57.16 (1.57) *
1HU10+R2	21.71 (0.41) *#	11.86 (0.33) *#	8.11 (0.13)	549.0 (7.7) *†#	38.19 (1.33) *	19.77 (0.68) *#	57.97 (1.94) *
2HU10+R2	20.88 (0.41) *#	12.13 (0.33) *	7.86 (0.13) †◊	543.1 (6.8) *†◊	34.93 (1.20) *†	18.63 (0.65) *#	53.55 (1.80) *

Values are presented as mean ± SE.

*** Indicates significant difference from baseline value; p<0.05, unpaired t-test.**

† Indicates significant difference from age-matched control value at same time point; p<0.05, unpaired t-test.

 # Indicates significant difference from month 9 pre-HU value within same group (i.e. 1HU10(+R2) or 2HU10+(R2)); p<0.05, unpaired t-test.

◊ Indicates significant difference from immediate preceding post-HU value within same group; p<0.05, unpaired t-t est.

‡ Indicates significant difference between 1HU7+R3 and 2HU10; p<0.05, unpaired t-test.

¤ Indicates significant difference between 1HU10 and 2HU10 at the same time point; p<0.05, unpaired t-test.

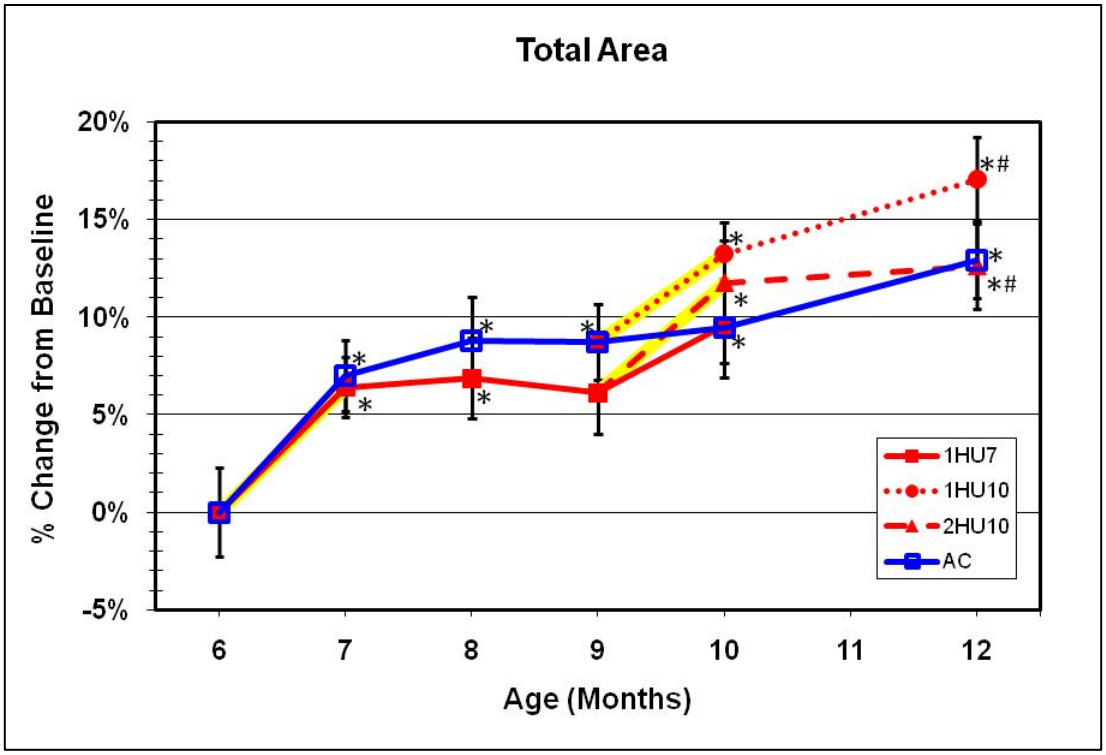

Fig. 22. Changes in total area of the distal femur metaphysis as a result of hindlimb unloading (HU) and ambulatory recovery. Yellow highlighting indicates periods of HU. Numerical values for total area are contained in Table 2. HU did not seem to have a dramatic effect, as there were no significant differences between groups within time points. For the HU bout that started at 6 months (1HU7), the post-HU values were significantly higher than baseline (BL6) but this change was almost identical to that for the aging controls (AC7). The effects of both HU bouts started at 9 months (1HU10 and 2HU10) suggest a trend toward higher values, but the post-HU values were not significantly different from the pre-HU values. The noticeable upward trend shows that bone was being deposited on the periosteal surface.

Values are presented as mean ± SE.

*** Indicates significant difference from baseline value; p<0.05, unpaired t-test.**

† Indicates significant difference from age-matched control value at same time point; p<0.05, unpaired t-test.

 # Indicates significant difference from month 9 pre-HU value within same group (i.e. 1HU10(+R2) or 2HU10+(R2)); p<0.05, unpaired t-test.

◊ Indicates significant difference from immediate preceding post-HU value within same group; p<0.05, unpaired t-t est.

‡ Indicates significant difference between 1HU7+R3 and 2HU10; p<0.05, unpaired t-test.

¤ Indicates significant difference between 1HU10 and 2HU10 at the same time point; p<0.05, unpaired t-test.

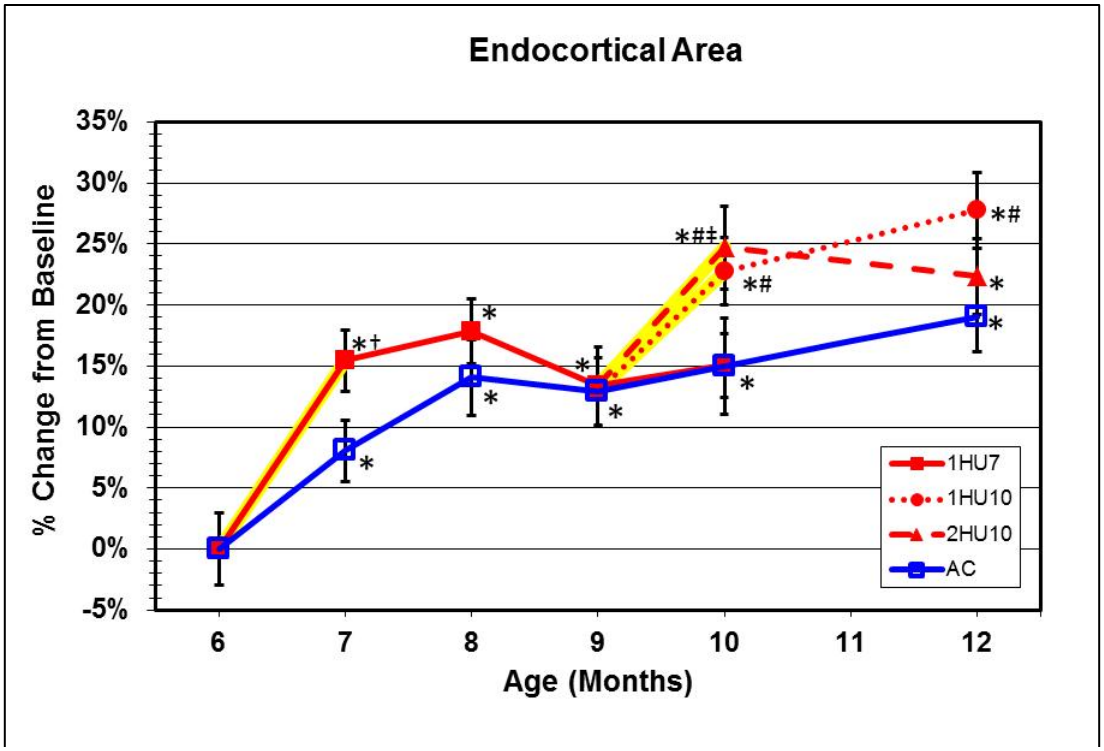

Fig. 23. Changes in endocortical area of the distal femur metaphysis as a result of hindlimb unloading (HU) and ambulatory recovery. Yellow highlighting indicates periods of HU. Numerical values for endocortical area are contained in Table 2. All groups exhibited an upward trend, indicating endocortical resorption, but all three HU bouts induced significantly more expansion of the cancellous compartment. The extent of increase in endocortical area due to HU (from pre-HU values) was 15.4% (p<.001) for 1HU7, 10.0% (p=.022) for 2HU10, and 8.7% (p=.018) for 1HU10. 1HU7 values were 6.8% higher than AC7 (p=.046), the only occasion where significant differences occurred relative to control groups.

Values are presented as mean ± SE.

*** Indicates significant difference from baseline value; p<0.05, unpaired t-test.**

† Indicates significant difference from age-matched control value at same time point; p<0.05, unpaired t-test.

 # Indicates significant difference from month 9 pre-HU value within same group (i.e. 1HU10(+R2) or 2HU10+(R2)); p<0.05, unpaired t-test.

◊ Indicates significant difference from immediate preceding post-HU value within same group; p<0.05, unpaired t-t est.

‡ Indicates significant difference between 1HU7+R3 and 2HU10; p<0.05, unpaired t-test.

¤ Indicates significant difference between 1HU10 and 2HU10 at the same time point; p<0.05, unpaired t-test.

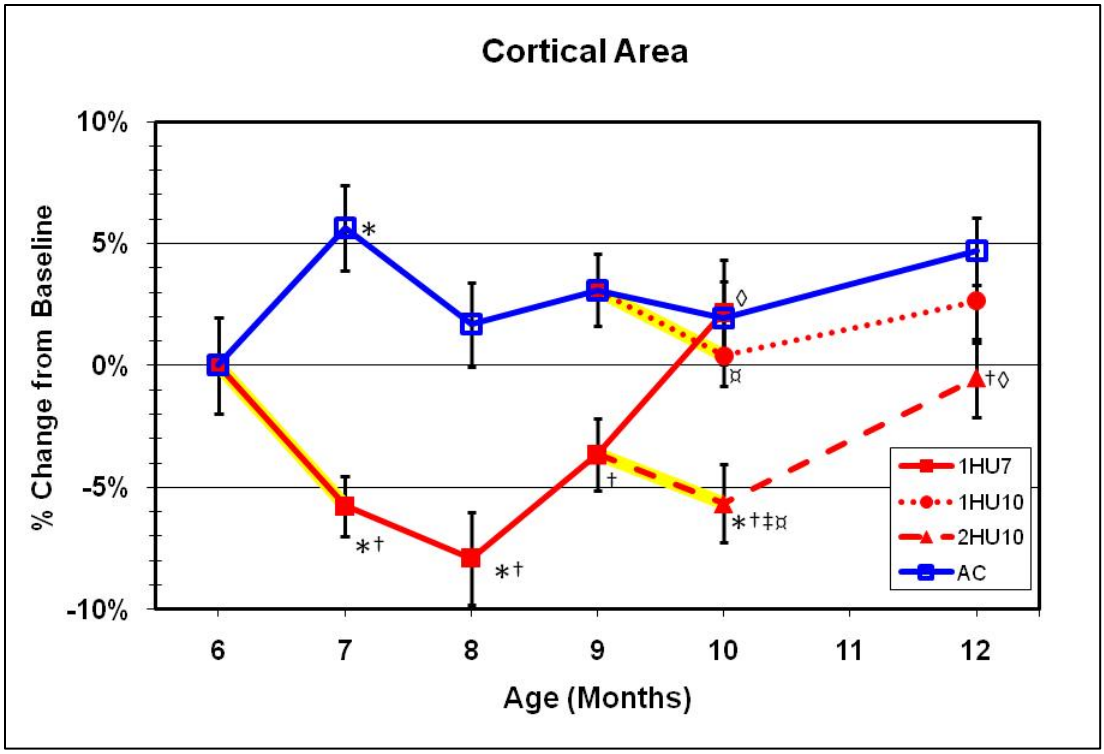

Fig. 24. Changes in cortical area of the distal femur metaphysis as a result of hindlimb unloading (HU) and ambulatory recovery. Yellow highlighting indicates periods of HU. Numerical values for cortical area are contained in Table 2.The initial HU caused a 5.8% decline relative to baseline (BL6) (p=.020), and this recovered to be insignificantly different from BL6 at 9 months, although still significantly lower than age-matched controls (AC9). After three recovery periods, cortical area fully recovered to both BL6 and aging control (AC10) levels. Both HU bouts that started at 9 months (1HU10 and 2HU10) induced reductions (2.7% and 2.1%, resp.) but the post-HU values were not significantly different from pre-HU values.

Values are presented as mean ± SE.

*** Indicates significant difference from baseline value; p<0.05, unpaired t-test.**

† Indicates significant difference from age-matched control value at same time point; p<0.05, unpaired t-test.

 # Indicates significant difference from month 9 pre-HU value within same group (i.e. 1HU10(+R2) or 2HU10+(R2)); p<0.05, unpaired t-test.

◊ Indicates significant difference from immediate preceding post-HU value within same group; p<0.05, unpaired t-t est.

‡ Indicates significant difference between 1HU7+R3 and 2HU10; p<0.05, unpaired t-test.

¤ Indicates significant difference between 1HU10 and 2HU10 at the same time point; p<0.05, unpaired t-test.

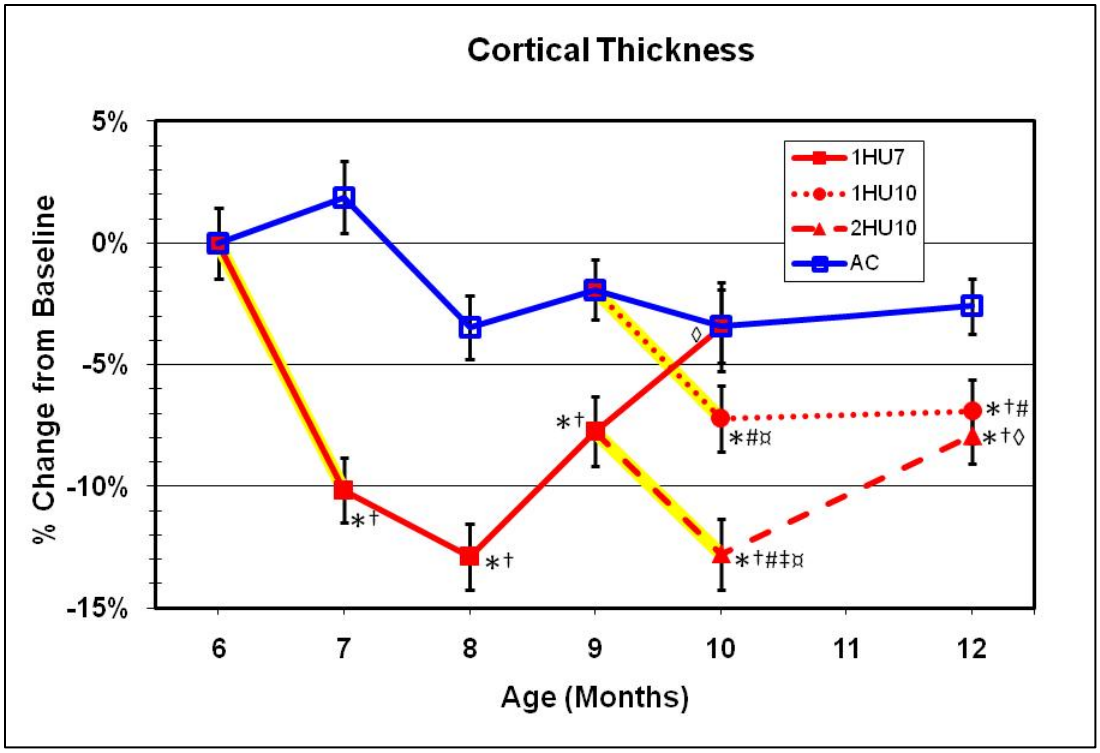

Fig. 25. Changes in average thickness of the cortical shell of the distal femur metaphysis as a result of hindlimb unloading (HU) and ambulatory recovery. Yellow highlighting indicates periods of HU. Numerical values for cortical thickness are contained in Table 2. Substantial thinning occurred as a result of HU, with 1HU7, 2HU10, and 1HU10 losing 10.2% (p<.001), 5.5% (p=.020), and 5.4% (p=.008), respectively, of their pre-HU values. Full recovery to control values required 3 months of ambulation after the initial HU. Neither of the two groups that completed unloading at 10 months (1HU10 and 2HU10) and were allowed to reload fully recovered relative to aging controls (AC12).

Values are presented as mean ± SE.

*** Indicates significant difference from baseline value; p<0.05, unpaired t-test.**

† Indicates significant difference from age-matched control value at same time point; p<0.05, unpaired t-test.

 # Indicates significant difference from month 9 pre-HU value within same group (i.e. 1HU10(+R2) or 2HU10+(R2)); p<0.05, unpaired t-test.

◊ Indicates significant difference from immediate preceding post-HU value within same group; p<0.05, unpaired t-t est.

‡ Indicates significant difference between 1HU7+R3 and 2HU10; p<0.05, unpaired t-test.

¤ Indicates significant difference between 1HU10 and 2HU10 at the same time point; p<0.05, unpaired t-test.

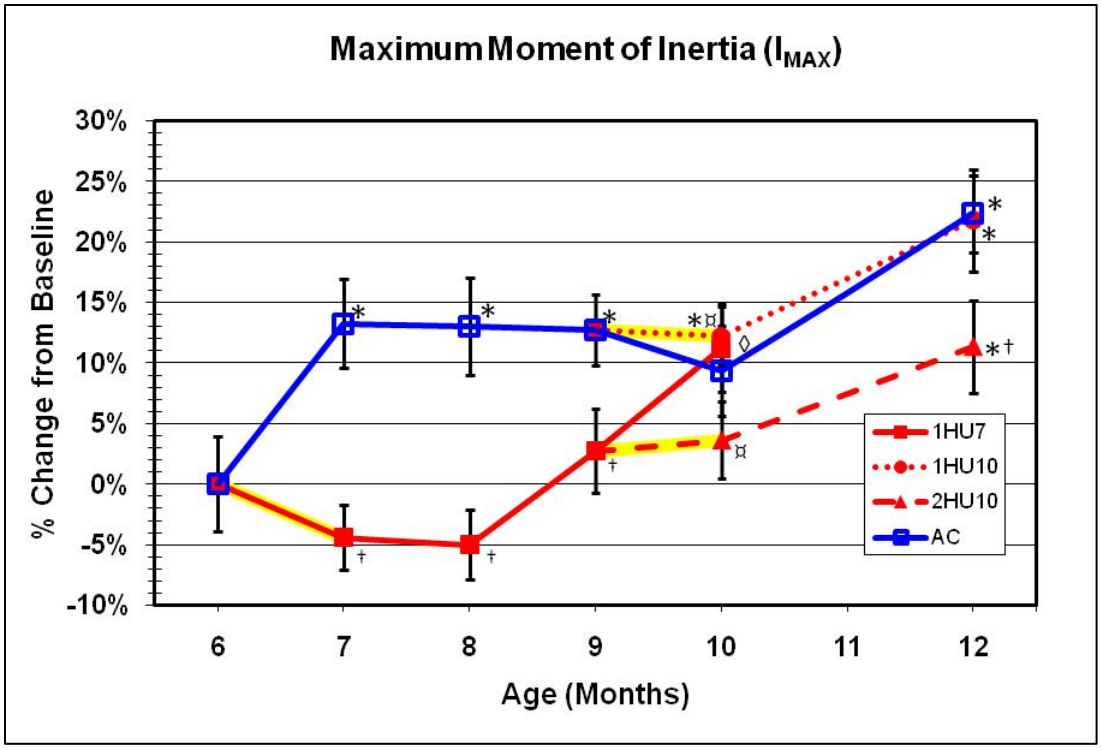

Fig. 26. Changes in the maximum moment of inertia (I_{MAX}) of the total cross-section of the distal femur metaphysis as a result of hindlimb unloading (HU) and ambulatory recovery. Yellow highlighting indicates periods of HU. Numerical values for I_{MAX} are contained in Table 2. This variable corresponds to the moment of inertia about an axis that runs approximately in the anterior-posterior direction. Results are quite similar to those for the I_P (Fig. 26). The initial HU (1HU7) prevented the increase exhibited by the aging controls over the same time period. AC7 was 13.3% higher than BL6 (p=.019), and 1HU7 was 15.6% lower than AC7 (p<.001). During the first recovery period following 1HU7, values remained significantly lower than aging controls. Values for 1HU7+R2 were 8.9% lower than age-matched controls (AC9) (p=.036), but recovery subsequently ensued, with 1HU7+R3 values returning fully to aging controls (AC10). Neither of the HU bouts that started at 9 months had much effect relative to pre-HU values or relative to aging controls. For recovery from 10 to 12 months, all three applicable groups (AC, 1HU10, 2HU10) tended to increase, but changes were not statistically significant.

Values are presented as mean ± SE.

*** Indicates significant difference from baseline value; p<0.05, unpaired t-test.**

† Indicates significant difference from age-matched control value at same time point; p<0.05, unpaired t-test.

 # Indicates significant difference from month 9 pre-HU value within same group (i.e. 1HU10(+R2) or 2HU10+(R2)); p<0.05, unpaired t-test.

◊ Indicates significant difference from immediate preceding post-HU value within same group; p<0.05, unpaired t-t est.

‡ Indicates significant difference between 1HU7+R3 and 2HU10; p<0.05, unpaired t-test.

¤ Indicates significant difference between 1HU10 and 2HU10 at the same time point; p<0.05, unpaired t-test.

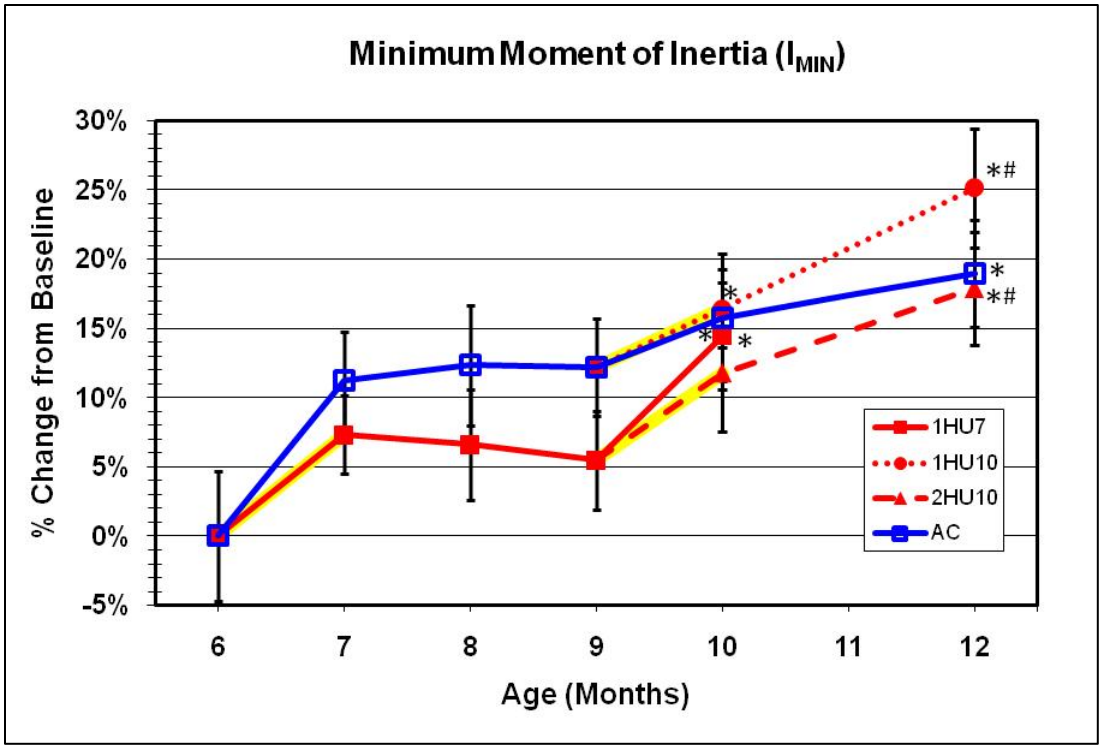

Fig. 27. Changes in the minimum moment of inertia (I_{MIN}) of the total cross-section of the distal femur metaphysis as a result of hindlimb unloading (HU) and ambulatory recovery. Yellow highlighting indicates periods of HU. Numerical values for I_{MIN} are contained in Table 2. This variable corresponds to the moment of inertia about an axis that runs approximately in the medial-lateral direction. Results are much different than those for the I_P (Fig. 26) and the I_{MAX} (Fig. 27). The increase in I_{MIN} from month 6 to 7 for the aging controls was indeed similar (11.2% here vs. 12.6% for I_P and 13.3% for I_{MAX}), but the response due to HU was quite different and distinct for I_{MIN}. Specifically, I_{MIN} increased for 1HU7 by 7.3% (p=.195) compared to slight decreases for I_P (-0.5%) and I_{MAX} (-4.4%). Based on the trends in the data, these results suggest that the changes giving rise to the differences between aging controls and HU exposed animals (1HU7) for I_P are due predominately to changes in the medial and/or lateral regions of the cross-section and not in the anterior or posterior regions. As with the I_P and I_{MAX}, the HU bouts starting at 9 months had little effect on I_{MIN}.

Values are presented as mean ± SE.

*** Indicates significant difference from baseline value; p<0.05, unpaired t-test.**

† Indicates significant difference from age-matched control value at same time point; p<0.05, unpaired t-test.

 # Indicates significant difference from month 9 pre-HU value within same group (i.e. 1HU10(+R2) or 2HU10+(R2)); p<0.05, unpaired t-test.

◊ Indicates significant difference from immediate preceding post-HU value within same group; p<0.05, unpaired t-t est.

‡ Indicates significant difference between 1HU7+R3 and 2HU10; p<0.05, unpaired t-test.

¤ Indicates significant difference between 1HU10 and 2HU10 at the same time point; p<0.05, unpaired t-test.

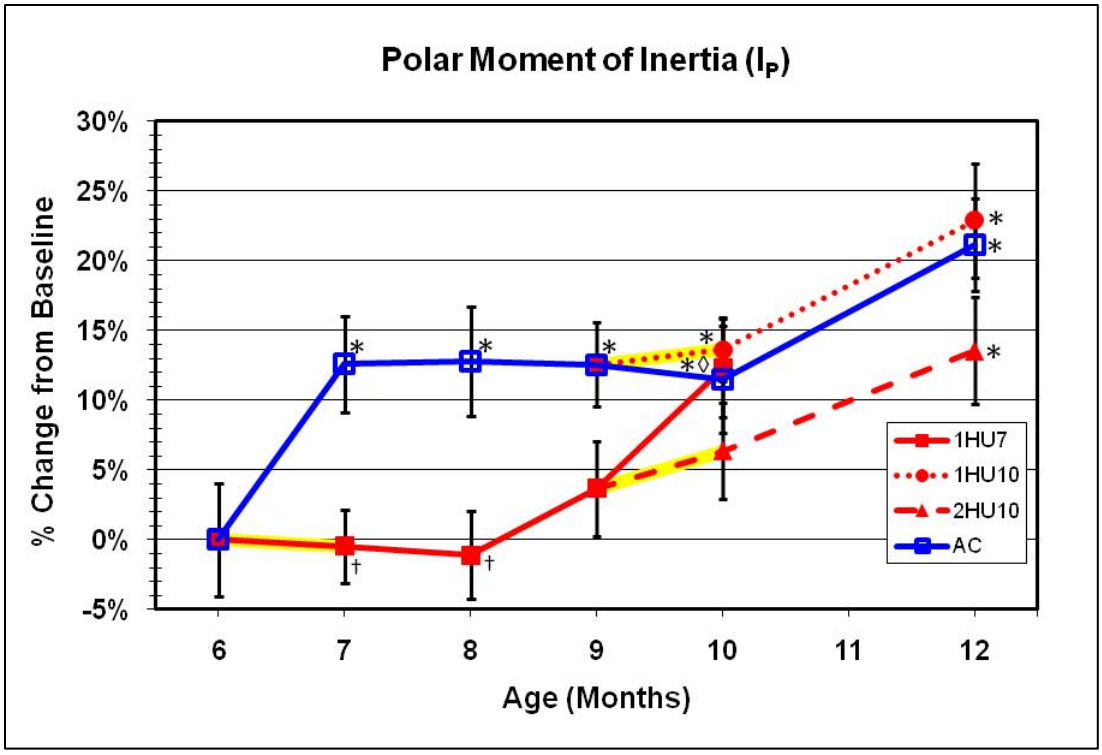

Fig. 28. Changes in polar moment of inertia (I_P) of the total cross-section of the distal femur metaphysis as a result of hindlimb unloading (HU) and ambulatory recovery. Yellow highlighting indicates periods of HU. Numerical values for I_P are contained in Table 2. Effects of the initial HU (1HU7) were to prevent the increase exhibited by the aging controls over the same time period. The mean for AC7 was 12.6% (p=.025) higher than BL6, and the mean for 1HU7 was 11.6% lower than AC7 (p=.005). During the first recovery period following 1HU7, values remained significantly lower than aging controls, but recovery ensued subsequently. Values for 1HU7+R2 were 7.9% lower than age-matched controls (AC9) (p=.060), an insignificant difference. After one more recovery period, 1HU7+R3 values returned fully to aging controls (AC10). Neither of the HU bouts that started at 9 months had much effect relative to pre-HU values or aging controls. All three applicable groups (AC12, 1HU10, 2HU10) tended to increase during recovery from 10 to 12 months, but changes were not statistically significant.
Values are presented as mean ± SE.
*** Indicates significant difference from baseline value; p<0.05, unpaired t-test.**
† Indicates significant difference from age-matched control value at same time point; p<0.05, unpaired t-test.
 # Indicates significant difference from month 9 pre-HU value within same group (i.e. 1HU10(+R2) or 2HU10+(R2)); p<0.05, unpaired t-test.
◊ Indicates significant difference from immediate preceding post-HU value within same group; p<0.05, unpaired t-t est.
‡ Indicates significant difference between 1HU7+R3 and 2HU10; p<0.05, unpaired t-test.
¤ Indicates significant difference between 1HU10 and 2HU10 at the same time point; p<0.05, unpaired t-test.

4.3 pQCT-Derived Strength Indices

Estimated, or calculated, strength indices (Table 3) were derived from data gathered from pQCT scans at the distal femur metaphysis. SSI (Fig. 29) was

automatically calculated by the scanning software while total CSI (Fig. 30), cancellous CSI (Fig. 31), and BSI (Fig. 32) were calculated using the relations described in Section 2.6. The response patterns for SSI and BSI track similarly to I_P and I_{MAX}: small losses for HU bouts relative to pre-HU values and age-related gains seen in aging controls were suppressed, but after 3 months of recovery there is essentially no difference between reloaded and control groups. The differences between pre- and post-HU values were not significantly different but both the first and second unloading bouts (groups 1HU7 and 2HU10, respectively) were significantly different from their ambulatory counterparts. The second HU served to again suppress growth.

In contrast, both total CSI and cancellous CSI exhibited substantial declines due to HU, especially for the initial HU bout that started at 6 months (1HU7), and both also recovered markedly from 8 to 10 months. Total CSI dramatically decreased in the 1HU7 group (-18.1%, $p<.001$) but recovered to BL6 and AC within 3 months of ambulation. Cancellous CSI declined 18.6% ($p=.074$) and thus behaved similarly to total CSI; however, the unloaded and recovery groups were not significantly different than baseline (except for 1HU10). An increase in the AC7 group is observed, with subsequent declines thereafter. The 1HU7 and 1HU7+R1 groups were significantly different from their corresponding AC group but not the baseline group. Other groups were all similar to their corresponding AC groups.

Table 3. Calculated strength indices for total and cancellous bone

	SSI (mm^3)	BSI (mm^3)	Total CSI (mg^2/mm^4)	Cancellous CSI (mg^2/mm^4)
6 Months Old				
BL6	14.77 (0.46)	2.386 (0.064)	7.52 (0.22)	1.13 (0.08)
7 Month Old				
AC7	16.23 (0.38) *	2.586 (0.056) *	8.03 (0.28)	1.31 (0.10)
1HU7	14.65 (0.27) †	2.249 (0.046) †	6.16 (0.19) *†	0.92 (0.08) †
8 Months Old				
AC8	16.18 (0.43) *	2.581 (0.059) *	7.59 (0.27)	1.27 (0.13)
1HU7+R1	14.65 (0.34) †	2.251 (0.060) †	5.96 (0.15) *†	0.91 (0.08) †
9 Months Old				
AC9	16.23 (0.34) *	2.616 (0.053) *	7.39 (0.22)	1.06 (0.07)
1HU7+R2	15.18 (0.36) †	2.420 (0.057) †◊	6.65 (0.21) *†	0.98 (0.08)
10 Months Old				
AC10	16.07 (0.48)	2.585 (0.061) *	7.23 (0.22)	1.02 (0.07)
1HU7+R3	16.23 (0.39) *◊	2.628 (0.059) *◊	7.37 (0.28) ◊	1.12 (0.08)
1HU10	16.09 (0.25) *¤	2.555 (0.044) *¤	6.57 (0.15) *†#	0.88 (0.06) *#
2HU10	15.12 (0.40) ¤	2.319 (0.061) †‡¤	6.13 (0.18) *†‡	0.97 (0.06)
12 Months Old				
AC12	16.96 (0.35) *	2.849 (0.048) *	7.39 (0.20)	1.01 (0.09)
1HU10+R2	17.12 (0.46) *	2.755 (0.072) *◊	6.84 (0.19) *	1.00 (0.08)
2HU10+R2	16.18 (0.41) *	2.608 (0.063) *†#◊	6.66 (0.18) *†◊	0.96 (0.08)

Values are presented as mean ± SE.

*** Indicates significant difference from baseline value; p<0.05, unpaired t-test.**

† Indicates significant difference from age-matched control value at same time point; p<0.05, unpaired t-test.

 # Indicates significant difference from month 9 pre-HU value within same group (i.e. 1HU10(+R2) or 2HU10+(R2)); p<0.05, unpaired t-test.

◊ Indicates significant difference from immediate preceding post-HU value within same group; p<0.05, unpaired t-t est.

‡ Indicates significant difference between 1HU7+R3 and 2HU10; p<0.05, unpaired t-test.

¤ Indicates significant difference between 1HU10 and 2HU10 at the same time point; p<0.05, unpaired t-test.

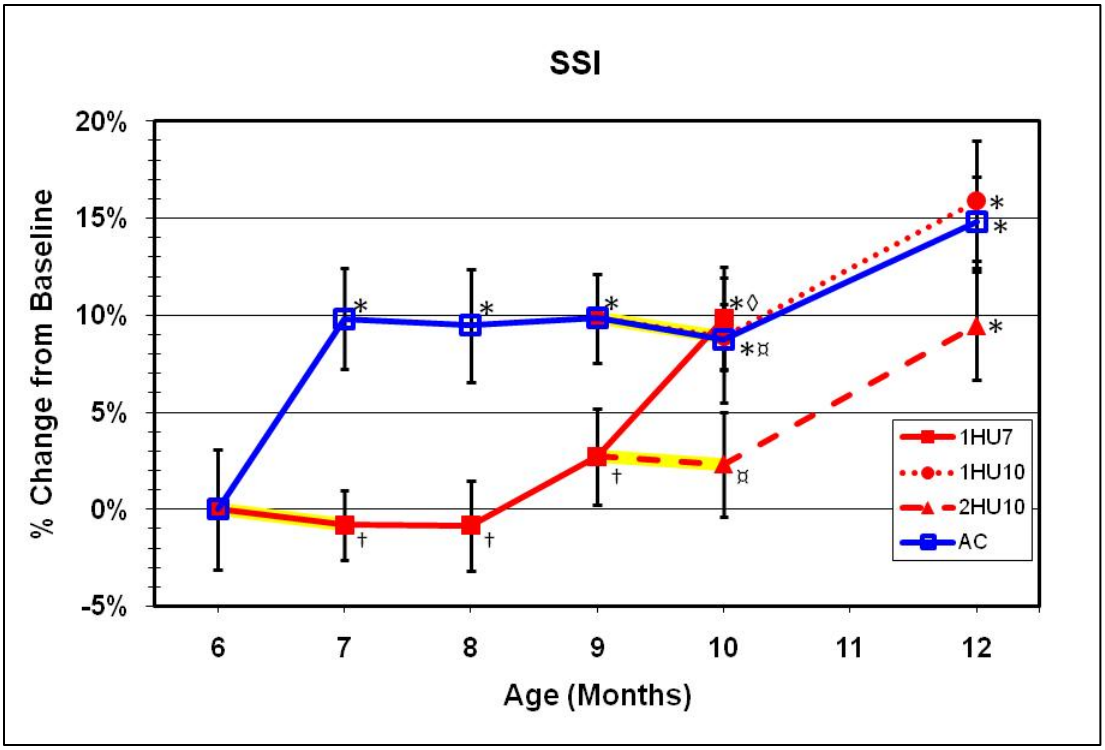

Fig. 29. Changes in the stress-strain index (SSI) of the distal femur metaphysis as a result of hindlimb unloading (HU) and ambulatory recovery. Yellow highlighting indicates periods of HU. Numerical values for SSI are contained in Table 3. The results are similar to the polar moment of inertia (I_P), and this is not surprising since I_P is used directly in calculating SSI. The main effect of the initial HU (1HU7) was to suppress the increase exhibited by the aging controls over the same time period. The mean for AC7 was 9.9% (p=.020) higher than BL6, and the mean for 1HU7 was 9.7% lower than AC7 (p=.002). During the first two recovery periods following 1HU7, SSI values remained significantly lower than aging controls, by 9.5% (p=.010) at 8 months and by 6.5% (p=.042) at 9 months, but recovered fully by 10 months. Neither of the HU bouts that started at 9 months had much effect in terms of change relative to pre-HU values. During recovery from 10 to 12 months, all three groups (AC, 1HU10, 2HU10) tended to increase at roughly the same rates, although neither of the recovery groups were significantly greater than their immediate pre- or post-HU groups.

Values are presented as mean ± SE.

*** Indicates significant difference from baseline value; p<0.05, unpaired t-test.**

† Indicates significant difference from age-matched control value at same time point; p<0.05, unpaired t-test.

 # Indicates significant difference from month 9 pre-HU value within same group (i.e. 1HU10(+R2) or 2HU10+(R2)); p<0.05, unpaired t-test.

◊ Indicates significant difference from immediate preceding post-HU value within same group; p<0.05, unpaired t-t est.

‡ Indicates significant difference between 1HU7+R3 and 2HU10; p<0.05, unpaired t-test.

¤ Indicates significant difference between 1HU10 and 2HU10 at the same time point; p<0.05, unpaired t-test.

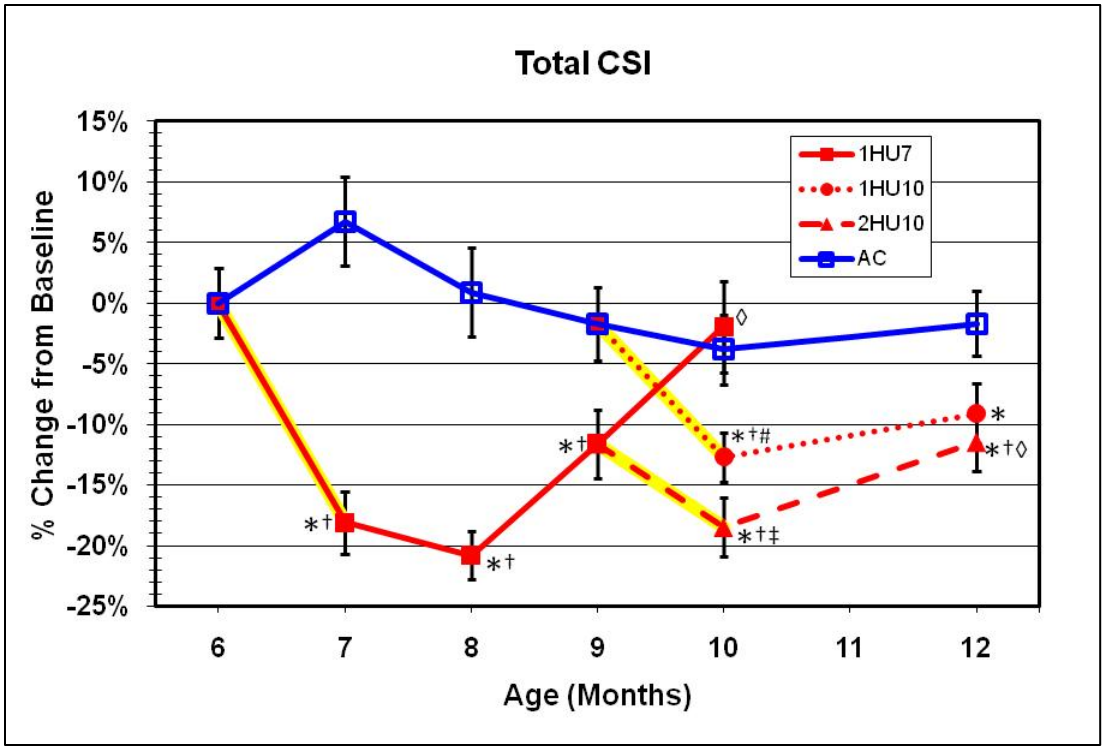

Fig. 30. Changes in the compressive strength index of the total cross-section of the distal femur metaphysis as a result of hindlimb unloading (HU) and ambulatory recovery. Yellow highlighting indicates periods of HU. Numerical values for total CSI are contained in Table 3. The initial HU (1HU7) produced a dramatic decrease in total CSI, which was 18.1% lower than BL6 (p<.001) and 23.3% lower than AC7 (p<.001). The deficit caused by HU actually increased slightly during the first month of reloading to be 20.7% lower than BL6 (<.001) and 21.5% lower than AC8 (p<.001). Total CSI values recovered substantially during the second month of reloading but remained significantly lower than both BL6 (-11.6%, p=.008) and AC9 (-10.0%, p=.023). Total CSI fully recovered to both BL6 and aging control (AC10) at 10 months. The effects of both HU bouts that started at 9 months were similar and led to substantial declines in total CSI, although both were more moderate than the reductions for 1HU7. Specifically, the declines from pre-HU to post-HU were 11.1% for 1HU10 (p=.004) and 7.8% for 2HU10 (p=.073). During recovery from 10 to 12 months, all three groups (AC, 1HU10, 2HU10) tended to increase slightly and similarly, although 1HU10 and 2HU10 were still 7.5% (p=.052) and 9.9% (p=.011) lower than AC12, respectively.

Values are presented as mean ± SE.

*** Indicates significant difference from baseline value; p<0.05, unpaired t-test.**

† Indicates significant difference from age-matched control value at same time point; p<0.05, unpaired t-test.

 # Indicates significant difference from month 9 pre-HU value within same group (i.e. 1HU10(+R2) or 2HU10+(R2)); p<0.05, unpaired t-test.

◊ Indicates significant difference from immediate preceding post-HU value within same group; p<0.05, unpaired t-t est.

‡ Indicates significant difference between 1HU7+R3 and 2HU10; p<0.05, unpaired t-test.

¤ Indicates significant difference between 1HU10 and 2HU10 at the same time point; p<0.05, unpaired t-test.

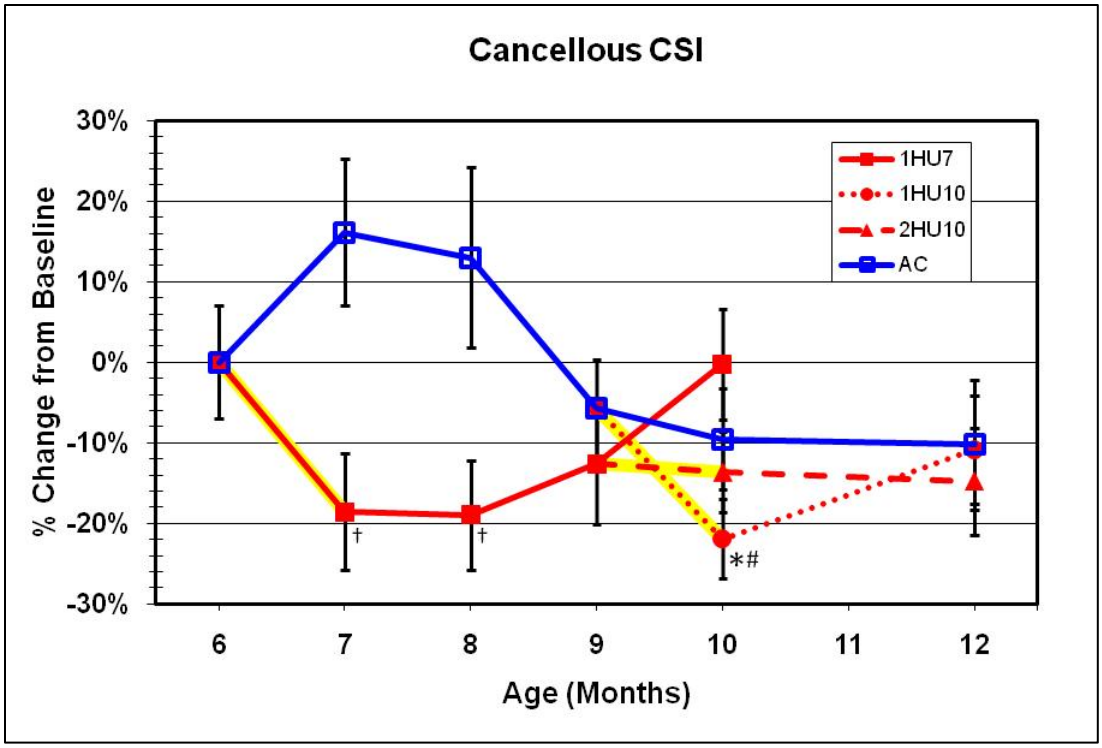

Fig. 31. Changes in compressive strength index of the cancellous region of the distal femur metaphysis as a result of hindlimb unloading (HU) and ambulatory recovery. Yellow highlighting indicates periods of HU. Numerical values for cancellous CSI are contained in Table 3. There are not as many statistically significant differences for this parameter due to higher levels of variability. For example, the decline due to 1HU7 was dramatic in terms of percent change (-18.6%) but the mean at 1HU7 is not significantly different from BL6 (p=.074). However, due to the increase in aging control (from BL6 to AC7), the value at 1HU7 is fully 29.8% lower than AC7 and statistically significant (p=.005). This significant difference remains for the first month after reloading, with 1HU7+R1 being 28.3% lower than AC8 (p=.023). There was no effect due to the second HU for the double-HU group (2HU10), but the single age-matched HU bout starting at 9 months (1HU9) did indeed induce a significant decline in cancellous CSI (-17.0%, p=.042).

Values are presented as mean ± SE.

*** Indicates significant difference from baseline value; p<0.05, unpaired t-test.**

† Indicates significant difference from age-matched control value at same time point; p<0.05, unpaired t-test.

 # Indicates significant difference from month 9 pre-HU value within same group (i.e. 1HU10(+R2) or 2HU10+(R2)); p<0.05, unpaired t-test.

◊ Indicates significant difference from immediate preceding post-HU value within same group; p<0.05, unpaired t-t est.

‡ Indicates significant difference between 1HU7+R3 and 2HU10; p<0.05, unpaired t-test.

¤ Indicates significant difference between 1HU10 and 2HU10 at the same time point; p<0.05, unpaired t-test.

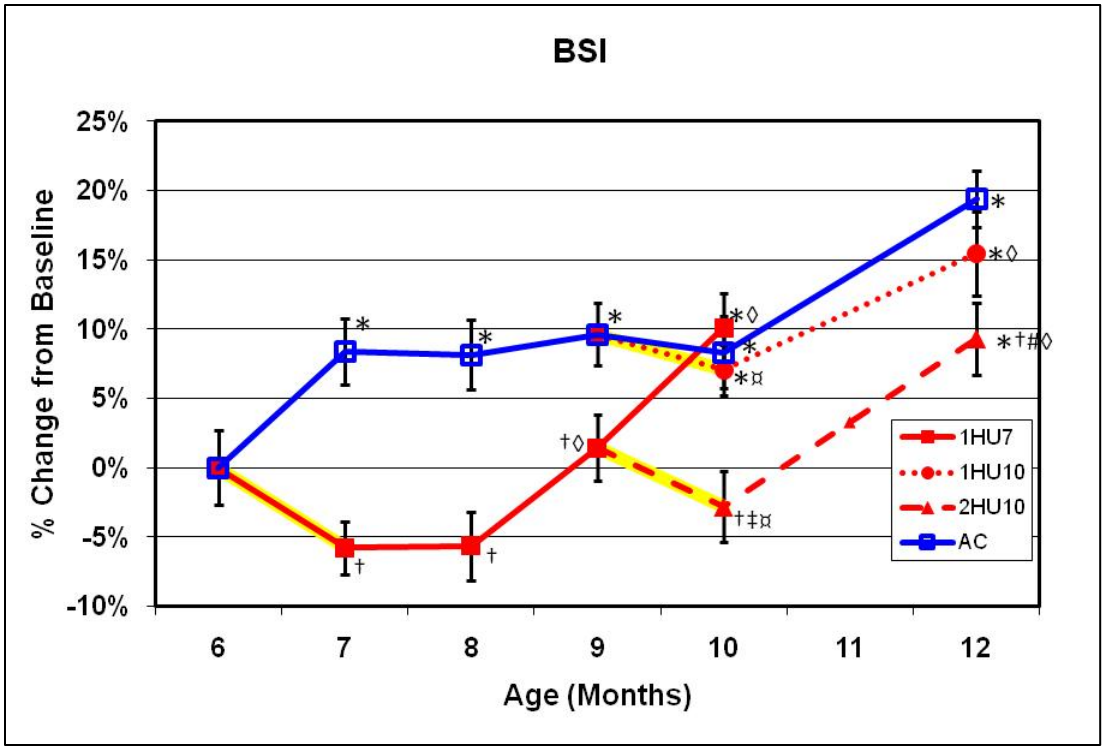

Fig. 32. Changes in bending strength index (BSI) of the total bone cross-section of the distal femur metaphysis as a result of hindlimb unloading (HU) and ambulatory recovery. Yellow highlighting indicates periods of HU. Numerical values for BSI are contained in Table 3. The percent changes due to HU are not very dramatic, with none of the HU bouts inducing statistically significant decreases from pre-HU to post-HU. However, the combination of an increase for aging controls and decrease for HU over the first month of the study led to significant differences between 1HU7 and aging controls at months 7, 8, and 9. Specifically, 1HU7 values were lower than aging controls by 13.0% (p<.001), 12.8% (p<.001), and 7.5% (p=.018), respectively. The HU bouts started at 9 months (1HU10 and 2HU10) induced slight declines in BSI, but these were not significant for either case. Recovery following the 9 to 10 month HU was significant for both cases (values at 12 months vs. 10 months), but aging controls also had similarly increased over the same time period.
Values are presented as mean ± SE.
*** Indicates significant difference from baseline value; p<0.05, unpaired t-test.**
† Indicates significant difference from age-matched control value at same time point; p<0.05, unpaired t-test.
 # Indicates significant difference from month 9 pre-HU value within same group (i.e. 1HU10(+R2) or 2HU10+(R2)); p<0.05, unpaired t-test.
◊ Indicates significant difference from immediate preceding post-HU value within same group; p<0.05, unpaired t-t est.
‡ Indicates significant difference between 1HU7+R3 and 2HU10; p<0.05, unpaired t-test.
¤ Indicates significant difference between 1HU10 and 2HU10 at the same time point; p<0.05, unpaired t-test.

4.4 Mechanical Testing Results

RPC mechanical testing was used to obtain the mecahanical properties of cancellous bone at the distal femur metaphysis (Table 4). Cancellous bone is comprised

of a complex arrangement of tiny rod-like trabeculae. Because of the complexity and structural variation, specimens did not all behave the same way when compressed, making an exact failure point sometimes difficult to identify. Because this study aimed to estimate intrinsic properties of the cancellous region, it was important to identify the point at which the specimen failed (i.e. the first "true" peak on the force-displacement curve) and not just look at the maximum compressive force observed after penetrating the region. An ideal force-displacement curve would start with a linear region, gradually peak, and then rapidly decline (indicating that failure had unambiguously occurred). Most of the specimens followed this pattern, but those that deviated from this mechanical behavior required close examination and review to ensure that a consistent criteria was applied to all specimens. This is a factor of any test that directly loads cancellous bone. Because of the behavior of cancellous bone, it was sometimes difficult or impossible to obtain a point where true yield occurred, therefore, the emphasis of material behavior should be placed on the properties related to ultimate stress, which was much easier to discern. Graphs for yield properties are located in the Appendix.

Ultimate stress (Fig. 33), elastic modulus (Fig. 34), and energy to ultimate (Fig. 35), all tended to have the same overall characteristics. One of the results which stands out is the large increase in mechanical properties of that occurs between baseline (BL6) and the aging control group at month 7 (AC7). Ultimate stress was 248.9% higher relative to baseline for the AC7 group ($p=.009$). In contrast, the 1HU7 group lost very little compared to baseline, decreasing only 14.2% ($p=.694$). Elastic modulus and energy

to ultimate also show similarly dramatic and significant changes over the first month. It is quite apparent that the initial HU bout significantly suppressed normal age-related increases in mechanical properties.

Focusing on ultimate stress and elastic modulus as the main results for mechanical properties, results show that reloaded groups steadily increased during recovery following the first HU (1HU7), while the aging controls steadily decreased over the same time period. The effects of the first HU gave rise to ultimate stress and elastic modulus values that were markedly lower compared to aging controls. Specifically, ultimate stress for 1HU7 was 75.7% lower than AC7 and elastic modulus was 65.3% lower. These differences persisted for the first month of recovery such that ultimate stress was 44.1% lower compared to AC8, but this was not statistically significant ($p=.116$). For elastic modulus, the difference was similar (40.4%) and it also reached statistical significance ($p=0.034$). All differences between the recovery and control groups disappeared by month 9. Interestingly, the recovery group at month 10 (1HU7+R3) was significantly higher than the age-matched control group (AC10) for both ultimate stress and elastic modulus. Losses were observed for both groups that were unloaded from months 9-10, with 1HU10 group having significant losses compared to its immediate pre-HU group in all of the strength variables except for energy to ultimate stress (which was the only variable for which 2HU10 experienced a significant loss). Also, the 2HU10 group tended to recover more than did the 1HU10 group.

Ultimate strain (Fig. 36) showed no meaningful response to HU or recovery. The only significant differences for ultimate strain occurred at month 12, where 1HU10+R2 and 2HU10+R2 were both significantly less than AC12.

Table 4. Estimated mechanical Properties of cancellous bone

	Elastic Modulus (Mpa)	Ultimate Stress (MPa)	Yield Stress (MPa)	Energy to Ultimate (mJ)	Energy to Yield (mJ)	Ultimate Strain (%)	Yield Strain (%)
6 Months Old							
BL6	18.80 (3.96)	0.44 (0.14)	0.35 (0.12)	64.8 (26.8)	37.9 (19.5)	4.48 (0.60)	3.27 (0.60)
7 Month Old							
AC7	48.05 (7.87) *	1.52 (0.36) *	1.36 (0.35) *	244.9 (79.0) *	171.9 (72.4)	4.46 (0.56)	3.63 (0.50)
1HU7	16.66 (3.30) †	0.37 (0.07) †	0.32 (0.06) †	49.7 (11.1) †	26.4 (6.0)	4.70 (0.41)	3.63 (0.31)
8 Months Old							
AC8	46.37 (6.51) *	1.21 (0.27) *	0.99 (0.24) *	177.2 (59.1)	118.2 (51.1)	3.88 (0.63)	3.14 (0.61)
1HU7+R1	27.65 (5.09) †	0.67 (0.18)	0.53 (0.14)	118.0 (29.7)	40.8 (13.2)	3.97 (0.56)	2.59 (0.33) ◊
9 Months Old							
AC9	28.44 (6.24)	0.74 (0.15)	0.56 (0.13)	111.6 (26.7)	50.4 (14.1)	5.27 (0.70)	3.43 (0.63)
1HU7+R2	30.84 (7.28)	0.80 (0.19) ◊	0.64 (0.15) ◊	105.7 (27.4) ◊	55.1 (14.7)	4.27 (0.42)	3.27 (0.43)
10 Months Old							
AC10	18.35 (3.62)	0.44 (0.09)	0.38 (0.07)	69.3 (22.3)	37.5 (9.1)	5.27 (0.67)	4.22 (0.67)
1HU7+R3	36.99 (8.31) *†◊	1.00 (0.21) *†◊	0.84 (0.18) *†◊	158.5 (44.2) ◊	84.7 (23.5) ◊	4.68 (0.51)	3.51 (0.48)
1HU10	11.22 (3.73) #	0.24 (0.11) #	0.18 (0.08) #	45.8 (32.2)	12.1 (6.5) †#	4.36 (0.64)	3.11 (0.60)
2HU10	22.26 (4.79)	0.43 (0.10) ‡	0.37 (0.09) ‡	44.0 (13.2) #‡	26.1 (6.1) ‡	4.42 (0.51)	3.78 (0.43)
12 Months Old							
AC12	34.13 (10.38)	1.01 (0.34)	0.70 (0.21)	152.2 (48.7)	54.9 (14.5)	6.23 (0.73)	4.57 (0.69)
1HU10+R2	19.22 (4.03) ¤	0.36 (0.07) †#¤	0.32 (0.06) ¤	34.1 (7.2) †#¤	20.3 (4.2) †#¤	4.17 (0.55) †	3.33 (0.49)
2HU10+R2	36.26 (5.49) *¤	0.82 (0.13) ◊¤	0.65 (0.10) ◊¤	106.1 (23.0) ◊¤	44.7 (9.5) ¤	4.26 (0.41) †	3.05 (0.32) †

*** Indicates significant difference from baseline value; p<0.05, unpaired t-test.**

† Indicates significant difference from age-matched control value at same time point; p<0.05, unpaired t-test.

 # Indicates significant difference from month 9 pre-HU value within same group (i.e. 1HU10(+R2) or 2HU10+(R2)); p<0.05, unpaired t-test.

◊ Indicates significant difference from immediate preceding post-HU value within same group; p<0.05, unpaired t-t est.

‡ Indicates significant difference between 1HU7+R3 and 2HU10; p<0.05, unpaired t-test.

¤ Indicates significant difference between 1HU10 and 2HU10 at the same time point; p<0.05, unpaired t-test.

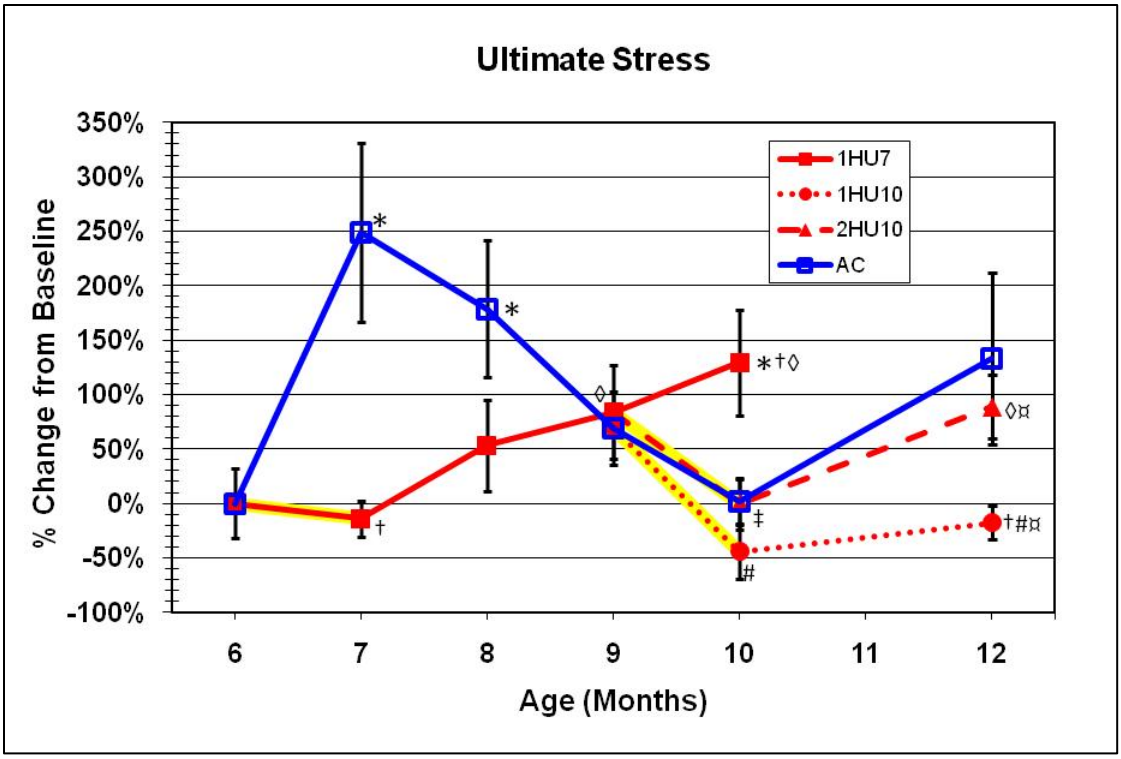

Fig. 33 Changes in ultimate stress of the distal femur metaphysis as a result of hindlimb unloading (HU) and ambulatory recovery. Yellow highlighting indicates periods of HU. Numerical values for ultimate stress are contained in Table 3.Relative to baseline (BL6), the loss of 14% (p=.694) experienced during HU was minor, especially compared to the 248.9% (p=.009) increase that occurred in the aging control group (AC7). This dynamic resulted in 1HU7 being 75.4% below AC7 (p=.004). However, this difference goes away after 1 recovery period due to the increase of the recovery groups and the decrease of control groups. After 3 recovery periods, 1HU7+R3 was significantly higher than BL6 (p=.029) and AC10 (p=.024). Both 1HU10 and 2HU10 experience losses relative to their immediate pre-HU groups, with only 1HU10's -67.2% being significant (p=.009). However, the control groups during months 9 and 10 also experienced similar losses. 1HU10 did not recover relative to pre- or post-HU vlaues, resulting in an end point that was 64.7% less than AC12 (p=.048) while 2HU10 had recovered relative to both and was only 19.1% below AC12 (p=.581).

Values are presented as mean ± SE.

*** Indicates significant difference from baseline value; p<0.05, unpaired t-test.**

† Indicates significant difference from age-matched control value at same time point; p<0.05, unpaired t-test.

 # Indicates significant difference from month 9 pre-HU value within same group (i.e. 1HU10(+R2) or 2HU10+(R2)); p<0.05, unpaired t-test.

◊ Indicates significant difference from immediate preceding post-HU value within same group; p<0.05, unpaired t-t est.

‡ Indicates significant difference between 1HU7+R3 and 2HU10; p<0.05, unpaired t-test.

¤ Indicates significant difference between 1HU10 and 2HU10 at the same time point; p<0.05, unpaired t-test.

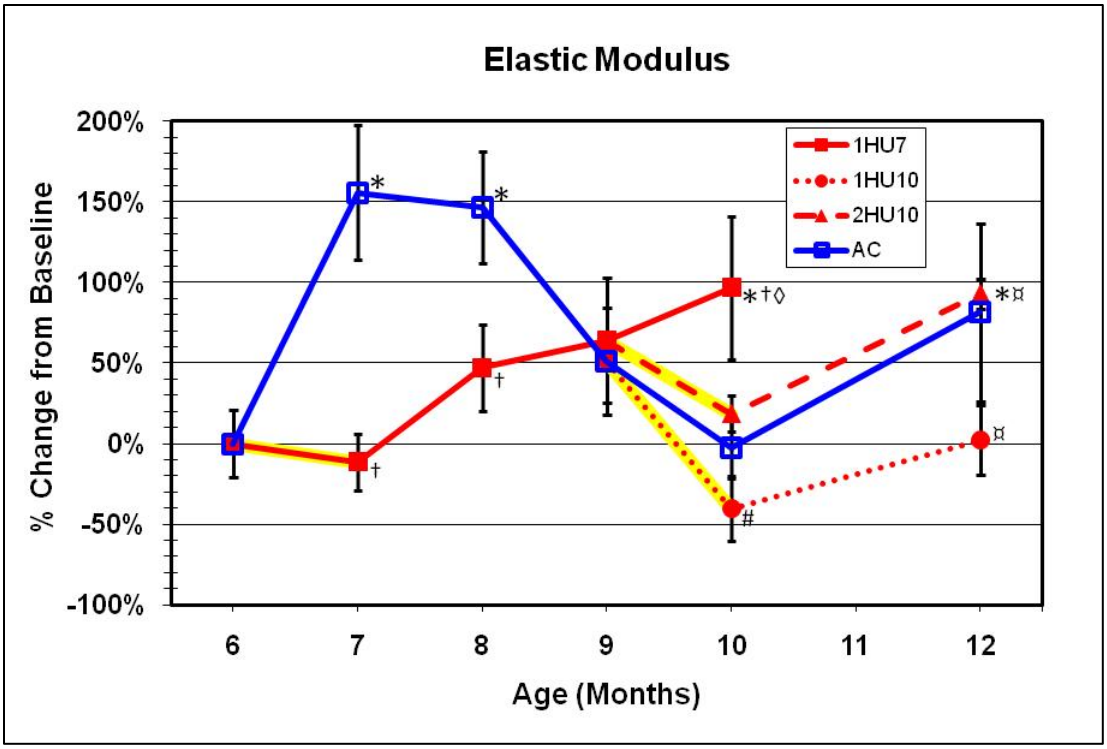

Fig. 34: Changes in elastic modulus of the distal femur metaphysis as a result of hindlimb unloading (HU) and ambulatory recovery. Yellow highlighting indicates periods of HU. Numerical values for elastic modulus are contained in Table 3. Relative to baseline (BL6), the unloaded (1HU7) group experienced a 11.4% (p=.680) drop while the corresponding control group (AC7) increased 155.7% (p=.009). After one recovery period, 1HU7+R1 was still -40.4% of the value of AC8 (p=.034). The recovery groups continued to increase while AC groups decreased until they were essentially equal at month 9. The opposite trajectories continued through month 10, when 1HU7+R3 was actully 101.6% greater than AC10 (p=.050). Like ultimate stress, 1HU10's value decreased significantly relative to immediate pre-HU (p=.020) values while 2HU10's did not (p=.327). 2HU10's loss and recovery matched very closely with controls during months 9-12. 1HU10 did recovery enough so that its month 12 value was not significantly different than its pre-HU (p=.214) or corresponding control group (p=.162).

Values are presented as mean ± SE.

*** Indicates significant difference from baseline value; p<0.05, unpaired t-test.**

† Indicates significant difference from age-matched control value at same time point; p<0.05, unpaired t-test.

 # Indicates significant difference from month 9 pre-HU value within same group (i.e. 1HU10(+R2) or 2HU10+(R2)); p<0.05, unpaired t-test.

◊ Indicates significant difference from immediate preceding post-HU value within same group; p<0.05, unpaired t-t est.

‡ Indicates significant difference between 1HU7+R3 and 2HU10; p<0.05, unpaired t-test.

¤ Indicates significant difference between 1HU10 and 2HU10 at the same time point; p<0.05, unpaired t-test.

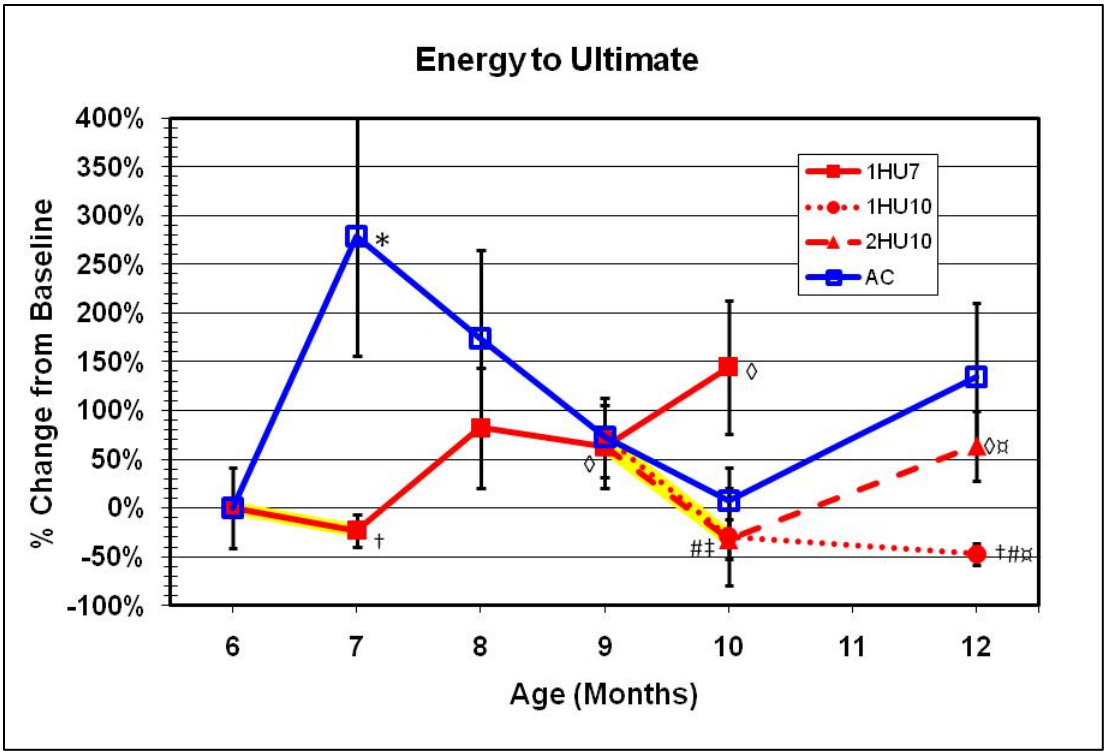

Fig. 35. Changes in energy to ultimate of the distal femur metaphysis as a result of hindlimb unloading (HU) and ambulatory recovery. Yellow highlighting indicates periods of HU. Numerical values for energy to ultimate are contained in Table 3. Relative to baseline (BL6), the unloaded (1HU7) group experienced a 23.3 % (p=..599) drop while the corresponding control group (AC7) increased 278.0% (p=.042). Significant differences between recovery and control values disappeared during recovery. After 3 recovery periods, 1HU7 was 144.7% greater than AC10 (p=.083). Although this difference was not significant, it followed the same trend as most of the other strength variables. 1HU10 and 2HU10 ended their respective HU periods having nearly identical values. However, only 2HU10 experienced a significant decrease relative to its immediate pre-HU group (p=.047). Following the behavior of most of the other strength variables, 2HU10 recovered to a much greater extent than did 1HU10, whose recovery group had a mean value slightly lower than its post-HU group.

Values are presented as mean ± SE.

*** Indicates significant difference from baseline value; p<0.05, unpaired t-test.**

† Indicates significant difference from age-matched control value at same time point; p<0.05, unpaired t-test.

 # Indicates significant difference from month 9 pre-HU value within same group (i.e. 1HU10(+R2) or 2HU10+(R2)); p<0.05, unpaired t-test.

◊ Indicates significant difference from immediate preceding post-HU value within same group; p<0.05, unpaired t-t est.

‡ Indicates significant difference between 1HU7+R3 and 2HU10; p<0.05, unpaired t-test.

¤ Indicates significant difference between 1HU10 and 2HU10 at the same time point; p<0.05, unpaired t-test.

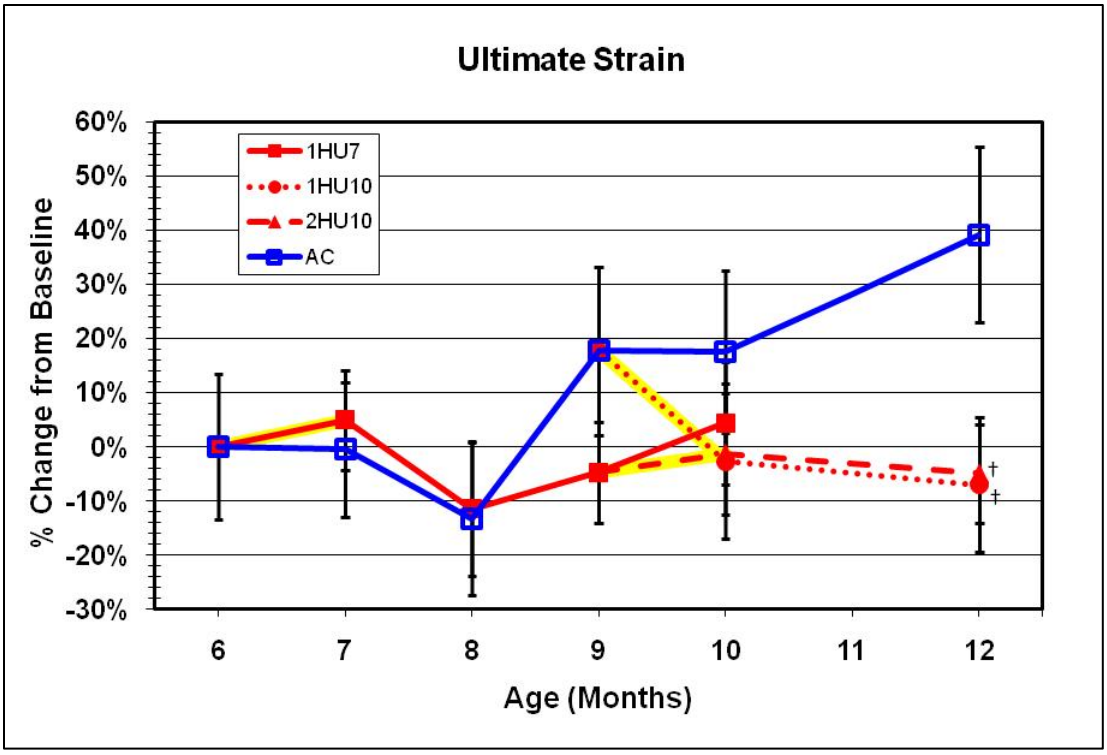

Fig. 36. Changes in ultimate strain of the distal femur metaphysis as a result of hindlimb unloading (HU) and ambulatory recovery. Yellow highlighting indicates periods of HU. Numerical values for ultimate strain are contained in Table 3. Strain values had a large distribution and so significant differences were few. The only significant differences occurred at month 12, where 1HU10's and 2HU10's recovery groups were 33.1% (p=.029) and 31.6% (p=.021) less than AC12, respectively

Values are presented as mean ± SE.

*** Indicates significant difference from baseline value; p<0.05, unpaired t-test.**

† Indicates significant difference from age-matched control value at same time point; p<0.05, unpaired t-test.

 # Indicates significant difference from month 9 pre-HU value within same group (i.e. 1HU10(+R2) or 2HU10+(R2)); p<0.05, unpaired t-test.

◊ Indicates significant difference from immediate preceding post-HU value within same group; p<0.05, unpaired t-t est.

‡ Indicates significant difference between 1HU7+R3 and 2HU10; p<0.05, unpaired t-test.

¤ Indicates significant difference between 1HU10 and 2HU10 at the same time point; p<0.05, unpaired t-test.

4.5 Comparison of Unloading and Recovery Characteristics

Table 5 is presented to facilitate comparisons between unloading-induced changes and normally-loaded recovery for the rat and ISS crew members. For all unloading variable, astronaut data are presented vs. pre-flight values (% pre-

unloading), as calculated at two regions in the hip (femoral neck and proximal femur) which were defined previously by Lang et al.[1,3]

There are two ways to characterize losses for the HU rats: relative to pre-HU (BL6) values (% pre-unloading) and relative to age-matched controls (% AC). In general, most variables for both rats and astronauts tended to behave similarly (i.e. a given variable either decreases or increases for both) even if the relative increases/decreases were not alike. The lone exception to this is total area/volume (the total area parameter for the rats uses volumetric data to define an average cross-section, so the two are analogous). Both of the astronauts' regions lose volume, whereas the rats' actually increases. Interestingly, HU losses defined by % AC match best with astronaut unloading results (as % pre-flight) for most variables. Exceptions are cancellous vBMD and total CSI, in which case the HU losses relative to baseline match better.

For each variable's recovery, astronaut data are presented two ways: relative to pre-flight (% pre-flight) and relative to values collected immediately post-flight (% post-flight). There are three ways to characterize recovery for the HU rat: relative to AC and BL6 (described above) as well as relative to post-HU values. All of the recovery groups for the month 6 HU are presented to see which, if any are consistent with similar losses for astronauts. The recovery periods for the rats were equal to 1, 2, and 3 times the duration of their unloading bout. Because the astronauts' missions were 4-6 months and the "recovery scans" were performed one year post-flight, the duration of recovery was somewhere between 2-3 times the duration of unloading for all of the subjects. No

single animal metric matched exactly with the recovery of the astronauts. The relative recovery values for the first HU recovery period (1HU7+R1) were generally lower than the astronaut recovery values. This is to be expected because the ratio of unloading: recovery is 1:1 for the rats as opposed to 1:2 for the astronauts. The 1HU7+R3 group also tends to have recovered to a greater extent than the astronauts when comparing to pre-unloading values. However, it matches quite well with the proximal femur data when looking at post-unloading recovery (with a major exception being BSI/Section Modulus). The 1HU7+R2 group tended to be the most similar to both astronaut sites when looking at recovery relative to pre-unloading values, but 1HU7+R3 matched the astronaut data more closely when recovery is defined relative to post-unloading. While none of the HU recovery groups accurately matched up with all of the respective astronaut variables, the 1HU7+R1 and 1HU7+R3 groups did provide a solid lower- and upper- bound for predicting the recovery of astronauts after one year (relative to post-unloading and pre-unloading values).

Table 5. Comparison of loss and recovery between hindlimb unloaded (HU) rats and astronauts*

	Immdeiately After Unloading			Recovery				
	1HU7	Astronaut Femoral Neck	Astronaut Proximal Femur	1HU7+R1	1HU7+R2	1HU7+R3	Astronaut Femoral Neck	Astronaut Proximal Femur
Total BMC								
% Pre-Unloading	-7.1%	-12.0%	-12.5%	-8.7%	-3.8%	3.0%	-5.4%	-2.2%
% AC	-12.8%	-	-	-12.5%	-6.5%	1.7%	-	-
% Post-Unloading	-	-	-	-1.7%	3.6%	10.9%	7.5%	11.8%
Tot Area/Volume								
% Pre-Unloading	6.4%	-2.7%	-2.0%	6.9%	6.1%	9.6%	4.3%	5.4%
% AC	-0.6%	-	-	-1.8%	-2.4%	0.1%	-	-
% Post-Unloading	-	-	-	0.4%	-0.3%	3.0%	7.2%	7.5%
Total vBMD								
% Pre-Unloading	-12.6%	-9.5%	-10.5%	-14.5%	-9.2%	-5.9%	-8.9%	-6.9%
% AC	-12.2%	-	-	-10.9%	-4.3%	1.3%	-	-
% Post-Unloading	-	-	-	-2.2%	3.9%	7.6%	0.6%	4.0%
Cortical BMC								
% Pre-Unloading	-8.3%	-13.0%	-13.7%	-10.6%	-4.5%	1.9%	-7.2%	-3.7%
% AC	-12.5%	-	-	-11.5%	-7.5%	0.0%	-	-
% Post-Unloading	-	-	-	-2.5%	4.1%	11.2%	6.7%	11.6%
Cortical Area/Volume								
% Pre-Unloading	-5.8%	-9.2%	-10.5%	-7.9%	-3.6%	2.2%	-2.4%	-0.4%
% AC	-10.8%	-	-	-9.4%	-6.5%	0.2%	-	-
% Post-Unloading	-	-	-	-2.3%	2.2%	8.4%	7.5%	11.2%
Cortical BMD								
% Pre-Unloading	-2.9%	-4.3%	-3.3%	-3.1%	-1.0%	-0.3%	-4.6%	-3.0%
% AC	-2.0%	-	-	-2.4%	-1.0%	-0.2%	-	-
% Post-Unloading	-	-	-	-0.2%	1.9%	2.7%	-0.4%	0.4%
Cancellous vBMD								
% Pre-Unloading	-16.4%	-15.4%	-14.5%	-17.8%	-12.8%	-7.0%	-11.0%	-9.0%
% AC	-19.3%	-	-	-16.8%	-5.2%	5.8%	-	-
% Post-Unloading	-	-	-	-1.7%	4.4%	11.3%	5.2%	6.5%
Total CSI								
% Pre-Unloading	-18.1%	-16.7%	-	-20.8%	-11.6%	-2.0%	-14.7%	-
% AC	-23.3%	-	-	-21.5%	-10.1%	2.0%	-	-
% Post-Unloading	-	-	-	-3.3%	7.9%	19.7%	2.4%	-
BSI								
% Pre-Unloading	-5.8%	-20.6%	-11.0%	-5.6%	1.4%	10.1%	-15.5%	-
% AC	-13.1%	-	-	-12.8%	-7.5%	1.6%	-	-
% Post-Unloading	-	-	-	0.1%	7.6%	16.9%	6.5%	-

*** Astronaut data are taken from Lang et al. with recovery values obtained 1 year post-flight[1,3]**
1HU7 = first HU starting at 6 mos. of age and ending at 7 mos.
+R1 = after 1 recovery period of 1 mo. (28 days)
+R2 = after 2 recovery periods of 2 mos. (56 days)
+R3 = after 3 recovery periods of 3 mo. (84 days)
2HU10 = second HU starting at 9 mos. of age and ending at 10 mos.
% Pre-Unloading = percent change Post- vs. Pre-HU for rats, Post- vs. Pre-flight for astronauts
% AC = percent difference between Post-HU and corresponding age-matched control
% Post-Unloading = percent change compared to immediate Post-HU for rats, Post-Flight for astronauts

Table 6 provides a summary comparing both unloading and recovery characteristics for the three HU cases. Recall that 1HU7 denotes the first HU of the

double-HU group, and 1HU7 started when the animals were 6 months of age and ended at 7 months. The 2HU10 designation signifies the second HU of the double-HU group, and this HU bout started when the animals were 9 months old and ended at 10 months. The 1HU10 group had a single bout of HU that started when the animals were 9 months old and ended at 10 months. The first three columns of Table 6 provide a convenient way to compare the unloading responses for each pQCT variable of interest. Comparing 1HU10 and 2HU10 gives insight into possible effects of prior HU exposure. The only difference between these two groups is that the 2HU10 animals experienced a previous HU bout (from 6 to 7 months). Similarly, comparing 1HU7 and 1HU10 provides a way to assess possible age effects. The only difference between these two is the age of the animals at the start of HU (3 month difference). For most variables listed in Table 6, the response for the first HU (1HU7) is more severe than the response for the single older HU (1HU10), suggesting that aging moderates the response to HU. The effects of HU are to induce a loss (or decrease in value) for the vast majority of variables, and for these the losses are generally higher for 1HU7 than for 1HU10. Total area and endocortical area actually increase during HU, and 1HU7 had greater increases than 1HU10 for both of their variables.

Comparing results in the three columns on the right of Table 6 provides a way to assess recovery characteristics for the three HU cases. There are three rows of results for each variable. The last, or third, row is probably the most relevant for focusing on recovery from immediate post-HU conditions. This row contains results as a percentage

of the immediate post-HU value. Positive percentages indicate some degree of increase during recovery, and negative values indicate continued decreases during recovery. Comparing 1HU10+R2 and 2HU10+R2 gives insight into any possible effects of prior HU exposure on recovery. For the vast majority of variables, the percentages are positive, indicating increases during recovery, but there is no consistent pattern for one case being higher or lower than the other. This suggests that there is no clear or consistent effect of prior HU exposure on recovery dynamics. Comparing 1HU7+R1 and 1HU10+R2 leads to a similar observation. The extent of recovery is higher for 1HU7+R2 for some variables and higher for 1HU10+R2 for other variables. Thus, there is also no clear pattern indicating any consistent effect of aging on recovery from HU.

Table 7 summarizes changes in mechanical properties of the cancellous bone in the distal femur metaphysis as estimated by RPC testing. The main properties of interest are the elastic modulus and ultimate stress, and the loss and recovery patterns for these are quite similar to one another (Figs. 33 and 34). Comparing results for 1HU10 and 2HU10 is complicated by the fact that the results are quite different depending on the reference used for the percent changes. That is, when comparing post-HU values to pre-HU values (% Pre-HU), both groups show substantial losses, with the losses for 2HU10 being less than those for 1HU10. However, when comparing post-HU values to corresponding aging controls (% AC), the 1HU10 group again exhibits markedly lower values, but the 2HU10 group indicates higher values for elastic modulus (+21%) and essentially no difference for ultimate stress (-2%). Similarly, comparing the

1HU7 and 1HU10 results to assess a possible age effect gives mixed or conflicting information depending on whether considering % Pre-HU or % AC results.

Table 6. Comparison of changes in densitometric and geometric properties resulting from hindlimb unloading (HU) at 7 and/or 10 months of age and subsequent recovery after two months

	Unloading			Recovery		
	1HU7	1HU10	2HU10	1HU7+R2	1HU10+R2	2HU10+R2
Total vBMD						
% Pre-Unloading	-12.6%	-8.0%	-6.9%	-9.2%	-7.8%	-3.4%
% AC	-12.2%	-6.0%	-8.9%	-4.3%	-5.8%	-5.5%
% Post-Unloading	-	-	-	3.9%	0.3%	3.8%
Total BMC						
% Pre-Unloading	-7.1%	-4.2%	-1.9%	-3.8%	-0.5%	2.8%
% AC	-12.8%	-2.7%	-6.8%	-6.5%	-2.4%	-5.8%
% Post-Unloading	-	-	-	3.6%	3.9%	4.8%
Total Area						
% Pre-Unloading	6.4%	4.1%	5.3%	6.1%	7.7%	6.1%
% AC	-0.6%	3.5%	2.1%	-2.4%	3.7%	-0.3%
% Post-Unloading	-	-	-	-0.3%	3.4%	0.8%
Cancellous vBMD						
% Pre-Unloading	-16.4%	-13.5%	-5.3%	-12.8%	-10.5%	-6.2%
% AC	-19.3%	-9.4%	-6.1%	-5.2%	-4.1%	-4.8%
% Post-Unloading	-	-	-	4.4%	3.5%	-1.0%
Cancellous BMC						
% Pre-Unloading	-4.1%	-5.4%	4.2%	-1.9%	2.5%	1.7%
% AC	-13.5%	-3.1%	2.2%	-4.3%	2.8%	-2.3%
% Post-Unloading	-	-	-	2.3%	8.4%	-2.4%
Endocortical Area						
% Pre-Unloading	15.4%	8.7%	10.0%	13.4%	13.2%	7.9%
% AC	6.8%	6.8%	8.4%	0.4%	7.3%	2.8%
% Post-Unloading	-	-	-	-1.8%	4.1%	-1.9%
Cortical vBMD						
% Pre-Unloading	-2.9%	-1.2%	-2.7%	-1.0%	-1.3%	0.0%
% AC	-2.0%	-1.1%	-3.5%	-1.0%	-2.7%	-2.3%
% Post-Unloading	-	-	-	1.9%	-0.1%	2.8%
Cortical BMC						
% Pre-Unloading	-8.3%	-3.7%	-4.6%	-4.5%	-1.7%	3.3%
% AC	-12.5%	-2.5%	-10.6%	-7.5%	-4.5%	-7.2%
% Post-Unloading	-	-	-	4.1%	2.1%	8.2%
Cortical Area						
% Pre-Unloading	-5.8%	-2.6%	-2.1%	-3.6%	-0.4%	3.3%
% AC	-10.8%	-1.5%	-7.5%	-6.5%	-2.0%	-5.0%
% Post-Unloading	-	-	-	2.2%	2.2%	5.5%
Cortical Thickness						
% Pre-Unloading	-10.2%	-5.4%	-5.5%	-7.7%	-5.1%	-0.2%
% AC	-11.8%	-3.9%	-9.7%	-5.9%	-4.4%	-5.5%
% Post-Unloading	-	-	-	2.7%	0.3%	5.6%
SSI						
% Pre-Unloading	-0.8%	-0.9%	-0.4%	2.7%	5.5%	6.6%
% AC	-9.7%	0.1%	-5.9%	-6.5%	0.9%	-4.6%
% Post-Unloading	-	-	-	3.6%	6.4%	7.0%

Table 6. (Cont.)

	Unloading			Recovery		
	1HU7	1HU10	2HU10	1HU7+R2	1HU10+R2	2HU10+R2
CSI (Total)						
% Pre-Unloading	-18.1%	-11.2%	-7.8%	-11.6%	-7.5%	0.2%
% AC	-23.3%	-9.2%	-15.2%	-10.1%	-7.5%	-9.9%
% Post-Unloading	-	-	-	7.9%	4.1%	8.6%
CSI (Cancellous)						
% Pre-Unloading	-18.5%	-17.2%	-1.2%	-12.6%	-5.5%	-2.4%
% AC	-29.9%	-13.7%	-4.6%	-7.4%	-0.7%	-5.0%
% Post-Unloading	-	-	-	7.3%	14.2%	-1.3%
BSI						
% Pre-Unloading	-5.8%	-2.3%	-4.2%	1.4%	5.3%	7.8%
% AC	-13.1%	-1.2%	-10.3%	-7.5%	-3.3%	-8.4%
% Post-Unloading	-	-	-	7.6%	7.8%	12.5%
I_{MAX}						
% Pre-Unloading	-4.4%	-0.5%	0.9%	2.7%	8.0%	8.4%
% AC	-15.6%	2.6%	-5.2%	-8.9%	-0.4%	-9.0%
% Post-Unloading	-	-	-	7.5%	8.5%	7.5%
I_{MIN}						
% Pre-Unloading	7.3%	3.8%	6.0%	5.5%	11.6%	11.8%
% AC	-3.5%	0.6%	-3.4%	-6.0%	5.2%	-0.9%
% Post-Unloading	-	-	-	-1.7%	7.5%	5.5%
I_P						
% Pre-Unloading	-0.5%	1.0%	2.6%	3.7%	9.2%	9.5%
% AC	-11.6%	1.9%	-4.6%	-7.9%	1.4%	-6.3%
% Post-Unloading	-	-	-	4.1%	8.2%	6.8%

1HU7 = first HU starting at 6 mos. of age and ending at 7 mos.
1HU10 = first HU starting at 9 mos. of age and ending at 10 mos.
2HU10 = second HU starting at 9 mos. of age and ending at 10 mos.
Group+R2 = after 2 recovery periods of 2 mos. (56 days total)
% Pre-Unloading = percent change Post- vs. Pre-HU
% AC = percent difference between Post-HU and corresponding age-matched control
% Post-Unloading = percent change compared to immediate Post-HU

Table 7. Comparison of changes in mechanical properties resulting from HU at 7 and/or 10 months of age and subsequent recovery after two months

	Unloading			Recovery		
	1HU7	1HU10	2HU10	1HU7+R2	1HU10+R2	2HU10+R2
Elastic Modulus						
% Pre-Unloading	-11.4%	-60.5%	-27.8%	64.1%	-32.4%	17.6%
% AC	-65.3%	-38.8%	21.3%	8.4%	-43.7%	6.2%
% Post-Unloading	-	-	-	85.1%	71.2%	62.8%
Ultimate Stress						
% Pre-Unloading	-14.2%	-67.2%	-45.8%	83.8%	-51.3%	2.6%
% AC	-75.4%	-45.7%	-2.4%	8.7%	-64.7%	-19.1%
% Post-Unloading	-	-	-	114.1%	48.4%	89.2%
Yield Stress						
% Pre-Unloading	-6.7%	-67.6%	-42.1%	83.5%	-43.8%	1.7%
% AC	-76.3%	-52.0%	-2.8%	13.0%	-54.9%	-7.7%
% Post-Unloading	-	-	-	96.8%	73.6%	75.5%
Ultimate Strain						
% Pre-Unloading	4.9%	-17.3%	3.6%	-4.7%	-21.0%	-0.2%
% AC	5.4%	-17.2%	-16.0%	-19.0%	-33.1%	-31.6%
% Post-Unloading	-	-	-	-9.2%	-4.4%	-3.6%
Yield Strain						
% Pre-Unloading	11.2%	-9.4%	15.7%	0.1%	-2.9%	-6.8%
% AC	0.1%	-26.3%	-10.3%	-4.6%	-27.1%	-33.2%
% Post-Unloading	-	-	-	-9.9%	7.2%	-19.4%
Energy to Ultimate						
% Pre-Unloading	-23.3%	-58.9%	-58.4%	63.2%	-69.4%	0.4%
% AC	-79.7%	-33.9%	-36.6%	-5.2%	-77.6%	-30.3%
% Post-Unloading	-	-	-	112.7%	-25.5%	141.5%
Energy to Yield						
% Pre-Unloading	-30.3%	-76.0%	-52.7%	45.4%	-59.7%	-18.9%
% AC	-84.6%	-67.8%	-30.6%	9.3%	-63.0%	-18.6%
% Post-Unloading	-	-	-	108.6%	68.1%	71.5%

1HU7 = first HU starting at 6 mos. of age and ending at 7 mos.
1HU10 = first HU starting at 9 mos. of age and ending at 10 mos.
2HU10 = second HU starting at 9 mos. of age and ending at 10 mos.
Group+R2 = after 2 recovery periods of 2 mos. (56 days total)
% Pre-Unloading = percent change Post- vs. Pre-HU
% AC = percent difference between Post-HU and corresponding age-matched control
% Post-Unloading = percent change compared to immediate Post-HU

5. DISCUSSION

The overall goal of this study was to quantify changes in mineral, geometric, and strength properties due to single and multiple bouts of extreme disuse, induced by hindlimb unloading (HU). One of the objectives was to examine whether this site was a good model for understanding microgravity-induced changes in the human hip.

5.1 Aging Control Dynamics

Aging controls (AC) were included in this study as an important reference. Even though animals are considered to be "adult" at this age (6+ months), changes in some parameters occurred and these changes must be noted in order to fully assess the effects of HU and recovery. pQCT outcome measures indicate that there is a noticeable but insignificant increase in total BMC, although not in density, during the first month of the experiment. Total vBMD decreases throughout the experiment and after 2 months, values were significantly less than baseline. Cortical BMC and cortical area track similarly, resulting in only mild fluctuations from baseline for cortical vBMD (no statistically significant differences). Meanwhile, cancellous vBMD decreases for every time point after AC7. The information gained by looking at the cancellous and cortical regions indicates that gradual reductions in age for cancellous vBMD are primarily responsible for the trend of lower total vBMD with age.

Cortical area stays slightly above baseline (with only AC7 being significantly different) while endocortical area increases, with all AC groups being significantly greater than baseline. Since endocortical area increases proportionally more than does total area, a mild thinning of the cortical shell occurs, but cortical thickness does not change significantly with age. The measures which are weighted by voxel density (moments of inertia, SSI, and BSI) track with the behavior of total area: a significant increase between baseline and AC7, relatively little change between AC7 and AC10, and a noticeable increase between AC10 and AC12.

Results obtained from RPC mechanical testing indicate that there is a significant increase in ultimate stress between baseline and the aging control group at month 7. Mechanical properties gradually decline over the next four months until they increase slightly between AC10 and AC12. The behavior of ultimate stress, yield stress, energy to ultimate, energy to yield, and elastic modulus results all follow this trend. Strain values do not differ significantly from baseline.

5.2 Effects of HU

The effects of HU can be evaluated by looking at the behavior of the outcome measures before and after each unloading period. There are two things that stand out: decreased bone mass and outward geometric expansion. Both the cancellous and cortical regions had significantly decreased mineral densities resulting from the early HU period. The insignificant reduction in cancellous BMC (relative to baseline) indicates

that resorption at the endosteal surface is the primary cause of decline in cancellous vBMD. The minimal decline in cancellous BMC is contrary to the findings of a previous study by Ju et al. which examined HU effects on the distal femur metaphysis of 5-week-old Wistar rats using micro-CT and found that various trabecular measures, as well as total bone tissue volume, decreased significantly during HU.[43] The Ju study does not give any direct information regarding the volume of the cancellous region, but the volume encompassed by the periosteum actually decreased slightly during the HU period. Several hindlimb unloading studies that examined the proximal tibia metaphysis also had similar findings to Ju et al.[20,22] Astronaut data relating to periosteal apposition and endocortical resorption are mixed. Lang et al. found that total volume decreased slightly during ISS missions[1], whereas Carpenter et al. saw a marked increase in total volume accompanied by a reduced cortical volume[4], more consistent with the results of this study.

Looking exclusively at the cortical region, it can be seen that HU caused endocortical resorption and did not hinder the natural periosteal apposition occurring in the aging control animals. The result is an outward expanding, yet thinning cortical shell. This is identical to the type of geometric changes that occur in men due to age-related remodeling of the tibia and femur.[44] The 1HU7 group experienced a significant increase in total area relative to baseline, while the 10-month-old HU groups experienced insignificant increases relative to their pre-HU values. However, none of the groups deviated significantly from corresponding AC groups. This indicates that HU

had no meaningful effect on total area. However, HU did have an effect on density-weighted measures that were affected primarily by changes in the area and distribution of the cortical region, such as all mass moments of inertia, SSI, and BSI. For these measures, there was not a significant decrease relative to baseline but the 1HU7 group was significantly lower than the AC7 group, indicating that normal age-related gains had been suppressed.

The effects of HU on mechanical properties was similar to that of the density-weighted geometric measures. None of the measures deviated significantly from baseline values; however, ultimate stress, energy to ultimate, and elastic modulus all were significantly lower than their age matched counterparts after the initial bout of HU. HU had no effect on strain values.

5.3 Effects of Recovery

During the first month of reloading, all pQCT-derived measures either continued the upward or downward trajectory that resulted from HU or the values remained essentially constant. No recovery occurred in the first month, by any measure. This delayed recovery was not observed by Allen et al., where density and geometric measures began recovering within the first 28 days of ambulation.[20] It should be mentioned that the study performed by Allen et al. examined the proximal tibia metaphysis, which may react differently than the distal femur metaphysis to changes in loading scenarios, as unloading-induced changes are site- and compartment-specific.[22]

However, significant recovery was evident for all outcome measures within 2-3 months after HU. Full recovery was most obvious after 3 months, where the 1HU7+R3 group was essentially identical to AC10 for all measures.

Total area remained relatively stagnant for two recovery periods and then increased slightly during the third, indicating that periosteal apposition slowed from the more rapid level observed during HU, but this also followed the age-matched controls closely. Endocortical area increased for one recovery period after unloading, decreased slightly during the next, and then increased slightly during the third, following the changes in the aging control groups between months 8 and 9. The cortical thickness, which dramatically decreased during HU, continued to drop during the first recovery period. It subsequently increased and made it up to control values at month 10 (3 recovery periods). What these results seem to indicate is that periosteal apposition slows down immediately after HU but endocortical resorption continues a while afterwards.

Mechanical properties began recovering immediately after HU. Ultimate stress and energy to ultimate were not significantly different from aging controls after 1 month of ambulation. Elastic modulus was similar to aging controls after 2 months of ambulation. Ultimate stress and elastic modulus values for the 1HU7+R3 group had fully recovered by every measure and were all significantly greater than the corresponding AC10 values, 1HU7 values, and baseline value. An increase in strength was expected after reloading occurred but the recovery groups overtaking control

groups was certainly unexpected, especially considering that the pQCT measures did not do the same. Strain values were not significantly different than baseline or aging control groups.

5.4 Effects of Second HU and Recovery

Performing two HU periods was meant to simulate the effects of an astronaut going on two missions. To determine whether changes in the second HU were due to aging or unloading, another pair of groups underwent a "delayed" single HU period at the same, older age; one of those groups was sacrificed immediately afterwards (1HU10) and the other was allowed to recover for two months (1HU10+R2). The second HU period had some seemingly contrary effects. Cortical vBMD experienced a significant drop relative to 2HU10's pre-HU value, similar to what happened during the first HU period; however, the 1HU10 group did not decrease significantly relative to pre-HU values for this variable. Cancellous vBMD exhibited the opposite effect: the loss for 1HU10 was significant while the loss for 2HU10 was not. The combination of both cortical and cancellous losses resulted in significant losses in total vBMD for both 1HU10 and 2HU10. Similarities in the changes between 1HU10 and 2HU10 for all of the geometric parameters and density-weighted strength indices indicate that the second HU period was not affected by the first. The positive recovery of mechanical properties was certainly hindered by the second HU, as is evidenced by the significant difference between the 3 month recovery group (1HU7+R3) and 2HU10. However, losses for

2HU10 were not as significant as those of 1HU10. Relative to pre-HU values, losses in pQCT variables for the 1HU10 group were generally not as substantial as those experienced by the 1HU7 group, indicating that age did not have a noticeably detrimental effect on the response to HU. This view is also supported by the fact that losses during the second HU tended to be more similar to those experienced by 1HU10 rather than 1HU7. However, aging did seem to have an effect on mechanical properties. There was a significant increase in mechanical properties in aging controls during the first month of the experiment, and HU served to suppress that increase. Losses experienced by 1HU10 were significant relative to its pre-HU group, which would seem to indicate that the aged HU actually induced losses rather than suppression of a natural increase. However, one factor that makes judging the age effect on the second HU difficult is the opposing dynamic of the aging controls and 1HU7 recovery groups. Ignoring the 1HU7+R3 group, it would appear as though the second HU had no effect and losses were simply due to aging. However, when the third recovery group is considered, it can be seen that the second HU suppresses the recovery occurring after the initial HU.

The final two months of recovery yielded some interesting results. Groups recovering from the single, aged HU (1HU10+R2) ended up slightly higher than those recovering from their second HU bout (2HU10+R2) for BMC and cross-sectional area in all regions. 2HU10+R2 recovered more substantially than 1HU10+R2 for total and cortical vBMD while their recovery was similar for cancellous vBMD. All strength indices

(except for cancellous CSI) had nearly identical recoveries for both groups. Looking at cortical thickness, the 1HU10+R2 group did not change compared to its post-HU value, whereas the 2HU10+R2 group increased during recovery.

Another notable observation was that mechanical properties decline more during the second HU than the first (relative to immediate pre-HU values) while the opposite is true for most pQCT variables. The reason for the differing pre-post losses in mechanical properties can likely be attributed to aging effects; the second HU was not suppressing the age-related increases that the first HU was, resulting in a greater overall loss during the second bout. Also, the pre-HU values for the second HU were greater than baseline (although not by a statistically significant amount), which is something that was not observed in most of the pQCT variables, including cancellous BMC and CSI. Recovery from the first and second HU bouts were similar in general, but cancellous and cortical pQCT variables had greater recovery after the second bout (relative to immediate pre-HU groups) while mechanical properties experienced a greater recovery after the first HU bout.

5.5 Comparison Between pQCT-Derived Measures and RPC Results

Several studies have documented that BMD alone does not always predict or relate to the strength of the cancellous or cortical bone, although it is certainly a major factor in determining fracture risk.[45,46,47,48] This study found that vBMD did not closely track the changes observed in mechanical properties during HU. For instance, there

were significant losses in total, cortical, and cancellous vBMD during the first HU period while aging controls increased only slightly over the same time period. However, HU results for ultimate stress, elastic modulus, and energy to ultimate showed a complete suppression of significant age-related increases that were very evident in the aging controls between months 6 and 7.Mechanical properties increased during the first recovery period even though all vBMD values were still decreasing, albeit not significantly. For the following two recovery periods, however, both vBMD and mechanical properties steadily increased. vBMD values decreased significantly below baseline after both the single and double HU bout (at month 10) but mechanical property behavior during the same time period decreased at about the same rate as aging controls. There was also not a strong relationship between RPC mechanical testing results and most other pQCT variables (as well as calculated measures). The variables that most accurately reflected the changes observed in RPC testing were cancellous BMC and cancellous CSI, which captured the HU-induced suppression of age-related increases, as well as other feature that were evident in the mechanical testing results. Upon examination of the cancellous data, it becomes apparent that the significant decrease in cancellous vBMD during the initial HU was primarily due to an increasing endocortical area rather than a significant loss of cancellous bone. It could be the case that pre- and post-HU mechanical properties were similar because the amount of cancellous bone in the compressed region had not significantly changed during HU. However, it is difficult to say whether this is the case because cancellous

bone strength depends on several factors, such as trabecular connectivity[27,49,50], that this study was unable to measure. This indicates that overall mineral and geometric properties are not sufficient to completely and accurately predict the mechanical behavior of cancellous bone. One important factor that could shed some light on the results is the extent of collagen cross-linking and fiber orientation. Multiple studies have shown that these factors contribute to mechanical properties[45,51], so having this information for the distal femur specimens could give valuable insight into unloading-induced changes. There was no discernable relation between pQCT parameters and ultimate strain, which is consistent with the results of a number of other studies[52,53,54,55,56], although others have observed an increase[57,58,59,60] or decrease[61,62] in ultimate strain as density increases.

Cancellous compartment parameters would be expected to provide the best predictions for mechanical properties obtained from RPC testing because RPC focuses on the cancellous region. Cancellous vBMD would seemingly be the best candidate for predicting cancellous mechanical properties but, because the density obtained from pQCT scanning is only an average for the region, even it does not tell the whole story. Goldstein et al. found that elastic modulus of cancellous bone varied by up to two orders of magnitude in the cross-section of a human tibia metaphysis, with the highest values being found at the region bordering the cortical shell and the lowest values being found in the center.[63] A visual inspection of RPC specimens as well as a study of pQCT density scans showed that there were noticeable density variations between

cancellous bone near the cortical shell and cancellous bone in the center of the region. Therefore, the region that is compressed during RPC is likely the weakest portion of the cross-section and, while RPC testing allows us to make comparisons between groups, it does not fully reflect the strength of the entire cross-section. However, if the platen size was increased to reach the true diameter of the endocortical circle, a significant portion of the compressive loads would be borne by cortical bone, defeating the purpose of determining the mechanical properties of only cancellous bone.

5.6 Similarity to Astronauts

Although the HU rat in this study and ISS crew members studied by Lang et al. generally followed the same positive/negative trends during unloading and recovery, the percent differences relative to all measures were not so similar that the distal femur metaphysis could accurately predict losses that would occur during extended stays in microgravity. Losses were generally, although not always, more substantial for the astronauts than for the rats. Interestingly, the HU results more closely match the astronaut losses when they are presented as percent difference from AC instead of percent difference from pre-unloading values. None of the three recovery groups consistently matched well with the astronaut data for every variable, but 1HU7+R2 and 1HU7+R3 tended to best mimic the astronaut femur losses relative to pre-unloading and post-unloading values, respectively. Also, the range of HU rat recovery was similar enough to the astronaut femur data that 1HU7+R1 and 1HU7+R3 could be used as a

general upper- and lower-bound for predicting unloading-induced losses. The major difference between the results of this study and the astronauts studied by Lang et al. is that periosteal apposition is observed in the rats during unloading, whereas periosteal resorption appears to be dominant in the astronaut femur. Conversely, Carpenter et al. observed an increase in periosteal size post-flight.[4] However, it should be noted that the study by Lang et al. examined 16 astronauts, twice as many as Carpenter et al. used.

6. LIMITATIONS

Much of the RPC results depend, in part, on where cancellous bone is deposited and resorbed within the cancellous compartment. The distribution of cancellous bone is very important for the RPC test. Many of the specimens had an obvious variation in trabecular density, with the anterior portion of the specimen having a higher density than the posterior. The variation is unavoidable because the growth plate's most proximal location is on the anterior side of the metaphysis. The posterior section of some of the specimens was porous enough to be considered essentially vacant. This directly impacted the RPC results because one of the primary assumptions of this test is that the specimen being tested is a continuum with the same cross-sectional area as the platens (since that is the area being directly compressed).[31] However, if certain areas are essentially devoid of trabeculae then the assumptions are not completely valid, as the actual stress on the tissue will be higher than the stress calculated using the platens.

It was decided that rats should begin the study when they reached 6 months of age because that is an age at which they are considered skeletally mature. However, it was obvious from large increases in several properties that there was still considerable growth occurring. In hindsight, it would seem more appropriate to have started the study at 7 months old. If this had been done, it is possible that the HU response of several properties would have been very different, especially mechanical properties.

Instead of HU suppressing natural increases (which occurred between months 6 and 7), it is more likely that mechanical properties would decrease significantly below baseline, as the vBMD parameters did. This is based on the fact that 1) a 7 month baseline group would have higher values than the 6 month baseline and 2) HU would not be acting against the increases observed between months 6 and 7.

7. CONCLUSIONS AND SUMMARY

Looking back at the hypotheses presented in Section 1.2, some expectations were right, others wrong, but most depend on how loss and recovery are defined. All bone mass and density measures were significantly lower than again controls after HU at 7 months (and all but cancellous BMC were significantly lower than baseline). I predicted that the strength of the cancellous compartment would recover more slowly than vBMD because trabecular architecture, which directly impacts cancellous bone strength, has been shown to recover more slowly. One assumption of this hypothesis was that mechanical properties would decrease significantly during unloading. However, the reduction in strength as a result of HU was minimal relative to baseline and it only increased during subsequent recovery periods. So in that regard, no recovery was necessary because there were no substantial losses. But compared to aging controls, the unloaded animals had significantly reduced mechanical properties, indicating that HU suppressed age-related increases. Recovery relative to aging controls (i.e. $p<.05$) occurred after 2 recovery periods for all vBMD variables (and 2-3 recovery periods for BMC measures) but ultimate stress and energy to ultimate had become similar to controls after the first month of recovery (elastic modulus required 2 months). From this perspective, the recovery of mechanical properties occurred more rapidly than recovery for mineral measures.

I also hypothesized that the second HU bout would be more detrimental than the first. Again, this depends on how you define recovery for each parameter. In general, the second unloading bout tended to be less detrimental than the first (relative to their immediate pre-HU values) when looking at pQCT values. Mechanical testing results can be looked at the same way: relative to pre-HU values, the second HU bout was most detrimental but when compared to aging controls, the first HU was most detrimental. When comparing the loss and recovery of mechanical properties relative to aging controls, it must be noted that significant natural growth appears to be occurring between months 6 and 7 and age-related losses are observed afterwards. Relative to immediate pre-HU groups, pQCT variables experienced greater recovery (relative to immediate pre-HU groups) after the second HU exposure while mechanical properties experienced a greater recovery after the first HU bout.

Despite the lower pre-HU "starting point" and equal HU duration, the 2HU group was not substantially lower than 1HU7 for most variables (pQCT and mechanical properties). This could be due to the losses reaching close to a "lower limit" that cannot be exceeded, regardless of how long or how often they are unloaded. A homeostatic level, such as that described above, has been observed in patients (<40 years old) with spinal cord injuries.[64] Garland et al. noticed that significant bone mineral loss happened very rapidly in the months immediately after injury, but measurements taken 5 years after injury were not significantly different than those taken 16 months after. This finding is relevant to this study because there is likely to be a point where

unloading-induced losses will begin to diminish, regardless of the number or duration of HU bouts, although there is not enough information to know whether the homeostatic level was reached in this study.

Mechanical properties measured through RPC testing tracked similarly with cancellous CSI (consequently, cancellous BMC also followed similar patterns of loss and recovery), although total CSI did not. Cancellous CSI captured the increase in strength during the first month as well as the subsequent decline. It should not be surprising that this index was the most accurate as it was solely meant to predict the strength of the cancellous region, and not the total volume. Because cancellous CSI is directed specifically at the cancellous region and neglects the cortical region, it is unlikely that it would be an accurate predictor of the mechanical properties if the specimen's entire cross-section was compressed. BSI captured changes in the HU and recovery groups but did not reflect the age-related losses observed in the control groups after month 7. One of the reasons that the other strength indices did not reflect changes observed in mechanical testing is that BSI and SSI (as well as the moments of inertia) are density-weighted predictors, which means that their results are also dependent on changes in the highly dense, outer cortical region.

The distal femur metaphysis of the rat did follow the same general loss and recovery patterns as the astronaut femoral neck and proximal femur. As predict, there were substantial differences between the magnitudes of losses. While none of the recovery periods reflected a consistent match with the astronaut femur data, the

1HU7+R2 and 1HU7+R3 groups were the most similar when recovery was defined relative to pre-unloading and post-unloading values, respectively. Also, the recovery groups were similar enough to the astronaut data that 1HU7+R1 and 1HU7+R3 could be used as a general upper- and lower-bound to predict recovery after missions. The only major difference between the Lang et al. results and the HU rat results is that the periosteal expansion was observed in the rats after unloading, but not in the astronauts.

REFERENCES

1. Lang T, LeBlanc A, Evans H, Lu Y, Genant H, Yu A. Cortical and trabecular bone mineral loss from the spine and hip in long-duration spaceflight. J Bone Miner Res. 2004;19:1006–1012.

2. Cauley JA, Lui LY, Ston KL, Hillier TA, Xmuda JM, Hochberg M, Beck TJ, Ensurd KE. Longitudinal study of changes in hip bone mineral density in Caucasian and African-American women. J Am Geriatr Soc. 2005;53:183–189.

3. Lang TF, LeBlanc AF, Evans HJ, Lu Y. Adaptation of the proximal femur to skeletal reloading after long-duration spaceflight. J Bone Miner Res. 2006;21:1224–1230.

4. Carpenter RD, LeBlanc AD, Evans H, Sibonga JD, Lang TF. Long-term changes in the density and structure of the human hip and spine after long-duration spaceflight. Acta Astronautica. 2010;67:71–81.

5. Morey-Holton ER, Globus RK. Hindlimb unloading of growing rats: a model for predicting skeletal changes during space flight. Bone. 1998;22:83S–88S.

6. Morey-Holton ER, Globus RK. Hindlimb unloading rodent model: technical aspects. J Appl Physiol. 2002;92:1367–1377.

7. Corcoran TA, Sandler RB, Myers ER, Leibowitz HH, Hayes WC. Calculation of cross-sectional geometry from CT images with application in postmenopausal women. J Comput Assist Tomogr. 1994;18:626–633.

8. Marshall D, Johnell O, Wedel H. Meta-analysis of how well measures of bone mineral density predict occurrence of osteoporotic fractures. Brit Med J. 1996;312:1254–1259.

9. Stone K, Seeley DG, Lui L, Cauley JA, Ensrud K, Browner WS, Nevitt MC, Cummings SR. BMD at multiple sites and risk of fracture of multiple types: long-term results from the study of osteoporotic fractures. J Bone Miner Res. 2003;18:1947–1954.

10. Seeman E, Delmas PD. Bone Quality – The material and structural basis of bone strength and fragility. N Engl J Med. 2006;354:2250–2261.

11. Cranney A, Jamal SA, Tsang JF, Josse RG, Leslie WD. Low bone mineral density and fracture burden in postmenopausal women. Can Med Assoc J. 2007;177:575–580.

12. Pasco JA, Seeman E, Henry MJ, Nicholson GC, Kotowicz MA. The population burden of fractures originates in women with osteopenia, not osteoporosis. Osteoporos Int. 2006;17:1404–1409.

13. Wainwright SA, Marshall LM, Ensrud KE, Cauley JA, Black DM, Hillier TA, Hochberg MC, Vogt MT, Orwell ES. Hip fracture in women without osteoporosis. J Clin Endocrinol Metab. 2005;90:2787–2793.

14. Christiansen BA, Kopperdahl DL, Kiel DP, Keaveny TM, Bouxsein ML. Mechanical contributions of the cortical and trabecular compartments contribute to differences in age-related changes in vertebral body strength in men and women assessed by QCT-based finite element analysis. J Bone Miner Res. 2011;26:974–983.

15. Rockoff SD, Sweet E, Bleustein J. The relative contribution of trabecular and cortical bone to the strength of human lumbar vertebrae. Calcif Tissue Res. 1969;3:163–175.

16. Keaveny TM, Hoffman PF, Singh M, Palermo L, Bilezikian JP, Greenspan SL, Black DM. Femoral bone strength and its relation to cortical and trabecular changes after treatment with PTH, alendronate, and their combination as assessed by finite element analysis of quantitative CT scans. J Bone Miner Res. 2008;23:1974–1982.

17. Holzer G, von Skrbensky G, Holzer LA, Pichl W. Hip fractures and the contribution of cortical versus trabecular bone to femoral neck strength. J Bone Miner Res. 2009;24:468–474.

18. Manske SL, Liu-Ambrose T, Cooper DML, Kontulainen S, Guy P, Forster BB, McKay HA. Cortical and trabecular bone in the femoral neck both contribute to proximal femur failure load prediction. Osteoporos Int. 2009;20:445–453.

19. Eswaran SK, Gupta A, Adams MF, Keaveny TM. Cortical and trabecular load sharing in the human vertebral body. J Bone Miner Res. 2006;21:307–314.

20. Allen MR, Hogan HA, Bloomfield SA. Differential bone and muscle recovery following hindlimb unloading in skeletally mature male rats. J Musculoskel Neuron Interact. 2006;6:217–225.

21. Maeda H, Kimmel DB, Raab DM, Lane NE. Musculoskeletal recovery following hindlimb immobilization in adult female rats. Bone. 1993;14:153–159.

22. Bloomfield SA, Allen MR, Hogan HA, Delp MD, Site- and compartment-specific changes in bone with hindlimb unloading in mature adult rats. Bone. 2002;31:149–157.

23. SEER Training Modules, National Cancer Institute. URL: training.seer.cancer.gov/anatomy/skeletal/tissue.html. Retrieved July 20, 2011.

24. Turner CH. On Wolff's law of trabecular architecture. J Biomech. 1992;25:1–9.

25. Han Y, Cowin SC, Schaffler MB, Weinbaum S. Mechanotransduction and strain amplification in osteocyte cell processes. Proc Natl Acad Sci USA. 2004;101:16689–16694.

26. Lemmon H. Methods for reduced platen compression test specimen cutting locations using micro-CT and planar radiographs. MS Thesis, Texas A&M University, College Station, TX. 2003.

27. Shen V, Birchman R, Xu R, Otter M, Wu D, Lindsay R, Dempster DW. Effects of reciprocal treatment with estrogen and estrogen plus parathyroid hormone on bone structure and strength in ovariectomized rats. J Clin Invest. 1995;96:2331–2338.

28. Meng XW, Liang XG, Birchman R, Wu DD, Dempster DW, Lindsay R, Shen V. Temporal expression of the anabolic action of PTH in cancellous bone of ovariectomized rats. J Bone Min Res. 1996;11:421–429.

29. Ke HZ, Shen VW, Qi H, Crawford DT, Wu DD, Liang XG, Chidsey-Frink KL, Pirie CM, Simmons HA, Thompson DD. Prostaglandin E2 increases bone strength in intact rats and in ovariectomized rats with established osteopenia. Bone. 1998;23:249–255.

30. Mosekilde L, Thomsen JS, Orhii PB, Kalu DN. Growth hormone increases vertebral and femoral bone strength in osteopenic, ovariectomized, aged rats in a dose-dependent and site-specific manner. Bone. 1998;23:343–352.

31. Hogan HA, Ruhmann SP, Sampson HW. The mechanical properties of cancellous bone in the proximal tibia of ovariectomized rats. J Bone Miner Res. 2000;15:284–292.

32. Oxlund H, Dalstra M, Ejersted C, Andreassen TT. Parathyroid hormone induces formation of new cancellous bone with substantial mechanical strength at a site where it had disappeared in old rats. Eur J Endocrinol. 2002;146:431–438.

33. Cuppone M, Seedhom BB, Berry E, Ostell AE. The longitudinal Young's modulus of cortical bone in the midshaft of human femur and its correlation with CT scanning data. Calcif Tissue Int. 2004;74:302–309.

34. Keyak JH, Lee IY, Skinner HB. Correlations between orthogonal mechanical properties and density of trabecular bone: Use of different densitometric measures. J Biomed Mater Res. 1994;28:1329–1336.

35. Cory E, Nazarian A, Vahid E, Vartanians V, Muller R, Snyder BD. Compressive axial mechanical properties of rat bone as functions of bone volume fraction, apparent density and micro-CT based mineral density. J Biomech. 2010;43:953–960.

36. Hasegawa Y, Schneider P, Reiners C. Age, sex, and gripstrength determine architectural bone parameters assessed by peripheral quantitative computed tomography (pQCT) at the human radius. J Biomech. 2001;34:497–503.

37. Dehority W, Halloran B, Bikle D, Curren T, Kostenuik P, Wronski T, Shen Y, Rabkin B, Bouraoui A, Morey-Holton E. Bone and hormonal changes induced by skeletal unloading in the mature male rat. Am J Physiol. 1999;276:E62–E69.

38. Garber M, McDowell D, Hutton M. Bone loss during simulated weightlessness: A biomechanical and mineralization study in the rat model. Aviat Space Environ Med. 2000;71:586–592.

39. Smith B, King J, Lucas E, Akhter M, Arjmandi B, Stoecker B. Skeletal unloading and dietary copper depletion are detrimental to bone quality of mature rats. J Nutr. 2002;132:190–196.

40. Müller A, Rüegsegger E, Rüegsegger P. Peripheral QCT: A low-risk procedure to identify women predisposed to osteoporosis. Phys Med Biol. 1989;34:741–749.

41. Lind PM, Lind L, Larsson S, Orberg. Torsional testing and peripheral quantitative computed tomography in rat humerus. Bone. 2001;29:265–270.

42. Ferretti JL, Capozza RF, Zanchetta JR. Mechanical validation of a tomographic (pQCT) index for noninvasive estimation of rat femur bending strength. Bone. 1996;18:97–102.

43. Ju Y-I, Sone T, Okamoto T, Fukunaga M. Jump exercise during remobilization restores integrity of the trabecular architecture after tail suspension in young rats. J Appl Physiol. 2008;104:1594–1600.

44. Ruff CB, Hayes WC. Sex differences in age-related remodeling of the femur and tibia. J Orthop Res. 1988;6:886–896.

45. Puustjärvi K, Nieminen J, Räsänen T, Hyttinen M, Helminen HJ, Kröger H, Huuskonen J, Alhava E, Kovanen V. Do more highly organized collagen fibrils increase bone mechanical strength in loss of mineral density after one-year running training? J Bone Miner Res. 1999;14:321–329.

46. Burr DB. The relationship among physical, geometrical, and mechanical properties of bone, with a note on the properties of nonhuman primate bone. Yearb Phys Anthropol. 1980;23:109–146.

47. Carbon R, Sambrok PN, Deakin V, Fricker P, Eisman JA, Kelly P, Maguire K, Yeates MG. Bone density of elite female athletes with stress fractures. Med J Aust. 1990;153:373–376.

48. Hui S, Slemenda CW, Johnston CC. Age and bone mass as predictors of fracture in a prospective study. J Clin Invest. 1988;81:1804–1809.

49. Ito M, Nishida A, Koga A, Ikeda S, Shiraishi A, Uetani M, Hayashi K, Nakamura T. Contributions of trabecular and cortical components to the mechanical properties of bone and their regulating parameters. Bone. 2002;31:351–358.

50. Kinney JH, Ladd AJ. The relationship between three-dimensional connectivity and the elastic properties of trabecular bone. J Bone Miner Res. 1998;13:839–845.

51. Ding M, Dalstra M, Danielsen CC, Kabel J, Hvid I, Linde F. Age variations in the properties of human tibial trabecular bone. J Bone Joint Surg. 1997;79:995–1002.

52. Ford CM, Keaveny TM. The dependence of shear failure properties of trabecular bone on apparent density and trabecular orientation. J Biomechanics. 1996;29:1309–1317.

53. Hansson TH, Keller TS, Panjabi MM. A study of the compressive properties of lumbar vertebral trabeculae: Effects of tissue characteristics. Spine. 1987;11:56–62.

54. Keaveny TM, Wachtel EF, Ford CM, Hayes WC. Differences between the tensile and compressive strengths of bovine tibial trabecular bone depend on modulus. J Biomechanics. 1994;27:1137–1146.

55. Lindahl O. Mechanical properties of dried defatted spongy bone. Acta Orthop. 1976;47:11–19.

56. Rohl L, Larsen E, Linde F, Odgaard A, Jorgensen J. Tensile and compressive properties of cancellous bone. J Biomechanics. 1991;24:1143–1149.

57. Kopperdahl DL, Keaveny TM. Yield strain behavior of trabecular bone. J Biomechanics. 1998;31:601–608.

58. Hvid I, Bentzen SM, Linde F, Mosekilde L, Pongsoipetch B. X-ray quantitative computed tomography: The relations to physical properties of proximal tibial trabecular bone specimens. J Biomechanics. 1989;22:837–844.

59. Keaveny TM, Watchtel EF, Ford CM, Hayes WC. Differences between the tensile and compressive strengths of bovine tibial trabecular bone depend on modulus. J Biomechanics. 1994;27:1137–1146.

60. Turner CH. Yield behavior of bovine cancellous bone. J Biomech Eng. 1989;111:256–260.

61. Hvid I, Jensen NC, Bunger C, Solund K, Djurhuus JC. Bone mineral assay: Its relation to the mechanical strength of cancellous bone. J Engineering in Medicine. 1985;14:79–83.

62. Mosekilde L, Mosekilde L, Danielsen CC. Biomechanical competence of vertebral trabecular bone in relation to ash density and age in normal individuals. Bone. 1987;8:79–85.

63. Goldstein SA, Wilson DL, Sonstegard DA, Matthews SL. The mechanical properties of human tibial trabecular bone as a function of metaphyseal location. J Biomechanics. 1983;16:965–969.

64. Garland DE, Stewart CA, Adkins RH, Hu SS, Rosen C, Liotta FJ, Weinstein DA. Osteoporosis after spinal cord injury. J Orthop Res. 1992;10:371–378.

APPENDIX

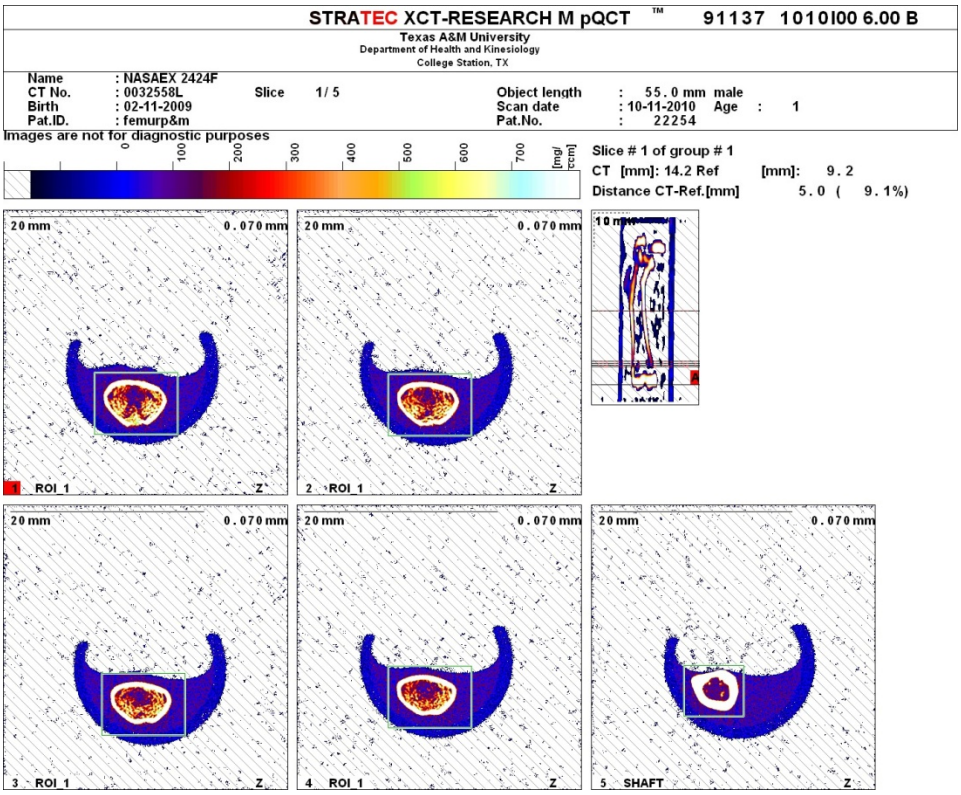
STRATEC XCT-RESEARCH M pQCT ™ 91137 1010100 6.00 B
Texas A&M University
Department of Health and Kinesiology
College Station, TX
Name : NASAEX 2424F
CT No. : 0032558L
Birth : 02-11-2009
Pat.ID. : femurp&m
Slice 1 / 5
Object length : 55.0 mm male
Scan date : 10-11-2010 Age : 1
Pat.No. : 22254
Images are not for diagnostic purposes
0 100 200 300 400 500 600 700 [mg/ccm]
Slice # 1 of group # 1
CT [mm]: 14.2 Ref [mm]: 9.2
Distance CT-Ref.[mm] 5.0 (9.1%)
20 mm 0.070 mm
1 ROI 1 Z
2 ROI 1 Z
3 ROI 1 Z
4 ROI 1 Z
5 SHAFT Z

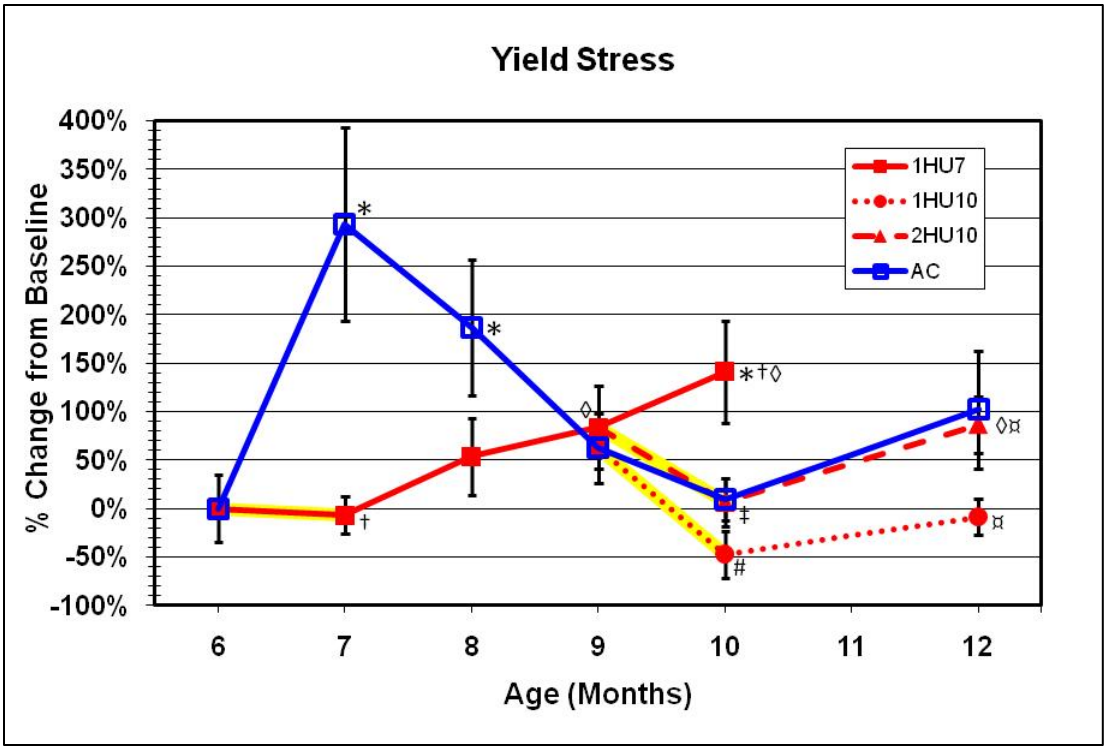
Yield Stress
% Change from Baseline
400%
350%
300%
250%
200%
150%
100%
50%
0%
-50%
-100%
6
7
8
9
10
11
12
Age (Months)
1HU7
1HU10
2HU10
AC

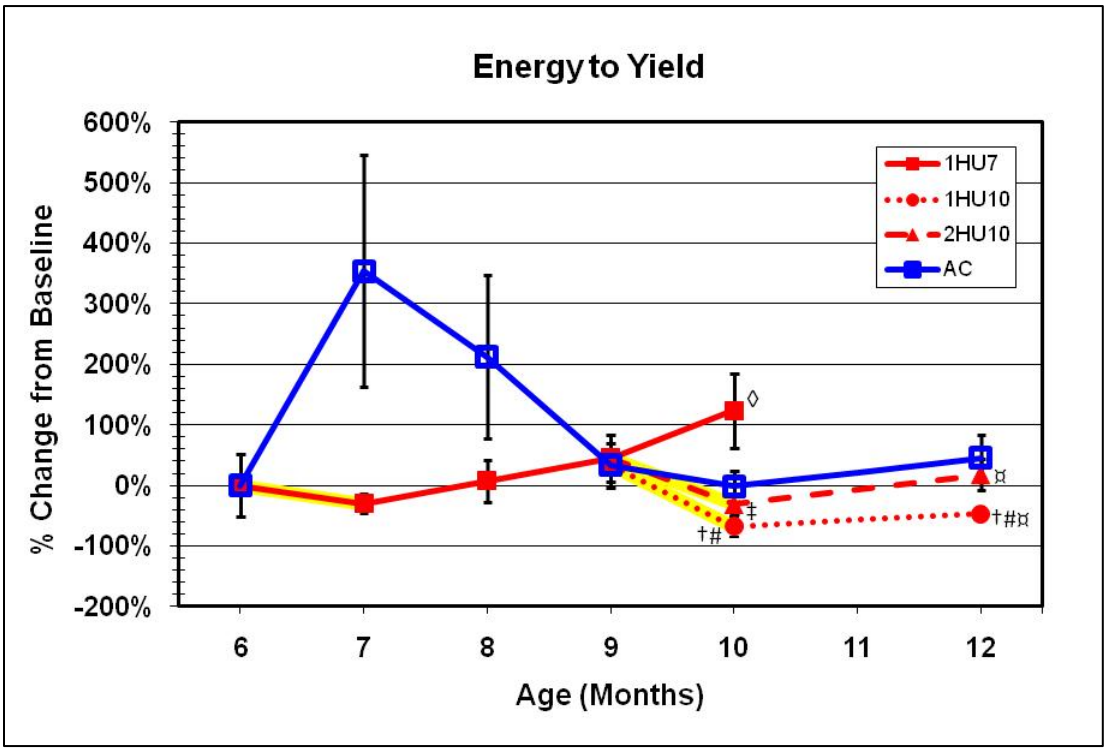
Energy to Yield
% Change from Baseline
600%
500%
400%
300%
200%
100%
0%
-100%
-200%
6
7
8
9
10
11
12
Age (Months)
1HU7
1HU10
2HU10
AC

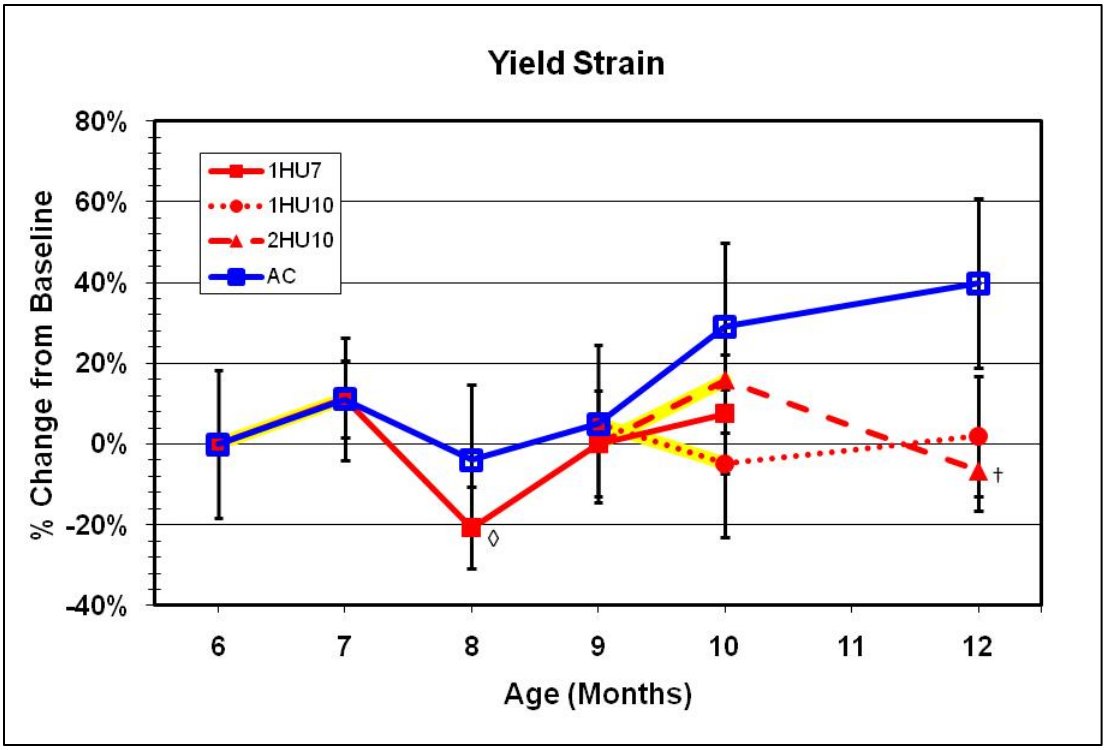
Yield Strain
80%
60%
40%
20%
0%
-20%
-40%
% Change from Baseline
1HU7
1HU10
2HU10
AC
◊
†
6
7
8
9
10
11
12
Age (Months)

VITA

Name:	Joshua Morgan Davis
Address:	Department of Mechanical Engineering 3123 TAMU College Station, TX 77843, C/O Dr. Harry Hogan
Email Address:	joshuadavis05@gmail.com
Education:	B.S., Mechanical Engineering, Texas A&M University, 2006 M.S., Mechanical Engineering, Texas A&M University, 2011